4.7 Carbohydrate-Metal Complexes: Structural Chemistry of Stable Solution Species

Thorsten Allscher, *Peter Klüfers**, *Peter Mayer*
Department Chemie und Biochemie, Ludwig-Maximilians-Universität München, Butenandtstr. 9, 81377 München, Germany
kluef@cup.uni-muenchen.de

Abstract

This review discusses the structural chemistry of metal complexes of carbohydrates and their derivatives with the focus on crystal structure and NMR data of stable solution species. There is evidence that the stability of these complexes is markedly increased when the carbohydrates operate as chelating polyolato ligands, this is, when they are multiply deprotonated polydentate ligands. The 1,2-diolato coordination mode resulting in five-membered chelate rings is most commonly observed. Small torsion angles within the 1,2-diolato moiety enable the chelation of small atoms while larger torsion angles are usually needed for the complexation of large atoms. Hence, as a consequence of the limited flexibility of the pyranose ring, pyranoidic 1,2-diols merely form less-stable complexes with small metal centers in marked contrast to furanoidic 1,2-diols. An additional contribution to the stability arises from hydrogen bonds, especially intramolecular ones, with the deprotonated ligator oxygen atoms acting as strong hydrogen-bond acceptors.

Keywords

Carbohydrate; Derivatives; Metal; Complex; Chelation; Solution structure; Crystal structure; NMR

Abbreviations

Ado	adenosine
AnEryt	anhydroerythritol
AnThre	anhydrothreitol
Arab	arabitol
Ara	arabinose
ax	axial
bpy	2,2′-bipyridyl
Bu	butyl
CD	cylodextrin
chxn	1,2-cyclohexanediamine
CIS	coordination-induced shift
Cp	cyclopentadienyl
Cyd	cytidine
DBU	1,8-diazabicyclo[5.4.0]undec-7-ene
dien	diethylenetriamine
dppp	1,3-bis(diphenylphosphino)propane
en	ethylenediamine
Eryt	erythritol
eq	equatorial
Et	ethyl

Fru	fructose
Gal	galactose
Gal1,6A$_2$	galactaric acid
Glc	glucose
Glc1A	gluconic acid
Glc1P	glucose-1-phosphate
Glc1,6An	1,6-anhydro-β-D-glucose (levoglucosan)
Glc1,6A$_2$	glucaric acid
Guo	guanosine
Ino	inosine
Ins	inositol
Lyx	lyxose
Man	mannose
Mann	mannitol
Me	methyl
Me$_3$tren	tris(N,N',N''-trimethyl-2-aminoethyl)amine
py	pyridine
Rib	ribose
Ribt	ribitol
Rul	ribulose
Sorb	sorbitol
Suc	sucrose
tach	1,3,5-triaminocyclohexane
Tre	α,α-trehalose
Thre	threitol
tpb	hydrido-tris(pyrazolyl)borate
tren	tris(2-aminoethyl)amine
Urd	uridine
Xyl	xylose
Xylt	xylitol
f	furanose
p	pyranose

1 Introduction

A central problem in the chemistry of carbohydrates is their polyfunctionality which usually leads to several possible coordination sites for metal atoms. As a consequence, in basic research the carbohydrates are often replaced by model ligands of reduced functionality in order to investigate the structure of carbohydrate–metal complexes. The most reliable structural information about solution and solid-state species is obtained by NMR spectroscopy and X-ray structure analysis of single crystals, respectively, both methods having developed significantly in the last years. Hence, we will focus on the structures of carbohydrate–metal complexes based on unambiguous data obtained by these two methods. The following carbohydrates and carbohydrate derivatives are included in this review: sugar alcohols, aldonic and

aldaric acids, anhydroerythritol, inositols, anhydro-sugars, glycosides, and reducing carbohydrates such as aldoses, ketoses, and glycuronates. Among the glycosides, the pyranosides and furanosides (mostly alkyl derivatives), nucleosides, non-reducing disaccharides, cyclodextrins, and polysaccharides are viewed. The nucleosides are the only non-*O*-glycosides considered in this review. Structures of simple addition products of carbohydrates and metal salts are not included either. Structures which should be included in this review, according to the requirements stated above, but have been reviewed elsewhere already, will mostly not be discussed again. Publications written in Chinese, Japanese, or Russian are not cited herein.

A summary of the historical development of reviews regarding carbohydrate–metal complexes can be found in a review written by Verchère et al. in 1998. Besides NMR and crystal structure data, they also consider other methods such as calorimetry and EXAFS spectroscopy [1]. Here a short listing of a selection of reviews written in the ensuing years: Complexes of the metals nickel(II), cobalt(III), and manganese(II,III) with *N*-glycosides derived from tris(2-aminoethyl)amine and aldoses have been reviewed by Yano [2] who has also written a summary on the structure and biological activity of complexes of transition metals with glycosylamines derived from sugar molecules and polyamines [3]. Nagy et al. discuss the coordination equilibria of carbohydrate–metal complexes in aqueous solution together with crystal structures [4,5] and summarize the application of EXAFS and XANES methods in the coordination chemistry of carbohydrates [6]. Solid-state and solution complexes with platinum-group metals are reviewed by Steinborn and Junicke [7]. The coordination chemistry of modified carbohydrates has been summarized by Alexeev et al. in two reviews [8,9]. The kinetics of proton-release reactions of aluminum(III) complexes with D-ribose and their stability has been reviewed by Petrou [10]. Chakravorty et al. describe heteroleptic vanadate chelate esters of monoionized diols and carbohydrates with tridentate auxiliary ligands [11]. The formation and the synthetic applications of carbohydrate-iron complexes possessing Fe–C bonds are discussed by Zamojski [12]. The metallation sites of nucleosides and nucleotides in ternary systems with polyamines has been summarized by Lomozik [13]. The metal complexation of oligo- and polysaccharides has also been reviewed. Metal-containing supramolecular catalytic systems may be achieved based on cyclodextrins and their derivatives ("cavitand" ligands) [14,15,16]. The metal-binding ability of chitosan under various conditions is discussed by Varma et al. [17].

In order to elucidate the coordination chemistry of individual carbohydrates, the following review will be carbohydrate-oriented instead of metal-oriented, that is, the structures of individual carbohydrates or, if only few structures are known, of a group of related carbohydrates are discussed en-block. We will start with complexes of simpler carbohydrates such as sugar alcohols or anhydroerythritol in order to derive the basics of metal coordination and will then proceed to typical carbohydrates.

2 Sugar Alcohols

The solution and solid state structures of the following sugar alcohols are discussed in separate sections: erythritol **1**, D-threitol **2**, xylitol **3**, D-arabitol **4**, ribitol **5**, D-mannitol **6**, dulcitol **7**, and D-sorbitol **8**.

1   2   3   4   5   6   7   8
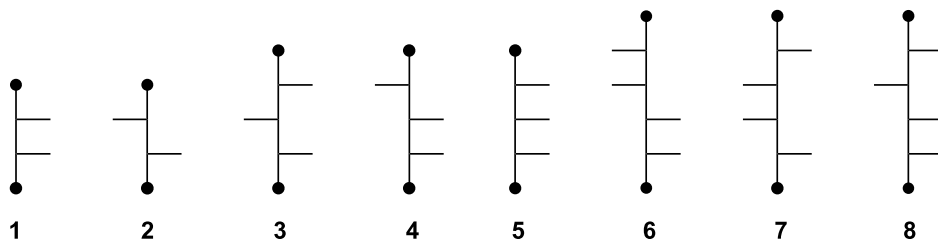
Carbon numbering: C1 is situated at the top of each chain.   ● = CH$_2$OH
Chiral sugar alcohols are depicted in their D-configuration.

2.1 Erythritol

Erythritol **1** is a tetraol with a central *erythro*-configured diol group. In combination with the terminal hydroxyl functions there are several conformations to act as a chelate ligand. In most of its characterized solid-state structures, erythritol is coordinated to two central atoms by acting as a bis-1,2-diolato ligand, at which the deprotonation of the hydroxyl groups is a consequence of the synthesis from alkaline solutions and/or complexation of more or less Lewis acidic central atoms. A complex of this type is obtained upon the reaction of erythritol with two equivalents of [(NH$_3$)$_2$Pd(OH)$_2$] in aqueous solution which leads to the centrosymmetric structure of **9** (❖ *Fig. 1*) [18].
In **9**, the C$_4$ chain of erythritol adopts a zigzag conformation with a torsion angle of 180° which is as much forced by the inversion symmetry of the complex as is the torsion angle of the central *erythro*-diolato group (180°). The terminal oxygen atoms are oriented to the same side of the C$_4$ chain as their adjacent *erythro*-oxygen atoms. The torsion angle of the resulting chelating diolato group is 46.2°. The solutions mentioned above contain **9** as the main species which is confirmed by a downfield shift ("coordination induced shift", CIS) of about 12 ppm of the carbon atoms involved in the five-membered chelate ring. The asymmetric monometallated complex **11** which might be stabilized by an intramolecular γ hydrogen bond (the donor and acceptor oxygen atoms are separated by a C$_3$ chain), is detected as a byproduct whereas **11** becomes the main species and **9** a byproduct in equimolar solutions of erythritol

9   10
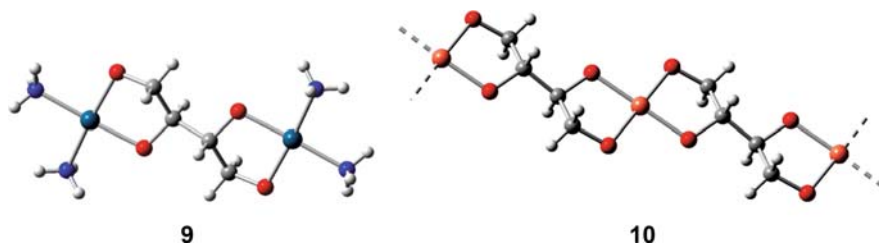
◾ **Figure 1**
Molecular structure of [{(NH$_3$)$_2$Pd}$_2$(ErytH$_{-4}$)] 9 in crystals of 9 · 2 H$_2$O and a section of the linear coordination polymer built up by [Cu(ErytH$_{-4}$)]$^{2-}$ 10 units in crystals of Na$_2$10 · Eryt · 12 H$_2$O

and [(NH$_3$)$_2$Pd(OH)$_2$] (CIS of the chelating carbon atoms 1 and 2 in **11**: 10.9 and 9.8 ppm, respectively, non-chelating carbon atoms 3 and 4: 0.9 and 1.0 ppm, respectively). A minor species of these equimolar solutions is the symmetric monometallated complex **12** (C1 CIS: −0.9 ppm, C2 CIS: 10.0 ppm).
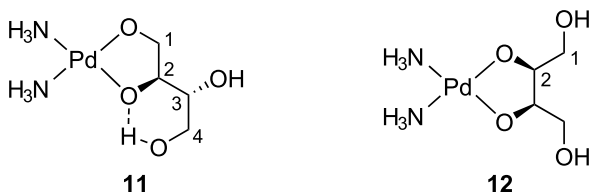

A similar species distribution is found for [(en)Pd(OH)$_2$]/erythritol solutions, and a crystal structure containing a binuclear complex analogous to **9** has been determined [19]. A solid-state structure of this type is also formed by ethylenediamine-copper(II) [20]. In strong alkaline aqueous solutions, the ethylenediamine-copper bond is cleaved and the formation of homoleptic complexes such as the linear coordination polymer **10** (❿ *Fig. 1*) is enabled [21].

The reaction of (dppp)Pt(CO$_3$) with four equivalents of erythritol produces the (dppp)Pt derivative of **11** as the major species, while the corresponding *erythro*-derivative **12** is obtained in small yield only (11%) [22].

While palladium(II) and copper(II) build solely 1,2-diolato complexes with erythritol which leads to five-membered chelate rings, boron(III) is involved in the six-membered rings as in the bis(phenylboronic acid ester) **13** (❿ *Fig. 2*). Erythritol adopts a zigzag conformation similar to that in **9** but the oxygen atoms are grouped alternatively on opposite sites of the C$_4$-chain. The six-membered chelate rings in half-chair conformation provide a suitable bond pattern for a boron center involved in the delocalized π-bond system of the phenyl substituent.

In solution, **13** is merely a minor species which is identified by a significant difference in the chemical shifts of its two symmetrically independent erythritol-C atoms: the terminal carbon atom is shifted by 2.8 ppm downfield while the inner carbon atom which is involved in two chelate rings is shifted by 2.8 ppm upfield. Most of the phenylboronic acid is bound in five-membered chelate rings similar to **9** (^{13}C shifts: 5.3 ppm for terminal C atoms, 6.5 ppm for inner C atoms) [23].
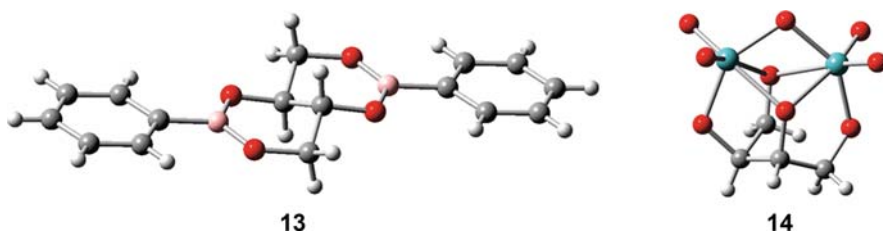
■ **Figure 2**
The crystal structure of (PhB)$_2$(ErytH$_{-4}$-$O^{1,3}$,$O^{2,4}$) **13** and the molecular structure of [Mo$_2$O$_5$(ErytH$_{-4}$)]$^{2-}$ **14** in crystals of [N(n-Bu)$_4$]$_2$**14**

In order to group all its hydroxyl functions on the same side of the C_4 chain, erythritol has to adopt a sickle conformation which is established as in the dimolybdate complex **14** (❯ *Fig. 2*). The torsion angle of the C_4 chain is 49.5°, the torsion angle of the central *erythro*-configured diol function is 34.4°. The sickle conformation allows the asymmetric facial coordination of two molybdenum centers with one terminal and one inner alkoxido function in a bridging mode. A dimolybdate complex with only triply deprotonated erythritol has been crystallized from more acidic solutions. The structure largely resembles the one in **14**, but the remaining proton at the bridging terminal hydroxyl function causes markedly increased Mo–O distances of 2.50 and 2.53 Å (in **14**: 2.27 and 2.29 Å [24]). NMR experiments reveal that the dimolybdate structure is retained in solution. All carbon atoms show a more or less strong downfield shift ($\Delta\delta$ between 6.6 and 18.5 ppm) [25,26]. Similar shifts are obtained for a ditungstate complex ($\Delta\delta$ between 6.1 and 18.1 ppm) whose asymmetry could be additionally characterized by the existence of two different ^{183}W signals [27]. The sickle conformation is also adopted by doubly and triply deprotonated erythritol in a Fe_{14} oxocluster which is stabilized by calcium(II) ions (torsion angles: 49.0°, 47.2° (C_4 chain), 44.2°, 48.7° (*erythro*-diol)) [28].

2.2 Threitol

Threitol **2** is a tetraol with a central *threo*-configured diol group. While erythritol has to adopt a sickle conformation in order to locate all its oxygen atoms on the same side of the C_4 chain, threitol attains this in its zigzag conformation.

In **15** and **16** (❯ *Fig. 3*), the zigzag conformation of L-threitol comes along with an approximately parallel alignment of the planes of carbon and oxygen atoms, respectively. The torsion angle of the C_4 chain is about 170° and the oxygen atoms occupy the corners of a rhomb.

Fourfoldly deprotonated L-threitol acts as a bis-1,3-diolato ligand in the V-shaped bis(phenylboronic acid ester) **15** (❯ *Fig. 3*), while the *erythro*-configured erythritol leads to the planar ester **13** (❯ *Fig. 2*). The significant CIS of the carbon atoms in **13** was also detected in solutions of **15** (2.1 ppm (terminal C), −5.9 (inner C)), however, 1,2-diolato species could not


15   **16**
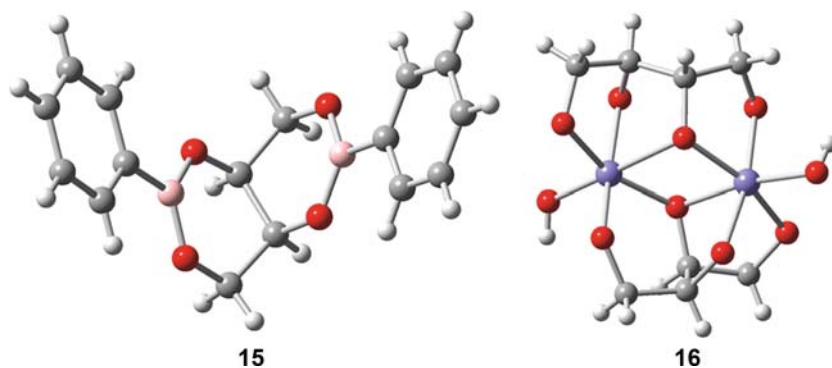
◼ **Figure 3**
The crystal structure of (PhB)$_2$(L-ThreH$_{-4}$-$O^{1,3}$,$O^{2,4}$) **15** and the molecular structure of [Fe$_2$(L-ThreH$_{-4}$)$_2$ (OH)$_2$]$^{4-}$ **16** in crystals of Ba$_2$**16** · 12.5 H$_2$O

be ascertained [23]. A structure of the type of **15** was also obtained with the bis(3,4-dibromomethyl) derivative of phenylboronic acid [29]. Five-membered chelate rings are described in the homoleptic borate ester **17** with doubly deprotonated D- and L-threitol in which the deprotonation occurs at the chelating central *threo*-configured diol group. Depending on the involved enantiomeric pairs of threitol (**17** presents the (*R,R*)-(*R,R*) form), three different complexes are formed. The CIS of the *threo*-C atoms are reported with 3.3 and 3.4 ppm, the terminal C atoms show a smaller CIS of 0.8 and 1.5 ppm [30].

In the sandwich-type complex anions **16** (❷ *Fig. 3*), eight out of ten oxygen atoms for the formation of an edge-sharing $(FeO_5)_2$-dioctahedron are provided from two fourfoldly deprotonated L-threitol ligands which show manifold complexing abilities. One of the *threo*-configured oxygen atoms of the two ligands is in the μ_2 mode, the others bind to one iron(III) center only. Both of the threitolato ligands act in the *fac*-1,2,3-triolato mode; additionally one acts as a 1,2-diolato and one as a 1,3-diolato ligand. The O–O distances in the chelate rings vary between 2.65 Å (five-membered ring) and 2.95 Å (six-membered ring). The O–C–C–O torsion angles are between 35° and 50° [31].

A more bent zigzag chain with a C_4 torsion angle of about 104° is present in the dinuclear C_2-symmetric rhenium(I) complex anion **18** (❷ *Fig. 4*). The terminal oxygen atoms of triply deprotonated L-threitol are in a bridging mode whereas the terminal oxygen atoms bind to one center only. A very short intermolecular distance between the latter non-bridging oxygen atoms of just 2.36 Å indicates a strong hydrogen bond between them and thus only triply deprotonated L-threitol is present. The torsion angle of the central *threo*-configured diolato group is 133.4°, the terminal diolato groups form torsion angles of about 56°. This complex has also been found in aqueous solution as well as in acetonitrile at a Re:L-Thre ratio of 2. The latter solution contains a minor trinuclear species which becomes the main species upon the addition of methanol and a Re:L-Thre ratio of 3. Deduced from a trinuclear complex with triply deprotonated glycerol, triply deprotonated L-threitol is expected to be in a μ_3 mode [32].


18   **19**
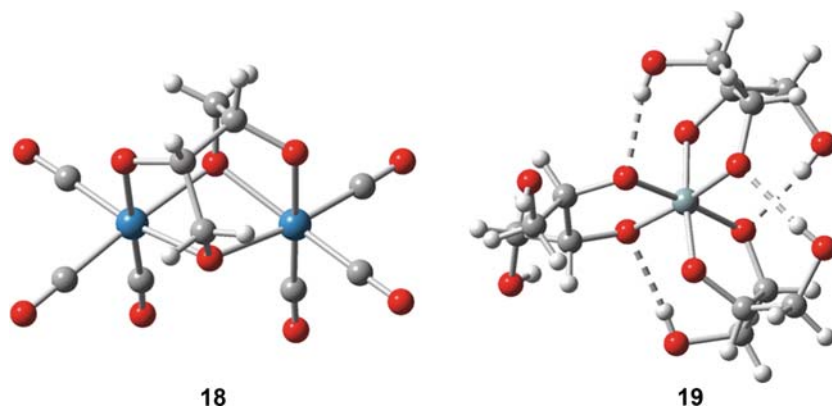
◨ **Figure 4**
The molecular structures of $[Re_2(CO)_6(L\text{-}ThreH_{-3})]^-$ **18** in crystals of NEt_4**18** · MeCN and $[\Lambda\text{-}Si(L\text{-}Thre2,3H_{-2})_3]^{2-}$ **19** in crystals of Rb_2**19** · 3 H_2O. *Dashed lines*: hydrogen bonds

With rubidium as the counterion, a mononuclear, approximately C_2-symmetric homoleptic silicate complex anion **19** (❯ *Fig. 4*) is formed by three L-threitolato ligands which are deprotonated at their central *threo*-configured chelating hydroxyl functions. The three polyols adopt two different conformations. Two ligands use their non-deprotonated hydroxyl functions to act as donors in intramolecular hydrogen bonds with deprotonated hydroxyl functions as acceptors. The acceptor functions of the two remaining deprotonated hydroxyl groups are used in hydrogen bonds to two water molecules. The third threitolato ligand adopts a conformation with a torsion angle of the C_4 chain of 95.1° which is significantly smaller than those observed for the other two ligands (144.6° and 136.2°, respectively). With cesium as counterion, a D_3-symmetric threitolato silicate anion $[\Lambda\text{-Si(D-Thre2,3H}_{-2})_3]^{2-}$ is obtained with all terminal hydroxyl groups being involved in intramolecular hydrogen bonds of the type in **19**. The torsion angles of the chelating *threo*-configured diolato group is in the range of 17–24° causing a bite of about 2.5 Å [33].

17   **20**   **21**

M = Mo,W
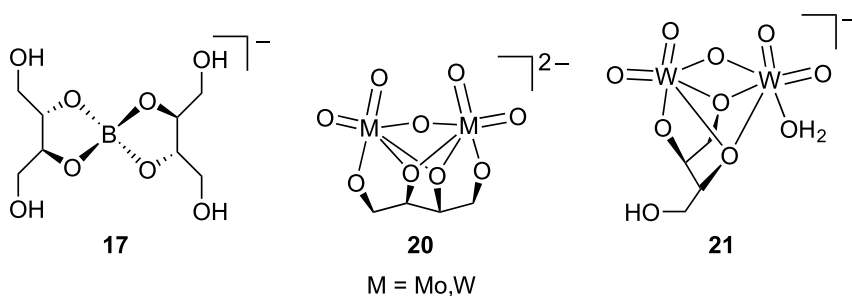
D- and L-threitol have been shown to form the C_2-symmetric dimolybdate **20** in which each molybdenum is facially coordinated by a 1,2,3-triolato group. The CIS of the *threo*-configured carbon atoms is reported with 9.8 ppm, the terminal carbon atoms have a CIS of 12.2 ppm [25,27]. This type of complexation is confirmed in a crystal structure with L-dithiothreitol as ligand [34]. The type of ditungstate complex formed with D- and L-threitol proves to be pH-dependent. At pH 7, the C_2-symmetric ditungstate **20** is formed (CIS *threo*-C: 9.2 ppm, terminal C: 10.5 ppm), while at pH 8–9 the asymmetric ditungstate **21** dominates. One terminal hydroxyl function is not involved in the complexation (CIS 1.8 ppm) while the other one now is in a bridging mode (CIS 9.5 ppm) together with one of the *threo*-configured hydroxyls (CIS 9.4 ppm). The second *threo*-configured hydroxyl is bound to one tungsten solely (CIS 13.1 ppm) [27,35].

22   **23**   **24**
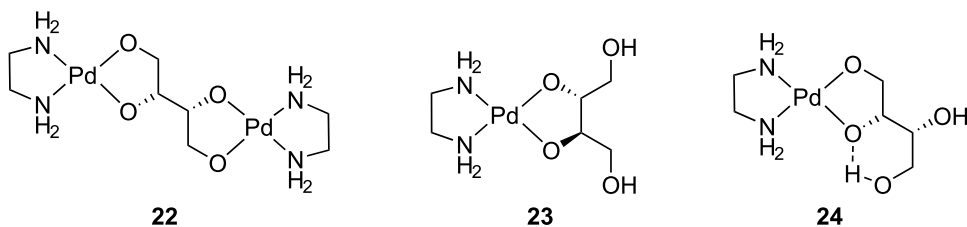
[Pd(en)(OH)$_2$] forms the solution species **22**–**24** with D-threitol with the species distribution strongly depending on the Pd:D-threitol molar ratio. In 1:1 solutions **23** is the main

species besides a minor fraction of **24**. Obviously the formation of chelate rings with a *threo*-configured diol group is more favored above an *erythro*-diol chelate formation such as in **12**, which was merely a minor species in the corresponding erythritol solutions. In 3:1 solutions the dimetallated complex **22** and the monometallated complex **23** coexist as main species [19]. Two monometallated products in the molar ratio of 3:2 are reported for the reaction of (dppp)Pt(CO_3) with four equivalents of *rac*-threitol. The major part corresponds to the (dppp)Pt-derivative of the *threo*-complex **23**, while in the minor part the terminal diol is coordinated similarly to **24** [22].

2.3 Xylitol

Xylitol **3** is a non-chiral, all-*threo*-configured pentitol which allows grouping of all its hydroxyl functions on the same side of the C_5 chain with a zigzag conformation. In the dinuclear cobalt(III) complex **25** (❯ *Fig. 5*) two entirely deprotonated zigzag conformers provide a proper O_{10} set of an edge-shared Co_2O_{10} dioctahedron, whereas in the similar diferrate(III) **16** (❯ *Fig. 3*) with the smaller all-*threo* configured L-threitol, two hydroxyls are required to complete the dioctahedron [36].

Fourfoldly deprotonated xylitol acts as a bis-1,2-diolato ligand in the dinuclear palladium(II) complex **26** (❯ *Fig. 5*). The remaining terminal hydroxyl function is employed in a short intramolecular δ hydrogen bond. The enhanced stability thereby makes **26** the dominating species in [Pd(en)$(OH)_2$]/xylitol solutions of the molar ratio 3:1 and even 2:1, whereas in the corresponding 3:1-solution with D-threitol the dimetallated species and the monometallated species **12** are formed in approximately equal amounts. The main species in equimolar solutions of [Pd(en)$(OH)_2$] and xylitol is the monometallated, *threo*-chelate complex [Pd(en)(Xylt2,3H$_{-2}$)] which is the hydroxymethyl homolog of the predominant [Pd(en)(Thre2,3H$_{-2}$)] complex. The isomeric complex with a terminal chelate formation, [Pd(en)(Xylt1,2H$_{-2}$)], is formed in small amounts only [19].

From solutions of (dppp)Pt(CO_3) and xylitol in a molar ratio of 1:4 two monometallated species are obtained. The formation of the 2,3-*threo* bound isomer (86%) is significantly preferred over the 1,2-terminal bound isomer (14%) [22].

25   **26**
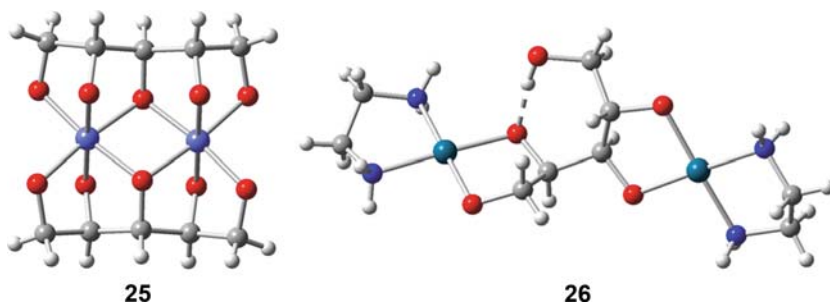
◧ **Figure 5**
The molecular structures of [Co$_2$(XyltH$_{-5}$)$_2$]$^{4-}$ **25** in crystals of Li$_5$**25** · 8 H$_2$O and [Pd$_2$(en)$_2$(Xylt1,2;3,4H$_{-4}$)] **26** in crystals of **26** · 4 H$_2$O. *Dashed line*: hydrogen bond

Three doubly deprotonated xylitol molecules act as 1,2-diolato ligands in the hexacoordinate silicate $[Si(Xylt2,3H_{-2})_3]^{2-}$ **27** (❯ *Fig. 6*) which is the hydroxymethyl derivative of the threitolato complex **19** (❯ *Fig. 4*) and, as a consequence, shows the same stabilizing intramolecular hydrogen bonds [33].
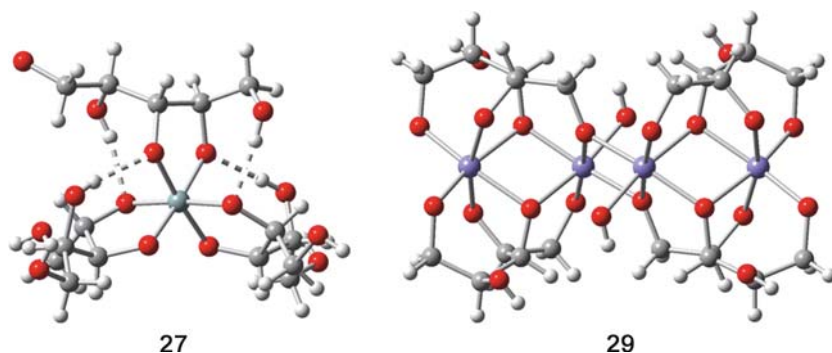
■ **Figure 6**
The molecular structures of $[Si(Xylt2,3H_{-2})_3]^{2-}$ **27** in crystals of Cs_2 **27** · 2 H_2O and $[Fe_4(rac$-Arab1,2, 3,5H$_{-4})_4(OH)_2]^{6-}$ **29** in crystals of Sr_4**29**(CO_3) · 33 H_2O. *Dashed lines*: hydrogen bonds

A hydroxymethyl derivative of the threitolato dimetallates **20** is also formed with the higher homolog xylitol, whereas the ditungstate proves to be stable at pH 7. At pH 8–9 xylitol acts as chelating ligand using its secondary hydroxyl functions similarly to **21**, while the primary hydroxyl functions are not employed for metal coordination.


28
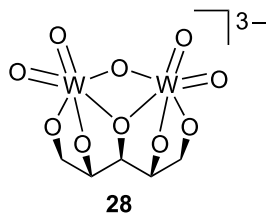
In the pH range of 9–12 the ditungstate **28** is formed with an entirely deprotonated xylitol exhibiting the same coordination pattern as in **25** (❯ *Fig. 5*): both metal centers are facially coordinated with the central alkoxido function in the μ_2 mode [25,26,27,35].

2.4 Arabitol

Arabitol **4** is a chiral pentitol bearing a *threo*- as well as an *erythro*-configured diol group. The centrosymmetric, tetranuclear ferrate(III) **29** (❯ *Fig. 6*) consisting of four edge-sharing FeO_6-octahedrons is formed by four fourfoldly deprotonated *rac*-arabitols in a conformation which enables coordination to the iron(III) centers with the terminal and the *threo*-configured oxygen atoms. The coordination sphere of the inner two iron centers is completed by a hydroxide lig-

and each—a structural feature adopted by the closely related threitolato complex **16** (❯ *Fig. 3*) as well [31].

A comparison of the structures **29** (❯ *Fig. 6*) and the palladium(II) complex **30** (❯ *Fig. 7*) clarifies the flexibility of arabitol to adopt a conformation which satisfies the structural requirements of the metal centers: in **29**, arabitol acts as a 1,3-diolato ligand and as a 1,2,4 triolato ligand with C3 in a μ_2 mode to achieve an octahedral coordination geometry, while D-arabitol acts as a bis-1,2-diolato ligand in **30**. The diolato moieties are *erythro*-linked, hence **30** could be considered a hydroxymethyl-Pd(en) derivative of **9** (❯ *Fig. 1*), with the hydroxyl forming a stabilizing intramolecular γ hydrogen bond. This species is also predominant in [Pd(en)(OH)$_2$]/D-arabitol solutions with excess [Pd(en)(OH)$_2$] and still is a minor species in equimolar solutions. Those contain the *threo*-complex [Pd(en)(D-Arab2,3H$_{-2}$)] as the only monometallated species [19].

30   31
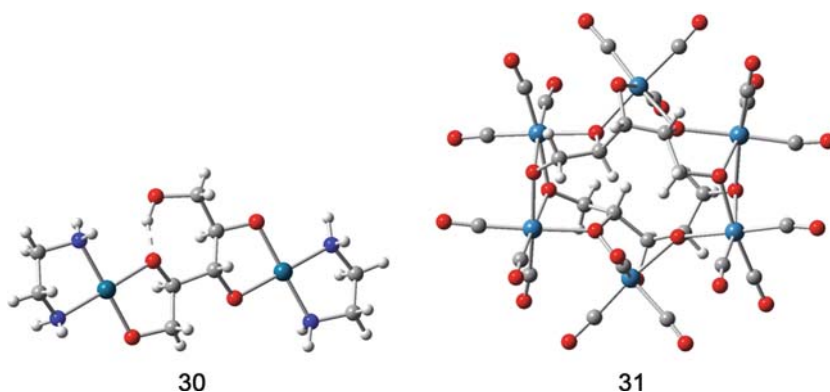
❐ **Figure 7**
The molecular structures of [Pd$_2$(en)$_2$(D-Arab1,2;3,4H$_{-4}$)] 30 in crystals of 30 · 7 H$_2$O and [Re$_6$(CO)$_{18}$(D-ArabH$_{-5}$)$_2$]$^{4-}$ 31 in crystals of (NEt$_4$)$_2$(DBUH)$_2$31. *Dashed line*: hydrogen bond

Two entirely deprotonated D-arabitol ligands are employed to connect the Re^I(CO)$_3$ centers in the hexanuclear cluster **31** (❯ *Fig. 7*). All but the central alkoxido function at C3 are in a bridging mode [32].

The dimolybdates and ditungstates found with arabitol are closely related to the complex anions **14** and **21**. Two dimolybdates are formed with D-arabitol ligands which adopt a sickle conformation with their *erythro*-configured end as in **14** (❯ *Fig. 2*), this is the C$_4$ chain from C2 to C5, in each case. The isomers differ in the coordination pattern: one isomer has C2 and C4 in the μ_2 mode, the other one C3 and C5 [25]. These isomers are the main species with tungsten(VI) as well, but a minor species is additionally formed in which the *threo* end of D-arabitol, this is C1 to C3, is used for complexation closely related to **21** [26,37].

2.5 Ribitol (Adonitol)

Ribitol **5** is a completely *erythro*-configured pentitol. No crystal structure analyses of a ribitol complex have been reported so far. However, solution studies have been performed with palladium(II) and with molybdenum(VI) and tungsten(VI).

Studies with palladium(II) revealed that in [Pd(en)(OH)$_2$]/ribitol solutions with a molar ratio of 3:1 or 2:1 the dimetallated complex [Pd$_2$(en)$_2$(Ribt1,2;3,4H$_{-4}$)] is formed as main species. The remaining terminal hydroxyl function is employed in an intramolecular δ hydrogen bond to O2 causing the enhanced stability compared to the minor, bis(terminal) species [Pd$_2$(en)$_2$(Ribt1,2;4,5H$_{-4}$)]. The monometallated terminal complex [Pd(en)(Ribt1,2H$_{-2}$)] is the main species in equimolar solutions. The detection of the isomeric complex [Pd(en) (Ribt2,3H$_{-2}$)] as a minor species gives reason to state that terminal chelation in *erythro* poly-ols is more favorable than a chelation with two adjacent secondary hydroxyl functions [19]. This is confirmed by the observation that (dppp)Pt^{2+} forms the terminal 1,2-diolato complex with ribitol with marked excess compared to the 2,3-*erythro* bound isomer (molar ratio 83:17, respectively) [22].

Molybdenum(VI) and tungsten(VI) are found to form only one of two possible isomeric *ery-thro*-type dimetallates analogously to **14** (❷ *Fig. 2*) with fourfoldly deprotonated ribitol. One of the terminal hydroxyl functions is not part of the coordination site. Even the formed isomer proves to have low stability due to unfavorable steric interaction between the terminal carbon atoms of the sickle conformer [25,26,37].

2.6 Mannitol

D-Mannitol **6** is a chiral hexitol having two terminal *erythro*-configured diol groups and a *threo* link between them.

Aqueous solutions containing [Pd(en)(OH)$_2$] and D-mannitol in a molar ratio of 3:1 or 2:1 yield the dinuclear complex **32** (❷ *Fig. 8*) as main species. The structure corroborates earli-er described preferences of Pd(en) in sugar alcohol complexes: the complexation occurs at two *erythro*-linked diol groups, one of which is *threo*-configured, the other one a terminal diol function. A δ hydrogen bond of the type O–H···O$^-$ similar to those in **26** (❷ *Fig. 5*) and **30** (❷ *Fig. 7*) stabilizes the complex, while the remaining terminal hydroxyl function is not involved in intramolecular hydrogen bonding. In 3:1 solutions this hydrogen bond is cleaved to an observable extent as the minor, trimetallated species [Pd$_3$(en)$_3$(D-Mann1,2;3,4;5,6H$_{-6}$)] is formed. Besides **32** (❷ *Fig. 8*), two mononuclear, *threo*-coordinated complexes are observed in equimolar solutions: [Pd(en)(D-Mann1,2H$_{-2}$)] and [Pd(en)(D-Mann3,4H$_{-2}$)]; *erythro* coordi-nation is not detected [19].

A more complex intramolecular hydrogen bond system is built in the platinum(II) complex **33** (❷ *Fig. 8*) in which the central *threo*-configured diol is the chelation site. A γ and a δ hydrogen bond, each starting at one of the terminal donor hydroxyl functions, end at one and the same alkoxido function. The other one is an acceptor in a more strained β hydrogen bond [22].

Affirmed by DFT calculations, the completion of an octahedral coordination sphere of trimethyl-platinum(II) in a dinuclear complex is accomplished with facial tridentately bonded D-mannitol (coordination mode: μ-κ^3O^1,O^2,O^4:κ^3O^3,O^5,O^6) [38].

In **34** (❷ *Fig. 9*), the silicon center is hexacoordinated through three central, *threo*-configured diol groups. The adjacent hydroxyl functions at C2 and C5 form stabilizing intramolecular hydrogen bonds similar to **19** (❷ *Fig. 4*) and **27** (❷ *Fig. 6*) [33].

Bonding through terminal- and *threo*-configured diol groups, which are *erythro*-linked, is observed in the tris(phenylboronic acid) ester **35** (❷ *Fig. 9*) while six-membered chelate rings
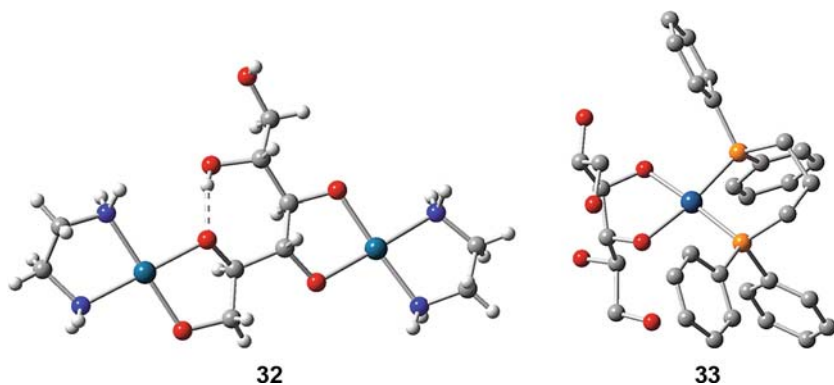
□ Figure 8
The molecular structures of $[Pd_2(en)_2(D-Mann1,2;3,4H_{-4})]$ **32** in crystals of **32** · 5 H_2O and (dppp)Pt(D-Mann3,4H$_{-2}$) **33** in crystals of **33** · CH_2Cl_2. *Dashed line*: hydrogen bond
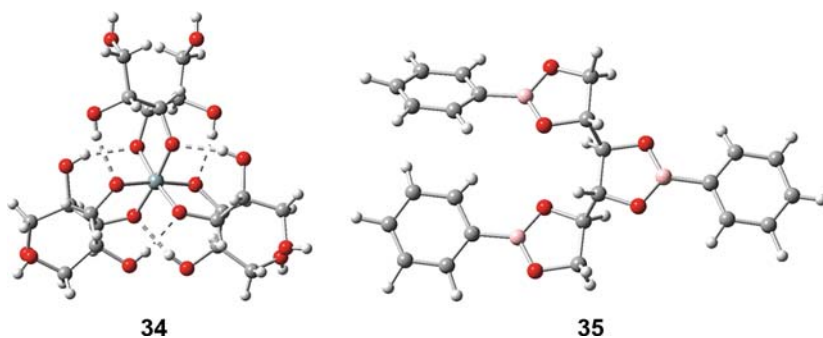
□ Figure 9
The molecular structure of $[\Lambda\text{-Si}(D\text{-Mann3,4H}_{-2})_3H_{-1}]^{3-}$ **34** in crystals of Na_334 · 12 H_2O and the crystal structure of $(C_6H_5B)_3(D\text{-MannH}_{-6})$ **35**. *Dashed lines*: hydrogen bonds

were formed with erythritol and L-threitol in **13** (❷ *Fig. 2*) and **15** (❷ *Fig. 3*), respectively [39]. Van Bekkum et al. suggest the formation of boron-mannitol monoester through bonding via the *erythro*-configured O2,O3 diol as well as via the *threo*-configured O3,O4 diol. The latter configuration is existent solely in the diester [30,40].

Two crystal structures of dimolybdates with different cations have been described. Both are of the type of **36** (❷ *Fig. 10*) and could be considered a dihydroxyethyl derivative of the erythritol complex **14** (❷ *Fig. 2*), whereas D-mannitol is only triply deprotonated in **36** similarly to an erythritol complex described above [24,41,42]. The structure of **36** (❷ *Fig. 10*) is retained in solution in two isomeric forms for molybdenum as well as for tungsten in a way similar to D-arabitol whose configuration matches the one of the coordination site of D-mannitol [25,26,37,43].
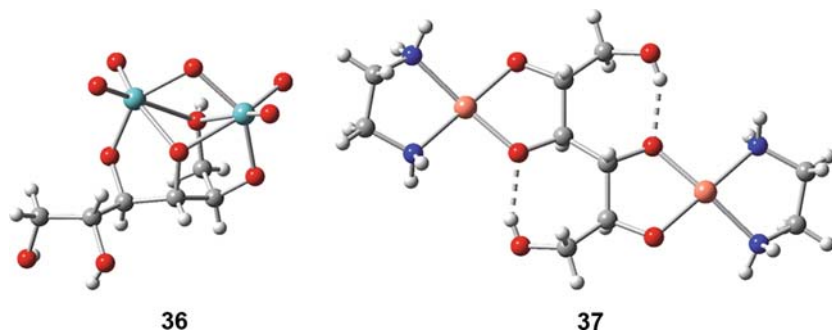
36   **37**

☐ **Figure 10**
The molecular structures of $[Mo_2O_5(\text{D-Mann}2,3,4H_{-3})]$ **36** in crystals of $Na36 \cdot 2\,H_2O$ and $[(en)_2Cu_2(Dulc2,3;4,5H_{-4})]$ **37** in crystals of $37 \cdot 7\,H_2O$

2.7 Dulcitol (Galactitol)

Dulcitol **7** is a non-chiral hexitol with two *threo*-configured diols linked by a central *erythro*-configured diol group. To emphasize the analogies in the coordination patterns, dulcitol may be regarded as a 1,4-di(hydroxymethyl) derivative of erythritol **1**. Ethylenediamine-copper(II), for example, is found to form the dinuclear complex **37** (❷ *Fig. 10*) which contains an erythritol substructure described above. The terminal hydroxymethyl groups form intramolecular δ hydrogen bonds resulting in an enhanced rigidity of the now *S*-shaped dulcitol [44]. This structural motif is found in several dulcitolato complexes of copper(II), nickel(II), and palladium(II). The strength of the established hydrogen bonds and thus the distances between the corresponding donor–acceptor pairs are basically a consequence of the Lewis acidity of the bonded metal-ligand fragment. In **37** the O–O distance is 2.53 Å while with the less Lewis-acidic $(tren)Ni^{2+}$ and $(Me_3tren)Ni^{2+}$ residues this distance is shortened to about 2.45 Å and 2.42 Å respectively [44]. In the copper-dulcitol compounds **37** (❷ *Fig. 10*) as well as in the linear coordination polymer comprising the substructure **10** (❷ *Fig. 1*) the donor–acceptor distances are about 2.62 Å [21].

Just a few species have been detected in solutions with ethylenediamine-palladium(II) at various Pd:dulcitol ratios. The only monometallated complex in equimolar solutions is $[Pd(en)(Dulc2,3H_{-2})]$ with Pd bound by a *threo*-configured diol moiety. Besides, a minor part is bonded in the dimetallated species $[Pd_2(en)_2(Dulc2,3;4,5H_{-4})]$, which is the main species in 2:1 and 3:1 solutions and whose solid-state structure resembles **37** (O–O distance 2.68 Å ❷ *Fig. 10*). A similar structure was obtained with ethylenediamine replaced by methylamine and isopropylidene-methyl-imine (O–O distance 2.54 Å. The fact that entirely deprotonated ducitol is obtained neither with $Cu(en)^{2+}$ nor with $Pd(en)^{2+}$ in solutions even with a metal:dulcitol ratio of 3 or higher, indicates the extraordinary stability of the *S*-conformation fixed by two intramolecular hydrogen bonds. The latter bonds are cleaved with the supporting ligand 1,3-bis(2′-dimethylaminoethyl)hexahydropyrimidine (tm-21:32-tet) which provides a suitable N_4 set to bind two palladium(II) centers which, in turn, could be bonded by a 1,2,3-bis-diolato moiety with the middle alkoxo function in a μ_2 mode. As a result a tetranuclear complex **38** (❷ *Fig. 11*) with entirely deprotonated dulcitol is obtained [19].

38 **39**
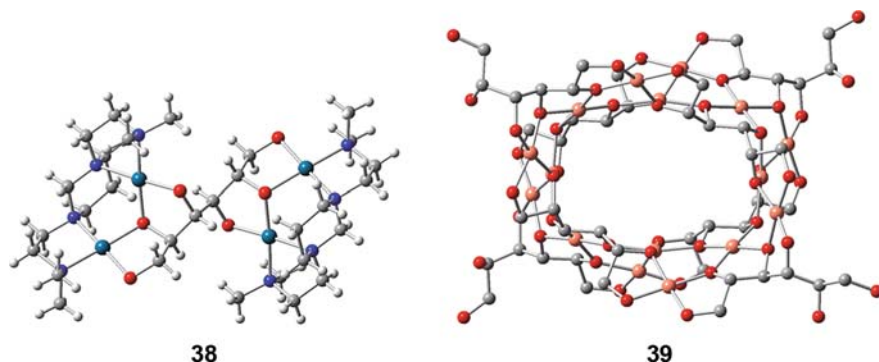
⬛ **Figure 11**
The molecular structures of $[Pd_4(tm-2,1:3,2-tet)_2(DulcH_{-6})]^{2+}$ **38** in crystals of $38Cl_2 \cdot 16\ H_2O$ and $[Cu_{16}(D-SorbH_{-6})_4(D-Sorb1,2,3,4H_{-4})_4]^{8-}$ **39** in crystals of $Li_839 \cdot 46\ H_2O$

Coordination via the *threo*-configured diol at O2 and O3 is also favored by $(dppp)Pt^{2+}$. Species using the central *erythro*-diol or one of the terminal non-stereogenic diols have been detected in small amounts only [22].

Molybdenum and tungsten also use the central tetraol set of dulcitol, however, in a sickle conformation, to form dimolybdates respectively ditungstates with a coordination pattern similar to that found in the erythritol complex **14** (❂ *Fig. 2*) [25,26,27,43].

2.8 Sorbitol (Glucitol)

D-Sorbitol **8** is a hexitol with its diol functions from C2 to C5 configured with the sequence *threo*, *threo*, *erythro*. The resulting C_1 symmetry is possibly the reason for the rather small number of characterized complexes since the crystallization as well as the NMR spectroscopic characterization is hampered by the usually obtained mixture of species.

To the best of our knowledge, published crystal structure data are available merely for a toroidal, hexadecanuclear copper(II) complex **39** (❂ *Fig. 11*) with eight multiply deprotonated D-sorbitol ligands. Half of them are completely deprotonated η^6,μ_5 hexaanions, the other half acts as μ_3 tetraanions with their *xylo*-configured C1–C4 subset. It was found that the magnetic coupling behavior is determined by the distribution of Cu–O–Cu angles and correlates with the ligand configurations of the chelating 1,2-diol entities [45].

Molybdenum is found to form four different dimolybdate(VI) complexes, all having proportions in the range of 21 to 32%. These are: two complexes with a central *threo*-configured diol of the type **20** with one of them using the C1–C4 subset, the other one using the C2–C5 subset, and two *erythro*-complexes of the type **14** (❂ *Fig. 2*) with the C3–C6 subset in two reversed orientations [25,26].

Coordination to the *xylo*-configured site C2–C4 similar to **21** is mainly observed for tungsten. Two minor species are the *erythro*-complexes employing the C3–C6 subset as molybdenum [27,37].

Boronic acid is reported to form esters with D-sorbitol in alkaline solution. Van Bekkum et al. suggest the formation of a monoester involving the *erythro*-configured diol while a mono- and a diester may be formed over a *threo*-configured site [40]. Tridentate D-sorbitol is found to occupy three of four coordination sites of the boron center in a ferrocene derivative with its hydroxyl functions at C2, C3, and C5 [46].

2.9 L-Iditol and Higher Sugar Alcohols

Further NMR studies were performed of molybdate(VI) and tungstate(VI) complexes with the hexitols **40** and **41**, the heptitols **42–46**, and the octitols **47** and **48**.
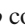

40   41   42   43   44   45   46   47   48
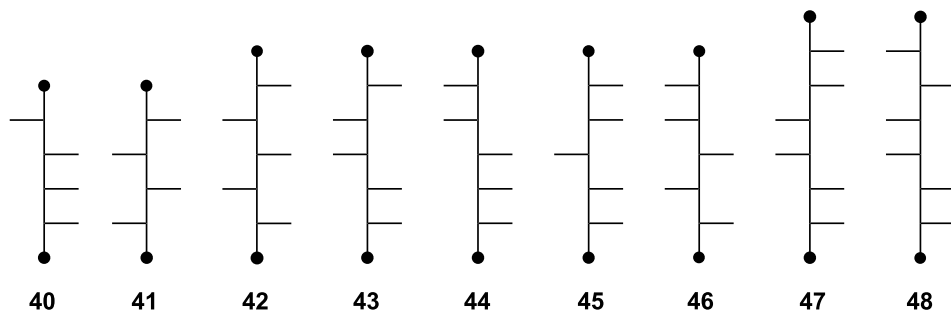
Carbon numbering: C1 is situated at the top of each chain.   ● = CH$_2$OH

An *erythro* complex similar to **14** (❯ *Fig. 2*) is established with the C2–C5 coordination site of D-altritol **40** [26]. L-Iditol **41** forms a C_2-symmetric dimolybdate(VI) complex in the pH range 5–10 using the all-*threo*-configured C2–C5 chelation site resulting in a structure similar to the threitol-complex **20**. A structure of the same type emerges with *meso*-glycero-ido-heptitol **42** with the all-*threo*-configured chelation site C2–C5. The corresponding ditungstate(VI) complexes are formed only at neutral pH ≤ 7. In the pH range 8–9, the hexitol **41** acts as a tridentate ligand with the chelation site C2–C4 to give a ditungstate(VI) of the type **21**, while the heptitol **42** acts as a pentadentate ligand in two isomers with a structure similar to **28**: the more stable isomer uses the C2–C6 chelation site, the other one uses the site C1–C5. In the pH range 9–12, the hexitol **40** also forms a complex similar to **28** [35].

D-glycero-D-galacto-heptitol **43** (perseitol) was first found to form a pair of isomers using the C2–C5 galacto site of chelation in dimolydate- and ditungstate complexes having a structure similar to **14** (❯ *Fig. 2*) [26,43]. A mixed bis-ditungstate complex was detected later. In this complex, one ditungstate is bound at the *erythro*-chelation site C4–C7, while the other ditungstate is coordinated through the *threo*-site C1–C3. The local structures at the two different sites resemble the structure types **14** (❯ *Fig. 2*) and **21**, respectively [37]. Bis-dimolybdate complexes have been observed with the octitols *meso*-erythro-*manno*-octitol **47** and D-erythro-L-gluco-octitol **48**, both comprising a C3–C8 perseitol **43** subset. In **47**, each of the two *eythro* chelation sites C1–C4 and C5–C8 is bound to a dimolybdate (for local structures compare with **14**, Fig 2). In contrast **48** binds one dimolydate in a *threo* complex at the chelation site C1–C4, the other is bound at the *erythro* chelation site C5–C8 (local structures **20** and **14**,

respectively). A less stable species with both ligands **47** and **48** uses the central *galacto* site C3–C6 to give *erythro* complexes (local structure compare with **14**, ❯ *Fig. 2*) [47].

D-Glycero-D-*manno*-heptitol **44** (volemitol) forms identical dimolydate and ditungstate complexes. The main species comprises the *arabino* chelation site C1–C4 with the local structure **14** (❯ *Fig. 2*) in two isomers. The same local structure is established in the other species which uses the C3–C6 chelation site. The reduced stability of the latter species is caused by the unfavorable steric interaction of the chelation site and the side chain [48].

Ditungstate complexes with the local structures **21** and **28** are observed with the ligands *meso*-glycero-gulo-heptitol **45** and D-glycero-L-gulo-heptitol **46**. The main species with tridentate **45** involves the central *xylo*-configured chelation site at C3–C5 resulting in a local structure **21** (at pH 9.9). A less stable complex is formed with the coordination site C2–C6 of pentadentate **45** (local structure **28**). Two isomers with the latter local structure **28** are obtained with **46** at pH 11.7. One uses the C3–C7 chelation site, the other binds ditungstate at the C2–C6 site. Local structure **21** is formed at pH 10.6, where **46** acts as tridentate ligand using its C4–C6 coordination site [49].

2.10 Regioselectivity and Stability

Though sugar alcohols provide various metal-binding sites, their complexation behavior is not as unpredictable as one might expect. Rules determining the chelation sites in ethylene-diamine-palladium(II) complexes with discrete chelate rings, that is with neither chelating alkoxo function being in a bridging mode, seem to count for other metal complexes of these type as well [19]:

1 The stability of chelate rings formed by *threo*-configured, *erythro*-configured and terminal diols increases in the sequence: *erythro* < terminal < *threo*.
2 The *erythro*-linked adjacent chelating diol functions are more stable than *threo*-linked ones.
3 An additional stability gain emerges upon intramolecular hydrogen bonding between donor hydroxy and an acceptor alkoxido moiety. The most stable type of hydrogen bond is the δ type, that is, a C_4-chain separates the hydrogen bond donor from the acceptor.

The prediction of chelation sites of sugar alcohols in multinuclear metal complexes with alkoxido functions in a bridging mode is rather difficult due to the influence of further factors such as the metal size and oxidation state or the distance of the O atoms of the ligand. However, based on a wealth of NMR solution data and supported by some crystal structures, rules regarding the regioselectivity and stability of the well-investigated dimolydate- and ditungstate-complexes of sugar alcohols could be established [25,27,35,37,43,48,49,50].

3 Aldonic and Aldaric Acids

The oxidation of the primary hydroxyl function at C1 of a sugar alcohol to a carboxyl function leads to the corresponding aldonic acid. Further oxidation of the remaining terminal hydroxyl function of an aldonic acid to a carboxyl function leads to an aldaric acid. Both, aldonic and aldaric acids easily form lactones through intramolecular condensation reactions. As an exam-

ple, the formation of D-gluconic acid γ-lactone **50** (also known as D-glucono-1,4-lactone) starting from D-gluconic acid **49** is depicted in ❯ *Scheme 1*.

49   **50**
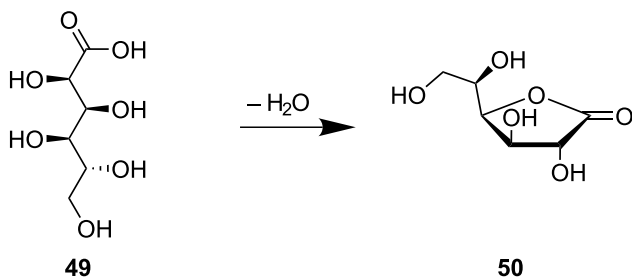
◻ **Scheme 1**

3.1 Aldonic Acids

In most of the D-gluconic acid **49** complexes known from the literature, the metal centers are bonded through the α-hydroxycarboxylate moiety and five-membered chelate rings are formed. While the carboxyl function is always deprotonated in these structures, it depends on the Lewis acidity of the metal or the pH of the solution, whether the α-hydroxyl residue is deprotonated or not. No deprotonation of the latter occurs in the solid-state structures of lead(II)- and manganese(II) D-gluconate (**58** and **59**, respectively, ❯ *Fig. 12*). Furthermore D-gluconic acid binds to both metal centers by a single carboxylate oxygen atom and to the manganese central atom in **59** (❯ *Fig. 12*) by the terminal alcoholic hydroxyl function which leads to a coordination polymer [51,52]. $Co^{III}(en)_2$ is also chelated by the α-hydroxycarboxylato moieties of D-gluconic acid and L-mannonic acid, respectively [53]. Magnesium(II) is reported to be coordinated by the α-hydroxycarboxylato moiety and the adjacent hydroxyl function at C3 [54].

49   **51**   **52**   **53**   **54**   **55**   **56**   **57**
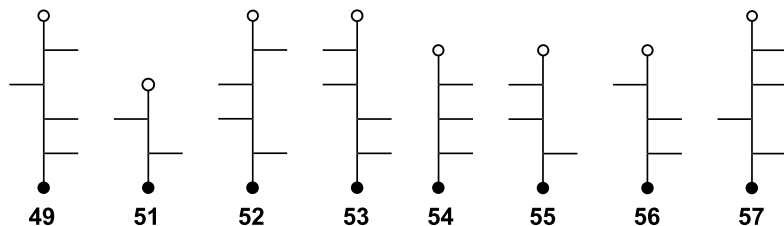
Carbon numbering: C1 is situated at the top of each chain.   ● = CH_2OH

○ = COOH

A stronger Lewis acid such as Me_2Sn^{2+} forces deprotonation of the α-hydroxyl function even at pH 5.5 (**60**). This coordination mode is also suggested for a copper(II)-D-gluconic acid complex [55]. In more alkaline solution (pH 8), the hydroxyl function at C4 is also deprotonated and Me_2Sn^{2+} is coordinated by the α-alkoxidocarboxylato moiety and O4 of tridentate
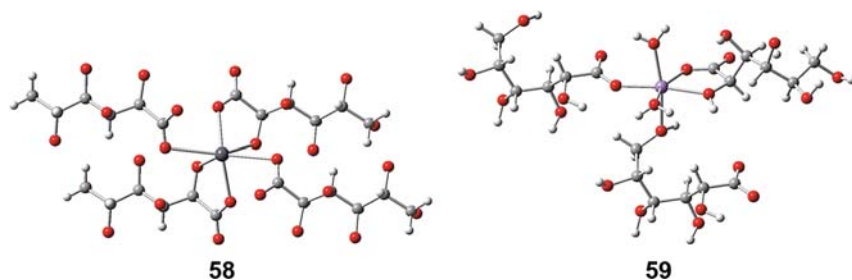
◘ **Figure 12**
Coordination of the central metals in the crystal structures of Pb(D-Glc1A1H$_{-1}$)$_2$ 58 and Mn(D-Glc1A1H$_{-1}$)$_2$ · 2 H$_2$O 59

D-gluconate [56]. This coordination mode is also observed in a praseodymium(III) complex in the pH range of 8–10 and an equimolar ratio of metal and ligand. At pH 6–7 and a molar ratio of ligand:metal greater than 2:1, complete deprotonation of all the hydroxyl functions at C1, C2, and C4 is not achieved. Now the praseodymium(III) center is coordinated by two tridentate D-gluconate ligands with three of four coordinating alcoholic hydroxyl functions not being deprotonated [57]. A similar coordination pattern is reported for the trimethyl-platinum(IV) complex **61** which was obtained from aqueous solution. Just the carboxyl function is deprotonated while the coordinating hydroxyl groups at C2 and C4 remain non-deprotonated. A D-threonic acid **51** derivative has been shown to bind to an octahedrally coordinated platinum(IV) center through its α-hydroxycarboxylate moiety [58]. The metals manganese, cobalt, nickel, copper, cadmium, mercury, lead, and zinc in the oxidation state +II are also reported to be coordinated by the O1,2,4 set of D-gluconic acid [59].

60
R = (CH(OH))$_3$CH$_2$OH
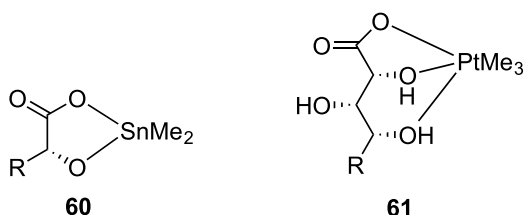
61
R = CH(OH)CH$_2$OH

In the pH range of 5–10, the trivalent metals aluminum, gallium, and indium are coordinated by the deprotonated hydroxyl function of C1–C4 of tetradentate D-gluconic acid [60]. Coordination with involvement of the carboxylate moiety is also reported for bismuth(III) in acidic solution. In alkaline solution, however, D-gluconic acid acts as a tetradentate ligand using its deprotonated secondary hydroxyl functions only [61]. Recently the crystal structure of [Cu$_4$\{μ-(α-D-Glc-1P)\}$_2$(μ-Glc1A1H$_{-1}$)$_2$(bpy)$_4$](NO$_3$)$_2$ has been reported in which the α-hydroxycarboylato moiety of gluconic acid is coordinated to one copper ion resulting in a five-membered chelate ring similar to **58** and **59** (❯ *Fig. 12*). Additionally the carboxylato oxygen atom links two copper ions. A linear coordination polymer complex is obtained with D-glucarate [62].

While structural information on complexes of molybdenum(VI) and tungsten(VI) with sugar alcohols is available for solid-state as well as for solution species, crystal structures have not been determined so far for the corresponding complexes with aldonic and aldaric acids (compare ❷ *Sect. 3.2*), that is, the following structural description is based solely on NMR spectroscopic data.

At pH 5–7 and with an excess of ligand, tungsten(VI) is coordinated by the α-alkoxidocarboxylato moiety of **49** similarly to **60**. However, a dinuclear species chelated by the alcoholic hydroxyl set of C3–C6 is observed when there is an excess of tungsten. Since the central diol at C4 and C5 is *erythro*-configured, the local structure might be similar to **14** (❷ *Fig. 2*). Additionally, coordination through the alcoholic hydroxyl functions at C2, C3, C5, and C6 is reported [63].

The α-alkoxidocarboxylato moiety of **49** is the chelation site in peroxido-complexes of molybdenum and tungsten as well. Similar structures are obtained with D-galactonic acid and L-mannonic acid [64].

Molybdenum and tungsten are coordinated by the α-alkoxidocarboxylato moiety of **52** in solutions with a molar ratio of ligand:metal of 2:1 in a pH range of 3–9. The stability of these chelates decreases with increasing pH. At a molar ratio of ligand:metal of 1:2 and with maximal stability at about pH 7.5, dinuclear complexes structurally similar to those formed by galactitol become the main species. The metal coordination is now established by the secondary alkoxido functions with a local structure similar to **14** (❷ *Fig. 2*). Additional species are found for molybdenum(VI) in weakly acidic solutions with a molar ratio of molybdenum:ligand of 2:1. Entirely deprotonated, hexadentate D-galactonic acid is bonded to two molybdenum centers through the alkoxido functions of the C1–C3 subset and the C4–C6 subset, respectively. Two molybdenum atoms may be bonded by fivefold deprotonated D-galactonic acid which acts as a pentadentate ligand through its secondary alkoxido functions in a sickle conformation and the carboxylate function [65].

L-Mannonic acid (L-enantiomer of **53**) is found to form similar complexes with molybdenum(VI) described above for D-galactonic acid, but additional species are found for tungsten(VI). An excess of ligand preferentially leads to the formation of mononuclear complexes with the α-alkoxidocarboxylato moiety of **53** as the chelation site, especially in the pH range of 3–6, while di- and tetranuclear species are enriched in solutions with an excess of metal. Three dinuclear species structurally analogous to those formed with D-mannitol are observed in neutral and weakly alkaline solutions. Coordination of the alkoxido functions in the positions 3 to 6 in a sickle conformation leads to a dimetallate complex with a local structure similar to **14** (❷ *Fig. 2*), while a zigzag conformation of the C2–C5 subset results in a structure similar to **20**. With L-mannonic acid these complexes are also detected with tungsten(VI). Finally a complex using the C1–C4 subset in a sickle conformation is observed mainly with molybdenum in solutions of a pH in a range of 3–7 [66].

Several structures of borate esters of aldonic acids have been described based solely on NMR spectroscopic data. Borate mono- and diesters are preferentially formed at the *threo*-configured diol sites of D-gluconic acid. Less stable esters are formed by bonding at the *erythro*-configured diol at C4 and C5. Still less stable are six-membered borolane rings as a result of bonding via O2 and O4. The 3,4- and 5,6-positions are occupied by borate anions resulting in a diborate ester. D-mannonic acid forms borate monoesters and two diastereomeric diesters preferentially through the *threo*-configured diol at position 3 and 4, while the *erythro*-configured diol at C4

and C5 leads to less stable esters. Additionally the formation of a diborate ester is also reported. The two borate moieties are bonded at the *threo*-configured 3,4-position and at the terminal diol in 5,6-position. Borate monoester- and diester formation has also been investigated with D-ribonic acid **54**, D-lyxonic acid **55**, D-arabinonic acid **56**, D-gulonic acid **57**. Four borate esters of ribonic acid have been found but further interpretation was prevented due to the large number of ^{13}C NMR signals. The *threo*-3,4-diol site is preferred in borate esters of lyxonic acid and gulonic acid, whereas the *threo*-2,3-position proves to be the most stable one in borate esters of arabinonic acid [40,67].

3.2 Aldaric Acids

Reactions in approximately neutral aqueous solutions lead to three solid-state structures of complexes of D-glucaric acid **62** (also known as D-saccharic acid) with the central metals aluminum(III), zinc(II), and copper(II), all exhibiting similar structure features: (a) both α-hydroxycarboxylate moieties of D-glucaric acid act as chelation sites, (b) deprotonation occurs at the carboxylate group and, in the case of bonding to the stronger Lewis acid aluminum(III), additionally at both α-hydroxy functions, and (c) the central hydroxyl functions in 3,4-position are never involved in metal coordination. A dinuclear complex **69** (❯ *Fig. 13*) is formed with aluminum(III) with one of the two α-alkoxido functions in a μ_2 mode [68], whereas coordination polymers are formed by the zinc(II) complex **68** (❯ *Fig. 13*) and by the copper(II) complex, for which no crystallographic data are available [69,70].


62   **63**   **64**   **65**   **66**   **67**
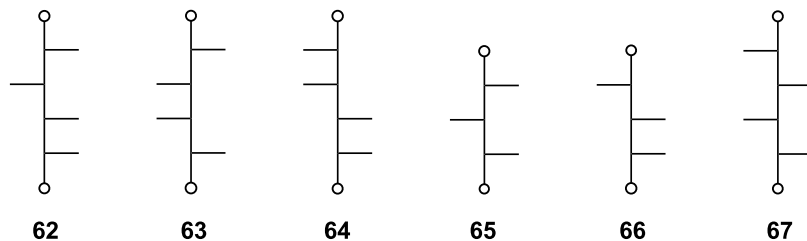
Carbon numbering: C1 is situated at the top of each chain.   ○ = COOH

Both α-hydroxycarboxylate moieties of galactaric acid **63** (also known as mucic acid) act as a chelation site for magnesium centers in the solid-state structure **70** (❯ *Fig. 14*), in which the galactarate is centrosymmetric and adopts a zigzag conformation [71]. Four galactarate molecules acting as bis(α-alkoxidocarboxylato) ligands and eight hydroxido ligands coordinate to six aluminum centers in a cyclic hexaaluminate **71** (❯ *Fig. 14*). This structure is obtained from a reaction in strongly alkaline solutions and combines carboxylato-, hydroxido- and alkoxido bonding to the aluminum centers.

Copper(II), however, shows a different complexation behavior with galactaric acid in strong alkaline media. A coordination polymer **72** (❯ *Fig. 15*) is formed by the copper atoms and the galactarate ions which act as *threo*-bis-diolato ligands. A polymer of the same type is formed with erythritol (compare **10**, ❯ *Fig. 1*) [72]. Carboxylato or hydroxido bonding is not observed in this copper complex. In weakly acidic solution with a pH of 4, however, copper(II) is chelated through an α-hydroxycarboxylate moiety of galactaric acid. Deprotonation
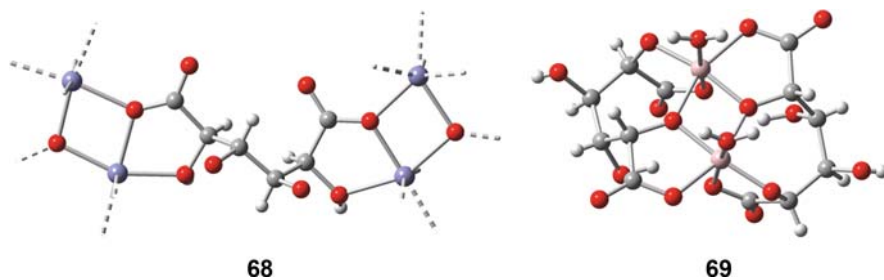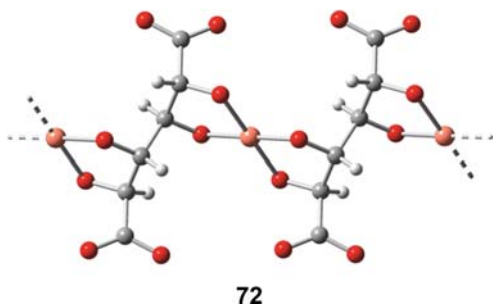
Figure 13
A part of the crystal structure of Zn(D-Glc1,6A$_2$1,6H$_{-2}$) **68** in crystals of **68** · 2 H$_2$O and the molecular structure of [{Al(D-Glc1,6A$_2$1,2;5,6H$_{-4}$)(H$_2$O)}$_2$]$^{2-}$ **69** in crystals of K$_2$**69** · H$_2$O. *Dashed lines*: indicate Bonds to adjacent oxygen atoms
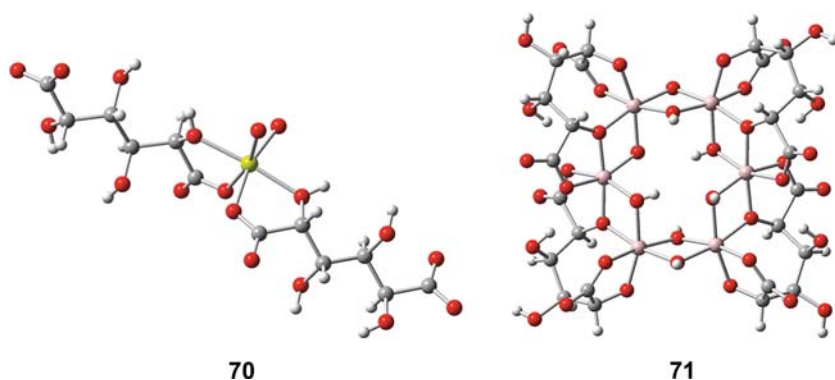
Figure 14
A section of the crystal structure of Mg(Gal1,6A$_2$1,6H$_{-2}$) · 2 H$_2$O **70** and the molecular structure of [Al$_6$(Gal1,6A$_2$1,2;5,6H$_{-4}$)$_4$(OH)$_8$]$^{6-}$ **71** in crystals of Na$_6$**71** · 21 H$_2$O

of the α-hydroxyl function is reported to occur at pH 7.5 [73]. These observations indicate for copper(II) that carboxylato bonding becomes more and more unfavorable with increasing pH. The following structures of complexes with aldaric acids are solely based on NMR spectroscopic data. Several complexes with both α-alkoxidocarboxylato residues of glucaric acid **62** as chelation sites are discussed with molybdenum(VI) and tungsten(VI) as central metals. Both β-hydroxyl functions are deprotonated in a less acidic solution of pH 4.5–6 and a double molar excess of metal whereupon a dinuclear complex is formed. At a higher pH of about 6–8.5, coordination through the carboxylato residue becomes unfavorable and chelation through the alkoxido functions at C2–C5 leads to a *threo*-complex similar to that described above for D-sorbitol [74]. As with D-galactonic acid, two molybdenum(VI) atoms are chelated through the alkoxido functions of the C1–C3 subset and the C4–C6 subset, respectively, of entirely deprotonated galactaric acid **63** in weakly acidic solutions with a molar ratio of molybdenum:ligand of 4:1. Obviously the strong Lewis acidity of molybdenum(VI) enables the carboxylate oxygen atom of galactaric acid to take over the part of the terminal, less acidic

72

◼ **Figure 15**
The solid-state structure of [Cu(Gal1,6A$_2$H$_{-6}$)]$^{4-}$ **72** in crystals of Na$_4$**72** · 12 H$_2$O. *Dashed lines* indicate bonds to adjacent oxygen atoms of the linear coordination polymer

alcoholic hydroxyl function in galactonic acid. The central diol functions are not involved in complexation in equimolar solution. However, in neutral solutions with an excess of molybdenum, the central diol function in combination with the adjacent alcoholic hydroxyl functions are arranged in a sickle conformation and form a dinuclear *erythro*-complex also found for galactitol [75]. Most of the complexes just described are also formed with tungsten(VI) as central metal [76].

Both, glucaric acid **62** and galactaric acid **63** form mono- and dinuclear peroxido complexes with molybdenum(VI and tungsten(VI). In all of them one or two α-alkoxidocarboxylato moieties are chelating the metal centers. The dinuclear species is predominantly formed in solutions with a molar ratio of metal:ligand of 2:1 [64].

The coordination behavior of molybdenum(VI) with D-mannaric acid **64** is similar to that with galactaric acid: two molybdenum atoms are bonded either by the two α-alkoxidocarboxylato moieties of fourfoldly deprotonated D-mannaric acid or by the alkoxido functions of the C1–C3 subset and the C4–C6 subset, respectively, of entirely deprotonated D-mannaric acid. Due to the *threo*-configuration of the central diol residue, a *threo* complex is established in neutral solutions with a molar ratio of Mo:ligand of 4:1 instead of an *erythro* complex which was observed with galactaric acid (compare structure **20** and **14** (❱ *Fig. 2*), respectively) [75]. The latter *threo* complex as well as a complex with the α-alkoxidocarboxylato moieties as chelation sites is also formed by tungsten(VI) [76].

In alkaline solutions of a pH of 11.5 containing calcium ions, aluminum(III) forms C_2-symmetric dinuclear sandwich-type complexes. D-glucaric acid **62** has to adopt a conformation which allows all coordinating alkoxido functions to point in the same direction. The aluminum centers are bonded by the *threo*-configured 2,3-site as well as by the *erythro*-configured 4,5-chelation site. Two *threo*-3,4-diolato moieties of two mannaric acid **64** ligands are the bonding sites of the tetrahedrally coordinated aluminum center. Tetrahedrally coordinated aluminum is also present in the bis-diolato complexes with xylaric acid **65** and D-arabinaric acid **66**, respectively; both complexes are formed in calcium-containing solutions. Xylaric acid is bonded to aluminum through its C2–C3 *threo*-diol function, at which the central hydroxyl function at C3 is in the μ_2 mode and is bonded to a calcium ion as well. A C_2-symmetric dinuclear complex is formed with D-arabinaric acid. The aluminum centers are coordinated to a C1–C2 α-hydroxycarboxylate moiety from one ligand and to a C3–C4

erythro-diol function from the other ligand. The complex formation is supported by calcium ions which are bonded at several sites of the complexes just described [77].

Borate mono- and diesters are preferentially formed of the *threo*-3,4-diol functions of glucaric acid **62** [40,67,78]. Several cations have been shown to have different effects on the borate-ester equilibria. Monovalent ions such as Na^I, K^I, and Ag^I hardly show any effect, whereas divalent cations with moderate polarizing abilities (Mg^{II}, Ca^{II}, Co^{II}, Ni^{II}, Sr^{II}, Cd^{II}, Ba^{II}) increase the diester formation. Strongly polarizing cations such as Al^{III}, Cu^{II}, Zn^{II}, Pr^{III}, and Pb^{II} induce dissociation of the borate diesters [79]. Monoesters and diesters with galactaric acid **63** are formed mostly through the *threo*-configured diols at 2,3-position. Diborate ester formation is also observed in which the two borate anions are bonded at the equivalent *threo*-configured diols in 2,3- and 4,5-position [40,67].

3.3 Regioselectivity and Stability

The electron-withdrawing effect of the carboxyl group markedly enhances the acidity of the adjacent α-hydroxyl group. As a consequence, the α-hydroxycarboxylate moiety becomes an attractive ligand mainly in acidic and neutral solutions in which sugar alcohols form complexes of low stability only, especially with metals of weak Lewis acidity. In alkaline solutions, however, the less acidic alcoholic hydroxyl functions are mostly preferred in complex formation. For these solutions the rules referring to the regioselectivity and stability of sugar-alcohol complexes may be valid for aldonic and aldaric acids as well.

4 Anhydroerythritol

Anhydroerythritol (AnEryt) or *cis*-oxolane-3,4-diol is a particularly well-suited ligand to investigate the coordination chemistry of carbohydrates as it can be considered to be a molecular cutout of important glycosides such as the nucleosides. On the one hand, its acidity is about the same as that of the glycosides, on the other hand, AnEryt is easily obtainable, configurationally stable in the entire pH range of interest, and chemically stable under alkaline conditions. AnEryt shares the latter two properties, which are critical for the glycoses, with the glycosides. Contrary to even glycoses, as a *meso* compound AnEryt gives rise to particularly simple ^{13}C NMR spectra. Finally, AnEryt is achiral, a property that is found to be beneficial for the crystallization of its complexes.

Usually the diolato $\kappa^2 O,O'$-AnErytH$_{-2}$ ligand forms five-membered chelate rings in the coordination compounds, the central atoms spanning a size range from boron(III) to lead(II). The unusual versatility of the AnErytH$_{-2}$ ligand is the result of the variability of a furanoidic ligand's bite, AnEryt being the prototype of this kind of ligand.

Coordination of central metal atoms with auxiliary ligands so that only two free binding sites remain, leads, in most cases, in combination with the deprotonation of the diol functions of AnEryt, to a predictable binding mode of $\kappa^2 O,O'$ as in the cases of cobalt(III), {RuNO}^{6}, oxo-rhenium(V) and palladium(II).

Four of the six binding sites of the octahedrally coordinated cobalt(III) in [(en)$_2$Co (AnErytH$_{-2}$)] are occupied by ethylenediamine ligands, $\kappa^2 O,O'$-AnErytH$_{-2}$ binds over the remaining two sites [80]. Caused by the *cis* conformation of the two diol functions of

AnEryt, the five-membered chelate ring is flat. An intramolecular hydrogen bond between the O1 atom of the AnEryt ring and an en ligand is responsible for the conformation of the complex (the conformation of the oxolane ring is $^{C4}T_{O1}$, distorted in the direction of E_{O1}). The Co–O bond length averages 1.88 Å.

Comparable conditions can be found for the structure of [*mer*-(dien)(NO)Ru(AnErytH$_{-2}$)] BPh$_4$·2 H$_2$O where four of six coordination sites were occupied by NO and *mer*-dien so that κ^2O,O'-AnErytH$_{-2}$ is once again the ligand for the remaining two binding sites with a O–C–C–O angle of $-22.1°$ [81]. Diolate-Ru(NO) bonding is governed by the *trans*-influence of the nitrosyl ligand. The Ru–O(*trans*) distance is with 1.94 Å markedly shortened compared with the Ru–O(*cis*) distance with 2.05 Å, the Ru–O(*trans*)–C angle is with 117.9° always more obtuse than the Ru–O(*cis*)–C angle with 112.1° and, most remarkably, considering the usual features of polyolato-metal structures, the O(*trans*) center does not act as a hydrogen-bond acceptor. On the other hand, O(*cis*) is a hydrogen-bond acceptor, as is usual. [(tpb)ReO(AnErytH$_{-2}$)] is also an octahedrally coordinated complex and built from equal amounts of two isomers, which differ in the orientation of the oxolanediolato ligand with respect to the (tpb)ReO fragment [82] (**73**, **74**).

73 **74**
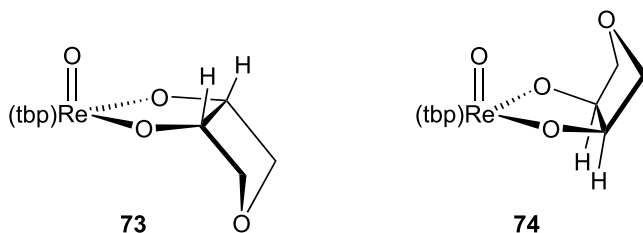
As known from the structure of [(en)$_2$Co(AnErytH$_{-2}$)], the O1 atom of the AnEryt ring in the *anti* isomer **73** of [(tpb)ReO(AnErytH$_{-2}$)] builds a hydrogen bond with the tpb ligand. No intramolecular hydrogen bonding can be found in the *syn* isomer **74**, the Re–O bond averages 1.93 Å in both cases. In contrast, the O–C–C–O angles of AnErytH$_{-2}$ differ in the case of *syn* and *anti* coordination, in compound **73** the angle amounts to $-1.6°$ and in **74** to $-19.3°$.

In the dinuclear anion [Re$_2$(CO)$_6$(μ-OMe)$_2$(μ-AnErytH$_{-1}$)]$^-$ **75**, AnEryt differs from the currently known coordination pattern [32]. A single monodentate κO-μ-AnErytH$_{-1}$ ligand takes one of the three alkoxido positions in the usual hexacarbonyl-trialkoxo-dirhenate(I) anion, leaving the other two for methoxido groups, as shown in ❯ *Fig. 16*. The second diol function forms an intramolecular hydrogen bond to the deprotonated diol function. The distances of the coordinated O atom to the two Re atoms average 2.17 Å and the O–C–C–O angle of AnErytH$_{-1}$ is 42.6°.

For the square-planarly coordinated palladium, the use of an auxiliary ligand leads to the expected κ^2O,O'-coordination of one AnErytH$_{-2}$. There are two known characterized complexes with [(bpy)Pd(AnErytH$_{-2}$)] · 6.5 H$_2$O and [(en)Pd(AnErytH$_{-2}$)] · 4 H$_2$O [83,84]. Two binding sites of the square-planarly coordinated palladium are occupied by bpy or en and two sites bind to the deprotonated AnErytH$_{-2}$. In both cases the Pd–O bond length averages 1.99 Å With 43.0°, the O–C–C–O angle of [(bpy)Pd(AnErytH$_{-2}$)] · 6.5 H$_2$O and 38.7°, the O–C–C–O angle of [(en)Pd(AnErytH$_{-2}$)] · 4 H$_2$O, the angles are closer to that of the κO-μ-AnErytH$_{-1}$ ligand than to the angles of the compounds introduced so far.

☐ **Figure 16**
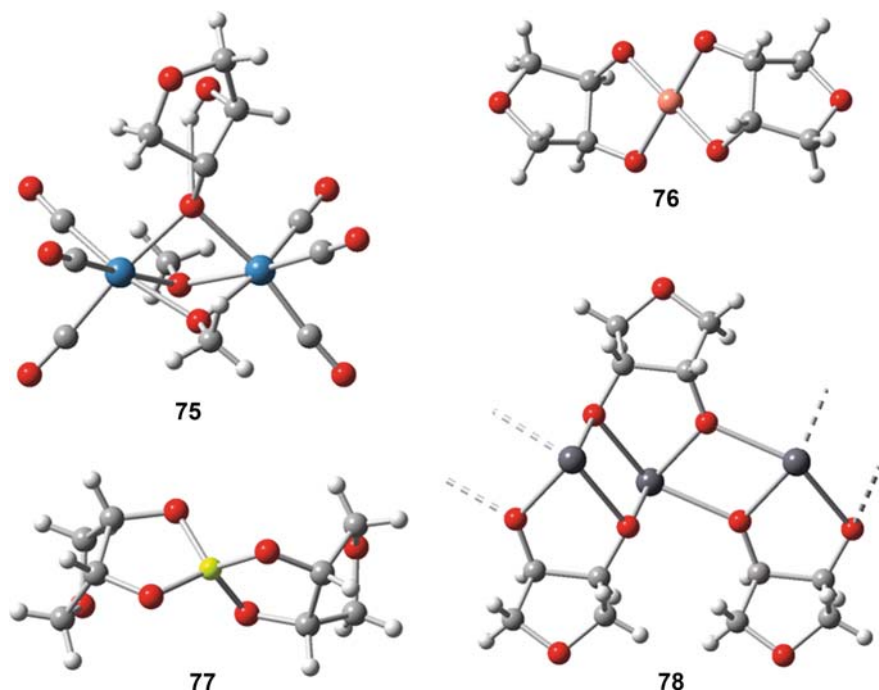X-ray structures of the anionic $[Re_2(CO)_6(\mu\text{-OMe})_2(\mu\text{-AnErytH}_{-1})]^-$ 75 in [K([18]crown-6)]75, $[Cu(AnErytH_{-2})_2]^{2-}$ 76 in $A_2$76 · 4 H_2O (A = Li, K, Na), $[B(AnErytH_{-2})_2]^-$ 77 in K77 · H_2O and a section of the linear coordination polymer built by Pb(AnErytH$_{-2}$) 78 in 78 · H_2O

When the central metal atom is free of auxiliary ligands there are more possibilities for coordination of AnEryt. Keeping to the square-planar coordination Cu(II) builds complexes with two AnEryt, as shown in ❷ *Fig. 16*. Three structures of the type $A_2[Cu(AnErytH_{-2})_2] \cdot 4\,H_2O$ (A_2**76** · 4 H_2O) with A = Li, Na and K [85,86] have been determined. The structures of Na and K on the one hand and Li on the other hand differ in the coordination of the alkali ions to the deprotonated diol functions of the Cu(AnErytH$_{-2}$) substructure. The Cu–O bond length averages 1.93 Å and the O–C–C–O angle of AnErytH$_{-2}$ grows in dependence on the cation from 33.7 (Li) to 35.4° (K).

Comparable coordination schemes with two AnErytH$_{-2}$ ligands exist for tetrahedrally coordinated metal centers, too. Boron(III), beryllium(II) and lead(II) build structures where the metal center is tetrahedrally coordinated with two AnErytH$_{-2}$ ligands [87,88], for example the structure of $K[B(AnErytH_{-2})_2] \cdot 2\,H_2O$ (K**76** · 2 H_2O) in ❷ *Fig. 16*.

According to the increasing atom size, the bond length increases from the B–O bond length with 1.47 Å over the Be–O bond length with 1.63 Å to an Pb–O bond length between 2.25 Å to 2.39 Å The boron compound shows two similar O–C–C–O angles of 12.0°, the beryllium compound an angle of 26.8° and a second of 0.8°.

As shown in ❷ *Fig. 16*, lead(II) forms not only monomers of $[Pb(AnErytH_{-2})_2]^{2-}$ but also polymers of Pb(AnErytH$_{-2}$) · H_2O (**78** · H_2O), which are chains of Pb(II) coordinated by

79

80   **81**
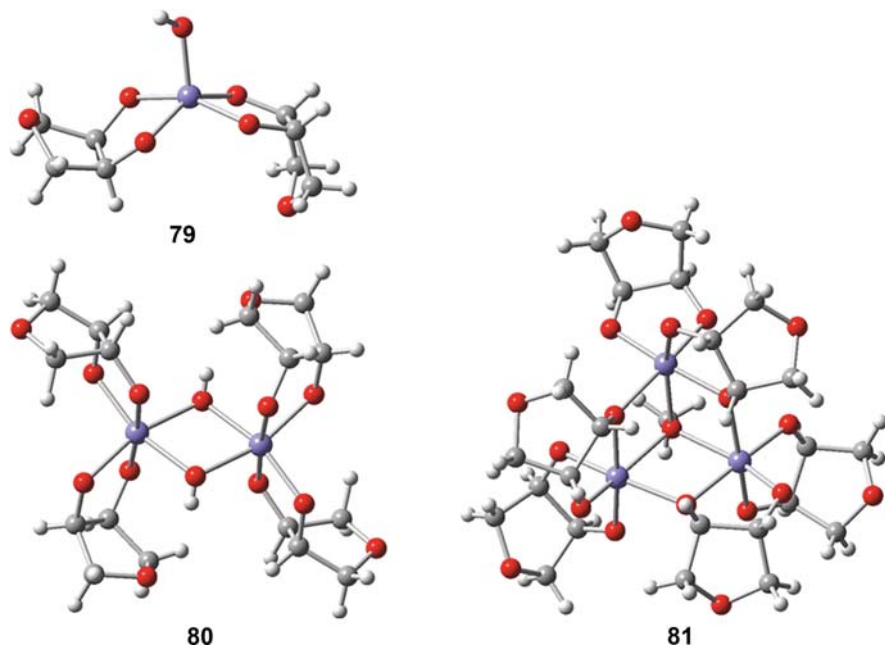
◫ **Figure 17**
X-ray structures of 79 in $Na_2[Fe(AnErytH_{-2})_2(OH)] \cdot 0.5\ NaNO_3 \cdot 3.5\ H_2O$, 80 in $Ba_2[Fe_2(AnErytH_{-2})_4(\mu\text{-}OH)_2] \cdot 12\ H_2O$, and 81 in $Na_4[Fe_3(AnErytH_{-2})_6(OMe)] \cdot 2.5\ NaNO_3$

four bridging O-atoms [89]. In contrast to the monomeric $[Pb(AnErytH_{-2})_2]^{2-}$, the Pb–O distances range between 2.24 and 2.47 Å the O–C–C–O angle of $AnErytH_{-2}$ averages 20°. $[Fe(AnErytH_{-2})_2(OH)]^{2-}$ **79**, $[Fe_2(AnErytH_{-2})_4(\mu\text{-}OH)_2]^{4-}$ **80** and $[Fe_3(AnErytH_{-2})_6(OMe)]^{4-}$ **81** are three anionic compounds with doubly deprotonated $AnErytH_{-2}$ ligands and iron(III) [90]. The three compounds are shown in ❂ *Fig. 17*. In the case of **79** there are two isomers caused of *syn* and *anti* orientation of AnEryt ligands. ❂ *Figure 17* only shows the *syn/anti* isomer, although the structure of the *anti/anti* isomer is also known. In **79**, iron(III) is square-pyramidally coordinated by two $AnErytH_{-2}$ and one hydroxido ligand. Nevertheless the ideal geometry varies at one coordinate of the Berry-pseudorotation at about 16.6% for the *syn/anti* isomer and at 27.6% for the *anti/anti* isomer. **80** is a $(\mu\text{-}OH)_2$ bridged dimer of **79** where both iron centers now are coordinated sixfold. Species **81** is a three-centered tetraanion where three of six diolato ligands bind to one of the iron atoms, the other three diolato ligands build $\eta^1{:}\eta^1,\mu_2$-bridges to a central μ_3-methoxidotriiron unit.

The distances between the iron centers and the O atoms vary depending on the compound. In **79**, the O atoms of the AnEryt ligands have distances between 1.93 and 1.98 Å to the iron center, in **80** the distances range from 1.96 to 2.02 Å and in compound **81** from 1.94 to 2.09 Å (❂ *Fig. 17*).

Similarly to iron(III), there are known mono-, di- and trinuclear compounds with silicium. Almost identical to **79** are the structures of $[M(AnErytH_{-2})_2(OH)]^-$ with M = Si **82** and Ge [91]. In $[SiPh(AnErytH_{-2})_2]^-$ [92] **83** a phenyl substituent occupies the apical position of the pyramidal coordination sphere instead of a hydroxyl residue (❂ *Fig. 18*).
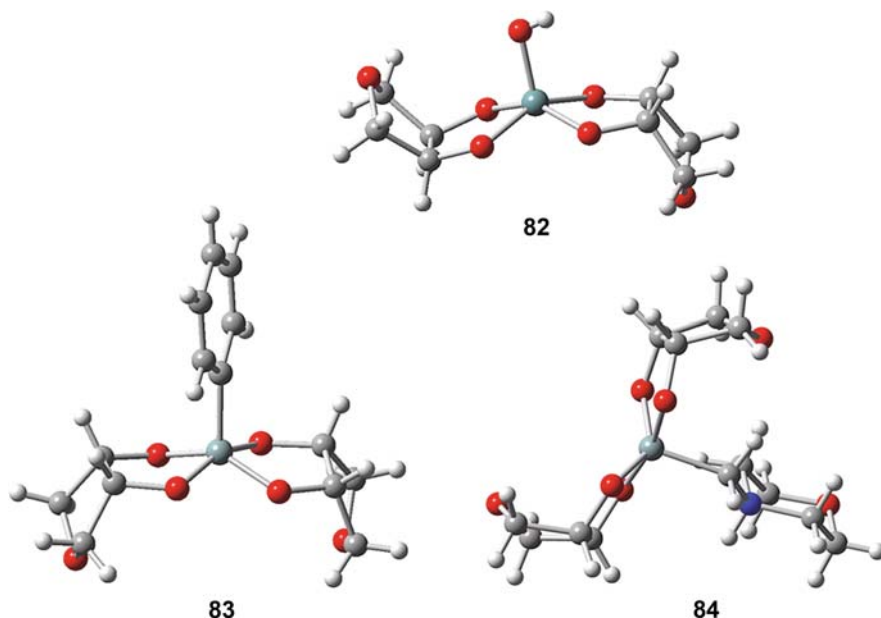
■ Figure 18
X-ray structures of 82 in Li[Si(AnErytH$_{-2}$)$_2$(OH)] · H$_2$O, 83 in K[SiPh(AnErytH$_{-2}$)$_2$] · 1.5 MeOH, and 84 in [(AnErytH$_{-2}$)$_2$SiCH$_2$NHC$_4$H$_8$O]

The anionic complex **82** crystallizes with different alkali cations which results in different conformations of the Si center in the crystal structure. In the case of **83**, *anti/anti* and *syn/anti* coordinated silicium centers exist in the crystal structure in equal parts.

The Si-O(AnErytH$_{-2}$) distances average 1.70 Å (Li) and 1.73 Å (Na, K, Cs), the AnErytH$_{-2}$ O–C–C–O angles are 14.1 and 9.7° for sodium and two times −3.5° for cesium.

In the case of silicium not only the various possibilities of coordination are of interest, the hydrolytic stability in neutral aqueous solution and the resulting biochemical relevance is of much greater importance. One approach in this direction is the introduction of a positive charge next to the Si center [93].

As can be observed in ❯ *Fig. 18*, the Si coordination polyhedra of [(AnErytH$_{-2}$)$_2$SiCH$_2$NHC$_4$H$_8$O] **84** and additionally [(AnErytH$_{-2}$)$_2$SiCH$_2$NHC$_4$H$_8$O] · H$_2$O in the crystal are strongly distorted trigonal bipyramids, in which each bidentate ligand spans one axial (O1, O3) and one equatorial site (O2, O4). The Si–O distances of the SiO$_4$C skeletons of **84** and **84** · H$_2$O range from 1.68 to 1.76 Å and the axial Si–O bonds (1.73–1.76 Å are significantly longer than the equatorial ones (1.68–1.71 Å. As seen in ❯ *Fig. 18*, the *syn/anti* geometry is observed in the crystals of **84**.

Taking into account the different possible orientations of the two oxolane rings, relative to the apical ligand, for the three compounds **82**, **83** and **84**, the existence of *syn/syn* isomers in addition to *syn/anti* and *anti/anti* isomers must be considered. Although there is some confusion in the literature [92,93,94,95,96,97] about the correct interpretation of the NMR data of silicate complexes, there is no doubt that the three above-mentioned compounds exist in solution. In ❯ *Fig. 19*, ^{29}Si and ^{13}C (DEPT-135) NMR spectra of **82** and **83** are shown.
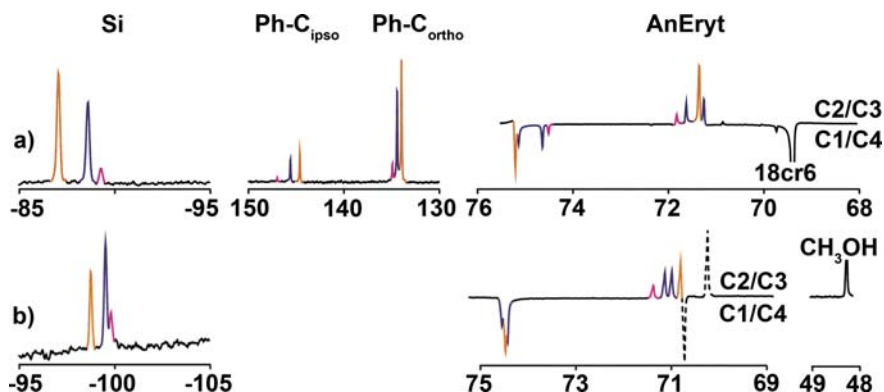
◼ **Figure 19**

^{29}Si and ^{13}C (DEPT-135) NMR spectra of pentacoordinate AnEryt–silicate species prepared from the diol, SiPh(OMe)$_3$ or Si(OMe)$_4$, and base at the molar ratio given in a) and b). Color code: orange: anti/anti; violet: syn/anti; pink: syn/syn isomer of the respective [Si(R)(AnErytH$_{-2}$)$_2$]$^-$ ion. a) R = Ph; base: KOMe/[18]crown-6; solvent: methanol; molar ratio: 2:1:2; total Si concentration: 0.38 mol kg^{-1}. AnEryt region in DEPT mode referenced to the [18]crown-6 signal. b) R = OH; base: LiOH; solvent: water; molar ratio: 3:1:1; total Si concentration: 0.54 mol kg^{-1}. The methanol signal stems from hydrolysis of the Si(OMe)$_4$ starting material and may be used as a reference for DEPT assignment. *Dashed line*: free AnEryt [92]

The ^{29}Si NMR spectrum in ❷ *Fig. 19* a) exhibits the signals of two major and one minor pentacoordinate species. According to the species in crystal structure, the two main signals are assigned to the *anti/anti* and *syn/anti* isomers, the minor peak to the *syn/syn* isomer.

In light of this assumption, interpretation of the ^{13}C NMR spectrum is straightforward. The ^{13}C DEPT-135 NMR spectrum is shown in ❷ *Fig. 19* a) on the right side. Both, the *anti/anti* and the *syn/syn* isomer have apparent C$_{2v}$ symmetry and should thus give rise to one signal for C2/C3 and one signal for C1/C4. The *syn/anti* isomer on the other hand, with its apparent C$_s$ symmetry, will show twice the number of signals. A special feature of the phenylsilicate spectra will gain significance in more complicated cases. ❷ *Figure 19* a) shows the ^{13}C NMR signals of the phenyl residue in addition to the diol signals. It should be noted that both the signals stemming from the *ipso*-carbon atom as well as the signals from the two *ortho*-carbon atoms mirror the ^{29}Si NMR spectrum.

The corresponding spectrum of an aqueous diolatosilicate solution is shown in ❷ *Fig. 19* b). The same rules could be applied to the ^{29}Si and ^{13}C NMR spectra of **84** in solution. Here the two main and one minor signals in the ^{29}Si NMR spectrum are found, too [97].

Contrary to prior interpretation [93], hydrolysis products dominate the NMR spectra of aqueous solutions of **84** at a pH value near to neutrality, particularly at a higher dilution, so the introduction of a positive charge next to the Si center does not prevent hydrolysis.

The properties of four-coordinate Si centers bonded to an alkylenedioxy substituent derived from a furanoidic diol also were investigated with the two isomeric oxolane-3,4-diols AnEryt and L-anhydrothreitol [92]. Thus, substitution of silicon with two phenyl residues leads to Ph$_2$Si(AnErytH$_{-2}$) **85** in the case of AnEryt. The molecular structure is that of a monomer. The five-membered chelate ring is almost planar, with a diol torsion angle close to 0°. Such geometrical parameters cannot be met by L-AnThre. However, this diol provides another example

that the inability to form a chelate ring must not be confused with a lack of reactivity. Thus, the solid-state structure of Ph$_2$Si(L-AnThreH$_{-2}$) **86** is not that of a monomeric chelate. Instead, an unstrained molecule with all bonding angles close to their ideal values is observed in a trimeric structure (❯ *Fig. 20*). Although 0° torsion is outside the range of achievable diol torsion angles, the great flexibility of furanoidic rings is obvious from the L-AnThre structure as well. To build the trimer, the diol torsion angles span almost the entire available 100° range of a furanoidic diol, with the actual values being between 82° and 165°.

According to the above-mentioned tetrahedrally coordinated compounds silicium could also build complexes with two AnErytH$_{-2}$ ligands, shown in ❯ *Fig. 20*, Si(AnErytH$_{-2}$)$_2$ **87** [92]. The average Si–O bond length amounts to 1.63 Å and is comparable to the bond length of [Be(AnErytH$_{-2}$)$_2$]$^{2-}$, the O–C–C–O torsion angles of the AnErytH$_{-2}$ ligands are −0.8 and −1.2° which differ from the Be compound noticeably. Furthermore there is a dimer form of **87** [92], also shown in **88** in ❯ *Fig. 20*. Here the Si–O bond length increases up to 1.72 Å and the O–C–C–O angles to −2.8 and −16.8°.
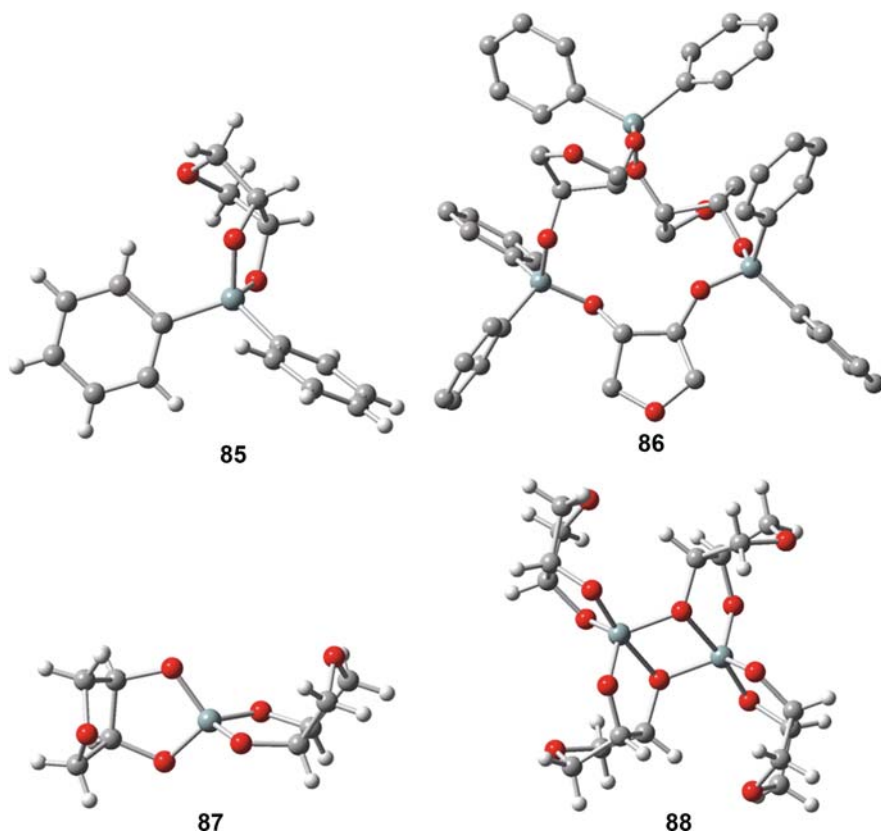
❏ **Figure 20**
X-ray structures of Ph$_2$Si(AnErytH$_{-2}$) 85, Ph$_2$Si(L-AnThreH$_{-2}$) 86, Si(AnErytH$_{-2}$)$_2$ 87, and [Si(AnErytH$_{-2}$)$_2$]$_2$ 88

In summary it may be said that AnEryt has a special position compared to the other polyols. The fact that AnEryt models a furanoside and not a pyranoside is of particular importance for dealing with small central atoms. Because of the smaller O–C–C–O torsion angle in the range from 0 to approximately 40°, the steric demand is smaller than that of pyranoses as could be shown for cobalt(III) complexes [80]. A *cis*-furanoidic diol thus appears to be a better choice than open-chain diols and, particularly, pyranoidic diol functions. The reason for the conformational flexibility of a furanose ring is its balance of strain. While open-chain diols experience Pitzer strain when twisted into an eclipsed conformation, and pyranoses are burdened with ring strain on being twisted towards 0° torsion, a furanose is characterized by a balance of the various types of strain over a pronounced range of torsions.

5 Inositols and Anhydro-Sugars

5.1 Inositols

There are nine various inositols or cyclohexane-1,2,3,4,5,6-hexaols, including one pair of isomers. The *myo*-inositol is the most widespread isomer of inositol and, excluding *allo*-, *cis*-, *epi*- and *muco*-inositol, all other inositols are of natural occurrence.

Myo-inositol is also the inositol, which is most investigated in connection with metal coordination. First of all, there are three known structures with magnesium, praseodymium and neodymium with the specific feature that the metal atoms coordinate to *myo*-inositol without deprotonation of the affected hydroxyl groups.

The magnesium atom in [Mg(*myo*-Ins)(H$_2$O)$_4$]Cl$_2$ (**89**Cl$_2$) [98] is coordinated to two *cis*-vicinal hydroxyl groups and four water molecules in an octahedral geometry. As a consequence of cation binding, the cyclohexane ring geometry in the vicinity of the coordination site is distorted. Deviations of nearly 15° from the norm occur in some torsion angles.


89
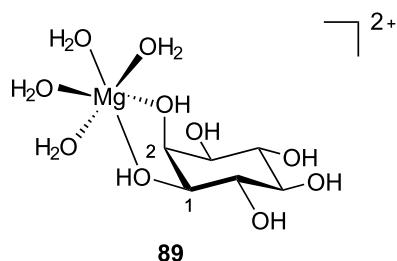
The intramolecular O$_{eq}$1 to O$_{ax}$2 distance is shortened 0.33 Å and that for O$_{eq}$3 to O$_{ax}$2, 0.11 Å from a normal value of 2.89 Å [99]. The decrease in the C–C–O angles for the C1–C2 bond could be an effect of the magnesium ion attraction to the hydroxyl groups. The torsion angles for bond C1–C2 differ by as much as 14° from those of *myo*-inositol.

Praseodymium and neodymium built almost identical structures with *myo*-inositol. In the crystal structures of [Pr(*myo*-Ins)]Cl$_3$ · 9 H$_2$O [100] and [Nd(*myo*-Ins)]Cl$_3$ · 9 H$_2$O [101], by trivalent lanthanide cations complexed *myo*-inositol, each Pr or Nb is coordinated to nine oxygen atoms, two from the inositol (two adjacent hydroxyl groups) and seven from water molecules

in a tricapped trigonal prism geometry, with Pr–O distances ranging from 2.47 to 2.69 Å and Nb–O distances ranging from 2.45 to 2.68 Å. The other two water molecules are hydrogen-bonded. No direct contacts exist between Pr/Nd and Cl.

These metal–hydroxyl interactions generally produce small conformational changes in the sugar at the metal-binding sites. Comparing uncomplexed *myo*-inositol with the Nd-inositol complex, the C–C, C–O distances and bond angles have only small changes.

In the complex of [(PO)(*myo*-InsH$_{-3}$)] **90** [102], the cyclohexane ring adopts the expected chair conformation, with the 2-, 4- and 6-hydroxyl groups being axial, equatorial and axial, respectively. There is an intramolecular hydrogen bond between the O6 atom as donor and O5 as acceptor. The three P–O single bonds, of average length 1.58 Å are all equivalent within significant error, as are the P–O–P bond angles with an average of 104.5°.

90   91a   91b
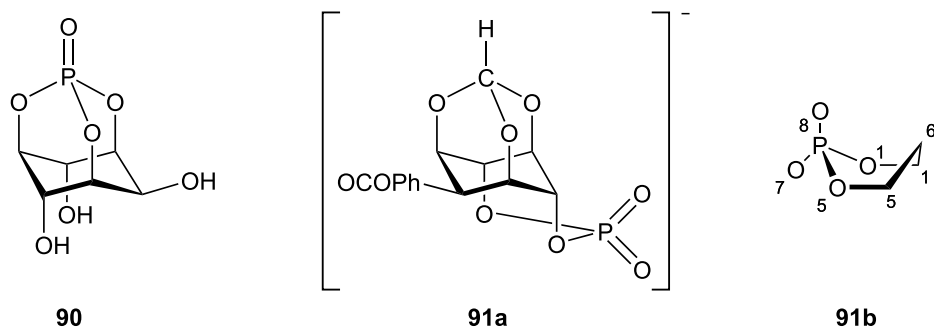
The six-membered 1,3,2-dioxaphosphorinane ring in the anionic 2-*O*-benzoyl-1,3,5-*O*-methylidyne-*myo*-inositol-4,6-cyclophosphate **91a** [103], however, has a boat rather than a chair conformation. The P–O bond distances involving the inositol residue are normal but longer than the mean value of 1.58 Å found by Neidle et al. [102] in **90**. Conspicuously, in **91b**, the six-membered 1,3,2-dioxaphosphorinane ring adopts a boat conformation, with P and C6 on the same side at distances of 0.61 and 0.68 Å respectively, from the mean plane through C1, C5, O1 and O5. This is different from the situation found in **90**, where all three six-membered 1,3,2-dioxaphosphorinane rings have chair conformations.

Furthermore, from *myo*-inositol and 1,2-*O*-isopropylidene-*myo*-inositol two tetracyclic phenyl-boronic esters [B$_3$(C$_6$H$_5$)$_3$(*myo*-InsH$_{-6}$)] **92** and [B$_2$(C$_6$H$_5$)$_2$(C$_3$H$_6$)(*myo*-InsH$_{-6}$)] **93** have been prepared [104], whereas **92** was determined by crystal structure, the structure of **93** was proved by ^{11}B and ^{13}C NMR spectroscopy. Compound **92** is a tetracyclic derivative of the less stable conformer of inositol (five axial hydroxyl groups and one equatorial) with two dioxaboroline rings at opposite faces of the six-membered ring and a dioxaborolidine ring bridging the C1 and C2 atoms at axial and equatorial positions. A similar structure was found for **93** with the difference that, bridging C1 and C2, there is a dioxolane ring. The boron atoms are planar with their attached atoms and stabilized by retrocoordination between the boron and oxygen and carbon atoms, respectively. The two phenyl rings that are in the same face of the molecule are essentially parallel, with a dihedral angle between planes of 28.3 ± 0.8°.

With *scyllo*-inositol boron builds a complex Na$_2$[B$_2$(OH)$_2$(*scyllo*-InsH$_{-6}$)] · 9 H$_2$O (Na$_2$**94** · 9 H$_2$O) [105], where an all-*cis-scyllo*-inositol builds a hexaoxadiamantane-like structure with two boron centers. The *scyllo*-inositol diborate anion itself comprises a rigid cage structure,

the C atoms in the inositol ring are in a chair conformation with normal distances and angles. The two B atoms, situated on either side of the ring, are each bonded axially to alternate ring C atoms via three O atoms with B–O bond distances of 1.48 to 1.51 Å and C–O distances of 1.42 to 1.45 Å. Completing the tetrahedral coordination, each B atom is bonded also to an OH at 1.42 Å.
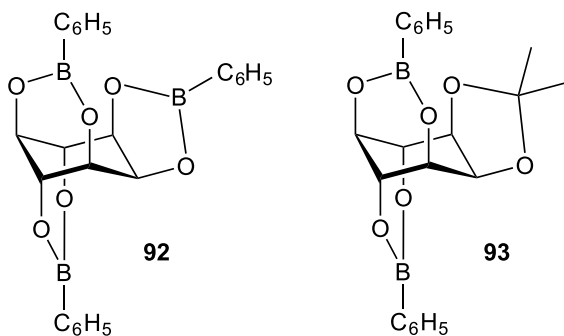

Corresponding to structure **94**, in aqueous alkaline solutions the existence of the two anionic tridentate borate esters [B(OH)(all-*cis*-1,3,5-triol-chxnH$_{-3}$)]$^-$ **95** and [B(OH)(*epi*-InsH$_{-3}$)]$^-$ **96** is proved by ^{11}B NMR spectroscopy [40]. The borate ester of all-*cis*-cyclo-hexane-1,3,5-triol has a chemical shift of −18.1 ppm, the ester of *epi*-inositol a chemical shift of −19.4 ppm.
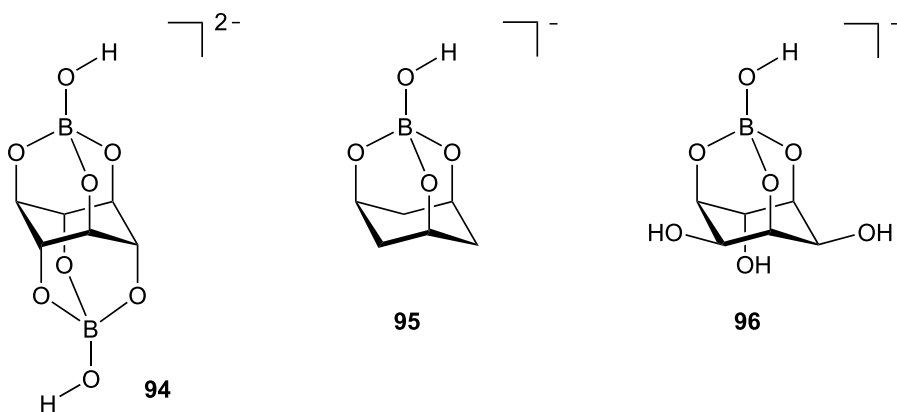
In the structure of [Co(tach)(*cis*-InsH$_{-1}$)](NO$_3$)$_2$ (**97**(NO$_3$)$_2$) [106], cobalt(III) is bound to the three amino groups of all-*cis*-1,3,5-triaminocyclohexane and to three axial oxygen donors of *cis*-inositol. The structure shows that only one of the coordinated hydroxyl groups of *cis*-inositol is deprotonated. Consequently, the Co–O$_H$ distance of 1.90 Å is significantly shorter than the corresponding Co–OH distances of 1.94 Å. Moreover, the C–O bond lengths of the coordinated alcoholic groups are slightly longer than the corresponding bond distance of the coordinated alkoxido group. In turn, the Co–N distance, which is *trans* to the alkoxido group, is significantly elongated, indicating a stronger *trans* influence of RO$^-$ compared with ROH.
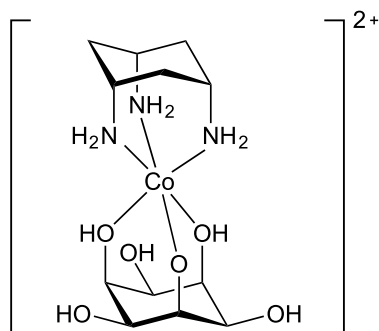
97   **98**
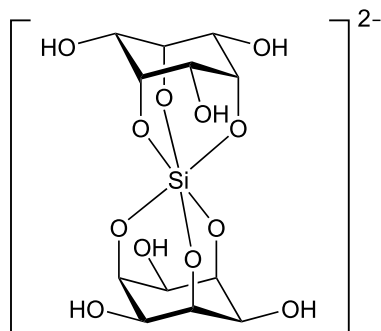
Without tach as auxiliary ligand $Cs_2[Si(cis\text{-}InsH_{-3})_2]$ (Cs_2**98**) [92] shows a bis-tridentate 1,3-diolate binding-*cis*-inositol complex. In contrast to the finding that a pyranoidic 1,2,3-triol like $^1C_4$-Me-β-D-Rib*p*, with its large torsional angles, is not so efficient an Si-chelator as a furanoidic diol, the significant enrichment of aqueous alkaline silicate solutions by hexaco-ordinate species on addition of *cis*-inositol is remarkable.

Besides these, to one metal atom coordinated *cis*-inositol complexes, there are two related fields of research. One is the complex coordination of metal atoms to the polyaminoalcohols, especially 1,3,5-triamino-1,3,5-trideoxy-*cis*-inositol, since the amino group can either act as additional donors for metal binding or serve as internal bases, facilitating the deprotonation and coordination of the hydroxyl groups [107].

The other field of research deals with *cis*-inositol-coated polyoxometalate clusters [108,109, 110]. $[OFe_6\{(cis\text{-}Ins)_6\text{-}21H\}]^{5-}$ and $[Ta_7O_{12}(cis\text{-}InsH_{-3})_6]^{7-}$ build polyoxometalate cores which are coordinated to *cis*-inositol on the outer binding sites. In the case of $[OFe_6\{(cis\text{-}Ins)_6H_{-21}\}]^{5-}$ there are five different modes of coordination of *cis*-inostiol to the Fe atoms, so that there is no preferred coordination mode recognizable. In the case of $[Ta_7O_{12}(cis\text{-}InsH_{-3})_6]^{7-}$, *cis*-inositol binds over the three *cis*-standing hydroxyl groups to the Ta atoms.

5.2 1,6-Anhydro-β-D-Glucose (Levoglucosan)

Currently there are three known structures of metal-coordinated 1,6-anhydro-β-D-glucose (Glc1,6An; levoglucosan). The cuprate anion of $Li_2[Cu(Glc1,6An2,4H_{-2})_2] \cdot 8\,H_2O$ is a homoleptic mononuclear 1,3-polyolato(2-) complex.

Generally, in terms of flexibility a chelate ligand is of limited variability, particularly when the ligator atoms are attached to a further cyclic fragment and above all, to a six-membered ring in its energetically favored chair conformation. In the coordination chemistry of carbohydrates, this general statement may be quantified for 1,2-diol fragments incorporated in pyranose rings. In cuprate(II) or cobalt(II) complexes of β-D-galactose, α-D-mannose and β-D-xylose, the mean O–O distance of the ligating diol groups is 2.67 ± 0.01 Å. This corresponds to a 0.19 Å reduction of the respective mean distance of 2.85 ± 0.02 Å in the uncomplexed methyl gly-copyranosides.

Assuming that a bicyclic pyranoidic carbohydrate will also be of restricted flexibility, the twofold reduction of the ligator atom distance (0.38 Å on coordination of cupric ions by 1,6-anhydro-β-D-glucose, compared with the above-mentioned 1,2-diolates, was unexpected due to the large O–O separation of 3.30 Å in the free anhydro sugar [111].

99   **100**   **101**
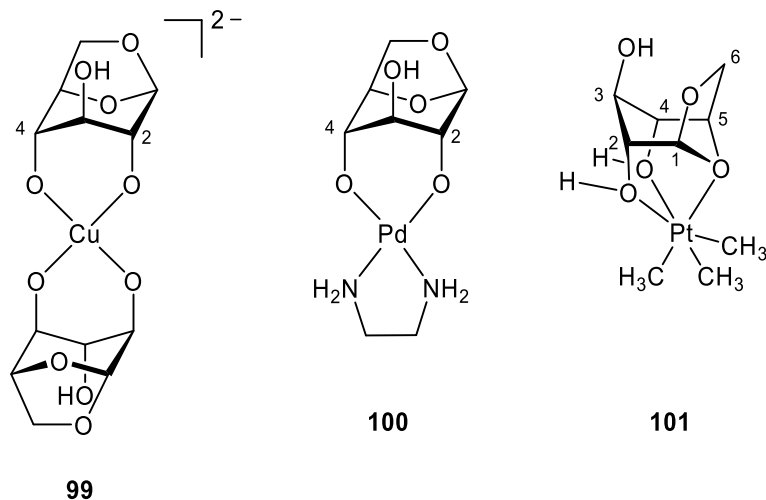
In the mononuclear cuprate(II) anion **99** (4 + 2)-coordinated Cu^{II} forms six-membered rings with doubly deprotonated levoglucosan ligands at a shorter Cu–O distance (Cu–O2, 1.95 Å Cu–O4, 1.99 Å. Two longer contacts are established with the O5 atoms of the pyranose rings. The chelate bonding mode is enabled by the astonishingly enhanced flexibility of the bicyclic ligand compared with simple pyranoses [112].

[(en)Pd(Glc1,6An2,4H$_{-2}$)] · H$_2$O (**100** · H$_2$O) is formed in a reaction from Pd-en and 1,6-anhydro-β-D-glucose [84]. Levoglucosan again can act as a 1,3-diolato ligand by bonding through O2 and O4. The distances between Pd–O2 and Pd–O4 amount to 2.04 Å and 2.05 Å the angle between O2–Pd–O4 to 97.0°. In fact, **100** is a six-membered-ring chelate complex and the molecular structure of **100** again shows flexibility of the bicyclic ligand, which undergoes distortion of the pyranose chair towards a boat conformation. In this distortion, greater flattening of the pyranose ring at C3 corresponds to an increasing O2–O4 distance. Conversely, in **100** the respective hydroxyl groups occupy a more axial position, and the 'bite' is smaller than in the free anhydro sugar. This can be compared with the even smaller O–O distance in Li$_2$**99** · 4 H$_2$O.

In [PtMe$_3$(Glc1,6An)]BF$_4$ (**101**BF$_4$) 1,6-anhydro-β-D-glucose acts as a neutral tridentate ligand which is coordinated through two hydroxyl groups (O2, O4) and an acetal oxygen atom (O5) of the glucopyranose ring. Thus, two five-membered rings and one six-membered 1,3,2-dioxaplatinacyclohexane ring are formed exhibiting a distorted half-chair and chair conformation, respectively. The cyclic system is not free from angle strain which is revealed particularly by the O–Pt–O angles. Two of them are distinctly smaller than 90° (O2–Pt–O5, 73.6°; O4–Pt–O5, 75.6°), whereas the C–Pt–C angles remain nearly orthogonal (88.1–89.9°). The two Pt–O bonds to the hydroxyl groups are almost equal (Pt–O2/O4, 2.25 Å. Contrarily, the Pt–O bond to the acetal oxygen is significantly longer (Pt–O5, 2.29 Å. This may be

explained in terms of the very low donor capability of the acetal oxygen atom and of the high *trans* influence of the methyl ligand [113].

6 Glycosides

Glycosides are obtained by conversion of the cyclic semiacetal form of aldoses and ketoses to an acetal. We will focus on the metal complexes and esters of the following glycosides: alkyl pyranosides, alkyl furanosides, non-reducing disaccharides, polysaccharides, and finally the nucleosides as a member of the group of *N*-glycosides.

6.1 Pyranosides

In the following, solid-state and solution structures of the pyranosides **102–107** and their protected derivatives will be described.
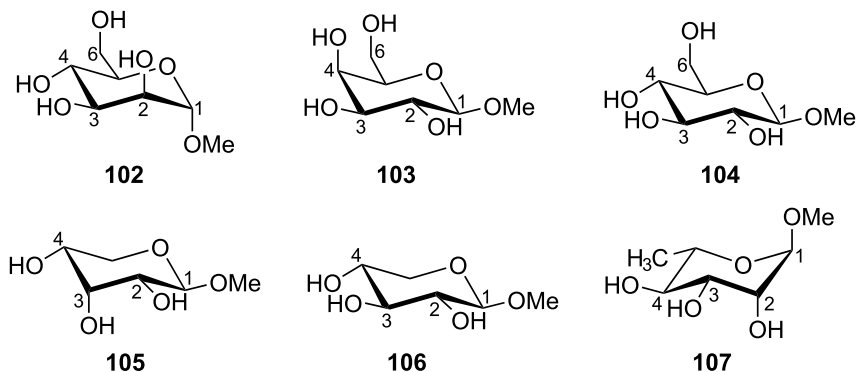
Methyl-α-D-mannopyranoside (Me-α-D-Man*p*) **102** is one of the structurally best-investigated compounds among the pyranosides. The reaction of equimolar amounts of Cu(OH)$_2$, ethylenediamine, and **102** in aqueous solution leads to a blue solution and crystals of the heteroleptic copper(II) complex [(en)Cu(Me-α-D-Man*p*2,3H$_{-2}$)] · 2 H$_2$O. The crystal-structure determination reveals that the copper center is coordinated in a square planar geometry (compare **37**, **39**, **72**) with two of the four coordination sites occupied by the *cis*-O2$_{ax}$,O3$_{eq}$ diolato moiety of **102** in a ^{4}C$_1$-conformation (ax = axial, eq = equatorial) [20]. The homoleptic cuprate **108** (❯ *Fig. 21*) is obtained by a reaction of Cu(OH)$_2$ with the double-molar amount of **102** in strong alkaline solution. The coordination pattern of the carbohydrate is similar to that observed in the just described heteroleptic complex: both pyranosides are in a ^{4}C$_1$-conformation and act as *cis*-O2$_{ax}$,O3$_{eq}$ diolato ligands. The preference of the *cis*-O2$_{ax}$,O3$_{eq}$ chelation site to the *trans*-O3$_{eq}$,O4$_{eq}$ site may be explained by the acidity of the hydroxyl functions (the acidity decreases in the sequence O2-H > O3-H > O4-H) as well as by the difference of the corresponding O–C–C–O torsion angles in **108** and in free methyl-α-D-mannopyranoside, respectively. The torsion angles of the chelating diolato moieties in **108** are 47.5° and 47.8°, respectively, which is about 8° less than the O2$_{ax}$–C–C–O3$_{eq}$
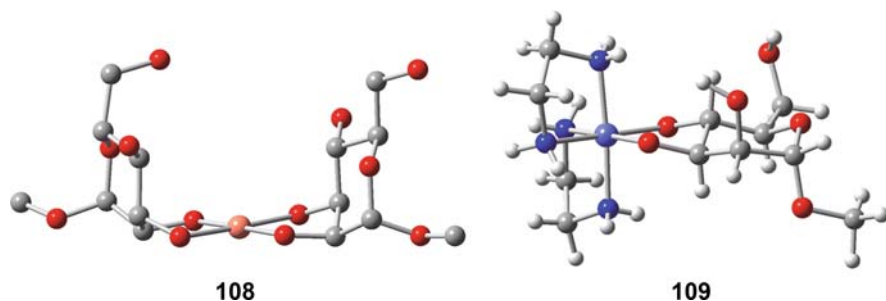
◼ Figure 21
The molecular structures of [Cu(Me-α-D-Man$p$2,3H$_{-2}$)(Me-α-D-Man$p$2,3,4H$_{-3}$)]$^{3-}$ 108 in crystals of Li$_3$108 ·
5 H$_2$O and Δ-[(en)$_2$Co(Me-α-D-Man$p$3,4H$_{-2}$)]$^+$ 109 in crystals of 109ClO$_4$ · NaClO$_4$ · 2 H$_2$O (hydrogen atoms
omitted for clarity in 108)

torsion angle and about 20° less than the O3$_{eq}$–C–C–O4$_{eq}$ torsion angle in free $^4C_1$-methyl-
α-D-mannopyranoside [114]. Obviously the diol residue causing less conformative strain of
the pyranoside is chosen as the chelation site [85].

Besides the conformative strain and acidity of the hydroxyl functions, however, steric factors
may also influence the selection of a chelation site. In the complex cation **109** (❂ *Fig. 21*), the
cobalt(III) center is coordinated by the *trans*-O3$_{eq}$,O4$_{eq}$ diolato moiety of **102**. The latter forms
a torsion angle of 53.9° which is just about 1.8° less than the *cis*-O2$_{ax}$,O3$_{eq}$ torsion angle of
free $^4C_1$-methyl-α-D-mannopyranoside. Thus only little deformation of the pyranoside would
be necessary with a *cis*-O2$_{ax}$,O3$_{eq}$ chelation site. However, a comparison of the structures **108**
and **109** (❂ *Fig. 21*) reveals that the latter site is unfavorable in **109** for steric reasons. The
involvement of an axially bonded oxygen atom in a five-membered chelate ring results in
an approximately perpendicular orientation of the planes of the chelate ring and the pyranose
ring (compare **108**), while the planes are coplanar with two equatorially bonded oxygen ligator
atoms (compare **109**). The perpendicular orientation is hampered in **109** by amino groups of
ethylenediamine below and above the CoO$_2$N$_2$ plane, while it is enabled in **108** in which the
coordination sites below and above the copper center are not occupied [80].

A three-dimensional, triply connected network is established in **110** (❂ *Fig. 22*) with tridentate
$^4C_1$-methyl-α-D-mannopyranoside **102** and bismuth(III) (the figure shows the symmetrically
independent bismuth atoms and mannopyranosides). Each of the carbohydrates acts as triolato
ligand and is bonded in five-membered chelate rings formed by the *cis*-O2$_{ax}$,O3$_{eq}$ as well
as by the *trans*-O3$_{eq}$,O4$_{eq}$ diolato moieties to two bismuth centers with O3 in the μ_2 mode.
The torsion angles of the *cis*-diols (48.3°, 49.4°) are smaller than those of the *trans*-diols
(55.4°, 57.4°) as is found in **108** (❂ *Fig. 21*) and in free methyl-α-D-mannopyranoside. The
two independent bismuth atoms bonded to the *trans*-O3$_{eq}$,O4$_{eq}$ diolato moieties are located
on sites which possess site symmetry 3 and are the branching points of the network [115].

Moreover, several vanadate chelate esters with O4- and O6-protected derivatives of $^4C_1$-
methyl-α-D-mannopyranoside have been structurally characterized. In all these esters the
remaining unprotected hydroxyl functions of the *cis*-O2$_{ax}$,O3$_{eq}$ diol residue act as the chela-
tion site. The dinuclear vanadate chelate ester **111** (❂ *Fig. 22*) is obtained with methyl-4,6-*O*-
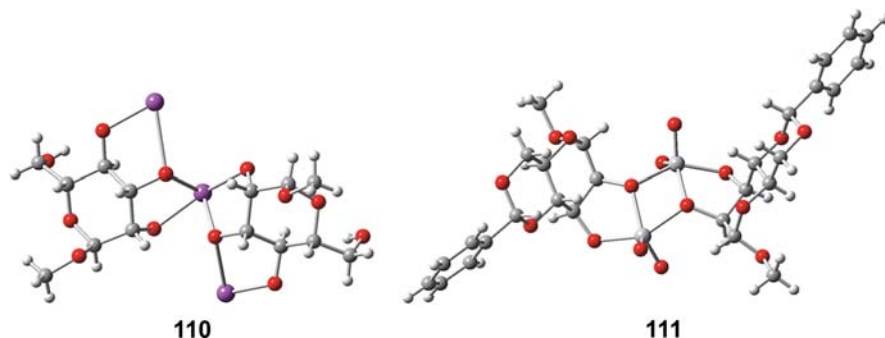benzylidene-α-D-mannopyranoside. The two VO$_2^{2+}$-centers are bridged by two O2-alkoxido

110   **111**

▣ **Figure 22**
The molecular structures of [Bi$_{5/3}$(Me-α-D-Man$p$2,3,4H$_{-3}$)$_2$]$^-$ 110 in crystals of Na$_2$110(OH) · 12 H$_2$O and [{VO$_2$(Me-4,6-O-benzylidene-α-D-Man$p$2,3H$_{-2}$)}$_2$]$^{2-}$ 111 in crystals of [NBu$_4$]$_2$111

functions and have a distorted trigonal-bipyramidal geometry. As a consequence of the small crystal radius of 0.60 Å of a penta-coordinated vanadium(V) [116] the torsion angles of the chelating *cis*-O2$_{ax}$,O3$_{eq}$ diolato functions are just 39.5° and 40.1° with O2–O3 distances of 2.49 Å and 2.50 Å respectively [117]. Only one of the two hydroxyl functions of the chelating *cis*-O2$_{ax}$,O3$_{eq}$ diol residue is deprotonated in the vanadate esters of methyl-4,6-di-*O*-methyl-α-D-mannopyranoside [118,119,120], and methyl-4,6-*O*-benzylidene-α-D-mannopyranoside [121], namely the one located in the *trans*-position to the *N*-ligator atom of the auxiliary ligands bonded tridentately to the vanadium(V) centers. A comprehensive review concerning this type of vanadate chelate esters has been written by Chakravorty et al. [11].
Methyl-β-D-galactopyranoside (Me-β-D-Gal$p$) **103** in its $^4C_1$-conformation comprises two adjacent diol functions: a *trans*-O2$_{eq}$,O3$_{eq}$ diol and a *cis*-O3$_{eq}$,O4$_{ax}$ diol. Analogously to methyl-α-D-mannopyranoside in **109** (❯ *Fig. 21*), methyl-β-D-galactopyranoside acts as chelating ligand in a bis(ethylenediamine)cobalt(III) complex through its *trans*-O2$_{eq}$,O3$_{eq}$ diolato moiety for sterical reasons [80]. A torsion angle of just 32.3° (55.6° in free Me-β-D-Gal$p$ [122]) is formed by the chelating *cis*-O3$_{eq}$,O4$_{ax}$ diolato group of methyl-β-D-galactopyranoside in the rhenium(V) complex **112** (❯ *Fig. 23*) while the torsion angle of the *trans*-O2$_{eq}$,O3$_{eq}$ diol is enlarged to 75.7° (62.9 in free Me-β-D-Gal$p$). A comparably strained pyranoside is present in methyl 3,4-*O*-isopropylidene-β-D-Gal$p$ [123]. NMR-experiments reveal that the oxolane ring is oriented towards the rhenium-bonded oxo group (*syn*-isomer) in solution as well, while the *anti*-isomer is detectable as intermediate only [82].
The *cis*-O3$_{eq}$,O4$_{ax}$ diol group of 2,6-*O*-protected derivatives of methyl-β-D-galactopyranoside is also reported to act as a chelation site in a vanadate ester [120], and in the phosphinite **113** (❯ *Fig. 23*) which incorporates a five-membered dioxophospholane ring [124].
Glucopyranosides include two almost equivalent *trans*-configured diol functions: the O2$_{eq}$, O3$_{eq}$ site and the O3$_{eq}$,O4$_{eq}$ site. This may cause the formation of mixtures of metal derivatives and be the reason for very limited structural information on metal complexes of unprotected glucopyranosides. Methyl-β-D-glucopyranoside (Me-β-D-Glc$p$) **104** is found to be coordinated to a (tren)Ni^{2+}-center (tren = tris(2-aminoethylamine)) by its O3$_{eq}$,O4$_{eq}$ diolato moiety in the solid state [125]. More structures are characterized for 4,6-*O*-protected glucopyranosides since their complexation behavior is more calculable. The dinuclear titanium(IV)
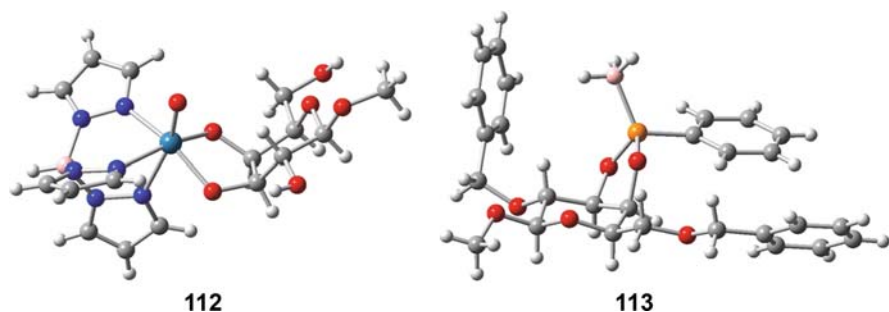
■ Figure 23
The crystal structures of [(tpb)ReO(Me-β-D-Galp3,4H_2)] 112 and methyl 2,6-di-O-benzyl-3,4-O-phenyl-phosphinediyl-β-D-Galp (P–B)borane 113

complex **114** (❷ *Fig. 24*) is formed with the 4,6-*O*-benzylidene derivative of **104** (a complex similar to **114** is obtained with the 4,6-*O*-naphthylmethylidene derivative of **104**), in which the latter acts as a bidentate but not as a chelating ligand [126]. Obviously the titanium(IV) center (crystal radius 0.56 Å [116]) is too small to be chelated by a *trans*-configured diol of a (gluco)pyranoside, while the next-in-size homolog zirconium(IV) (crystal radius for hexacoordinated Zr^{IV}: 0.86 Å [116]) is chelated in a dinuclear complex with the carbohydrate used in **114** [127]. Pentacoordinated tin(IV) (crystal radius 0.76 Å [116]) is of a size suitable to be chelated by such a ligand as well. In the dinuclear complex **115** (❷ *Fig. 24*) which has a constitution comparable to **111** (❷ *Fig. 22*), the *trans*-$O2_{eq},O3_{eq}$ diolato chelation site is coordinated to a $(n\text{-Bu})_2Sn^{2+}$ center while a second $(n\text{-Bu})_2Sn^{2+}$ center is bonded by the bridging O3-alkoxido function [128]. NMR studies reveal that the chelation of pentacoordinated vanadium(V) (crystal radius 0.60 Å [116]) with the *cis*-configured $O2_{ax},O3_{eq}$ diolato site of mannopyranoside is preferred over the *trans*-configured $O2_{eq},O3_{eq}$ diolato site of glucopyranoside [117].

■ Figure 24
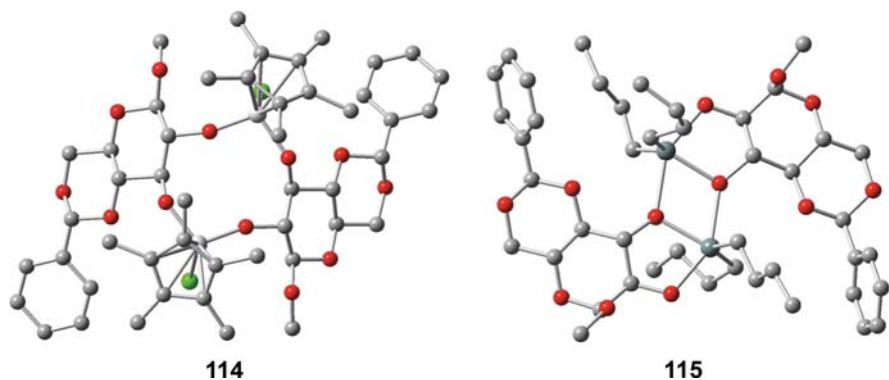The crystal structures of [(Cp*TiCl)-μ-(methyl 4,6-O-benzylidene-β-D-Glcp2,3H_2)]_2 114 and [(Sn(n-Bu)_2)-μ-(methyl 4,6-O-benzylidene-α-D-Glcp2,3H_2)]_2 115 (hydrogen atoms omitted for clarity)

A homoleptic cuprate similar to **108** (❯ *Fig. 21*) is formed with the $^1C_4$-conformer of methyl α-L-rhamnopyranoside **107** with the *cis*-O2$_{ax}$,O3$_{eq}$ diolato moiety acting as the chelation site [129]. However, chelation with the *trans*-O2$_{eq}$,O3$_{eq}$ diolato moiety of methyl-β-D-xylopyranoside (Me-β-D-Xyl*p*) **106** is observed in the heteroleptic copper(II) complex **116** (❯ *Fig. 25*), in which a water molecule is bonded to the now pentacoordinated copper center with a distance of 2.26 Å [130]. According to Shannon, the crystal radii of penta- and tetracoordinated (in a square planar geometry) copper(II) are 0.79 Å and 0.71 Å respectively [116]. A transformation of the more stable $^4C_1$-conformer of free methyl-β-D-ribopyranoside (Me-β-D-Rib*p*) **105** to the $^1C_4$-conformer is observed in the trinuclear rhenate **117** (❯ *Fig. 25*). A suitable arrangement of oxygen ligator atoms is provided by the all-*cis*-O2$_{ax}$,O3$_{eq}$,O4$_{ax}$ triolato moiety which is bonded to the Re$_3$-core with all alkoxido functions in the μ_2 mode [32].

116   **117**
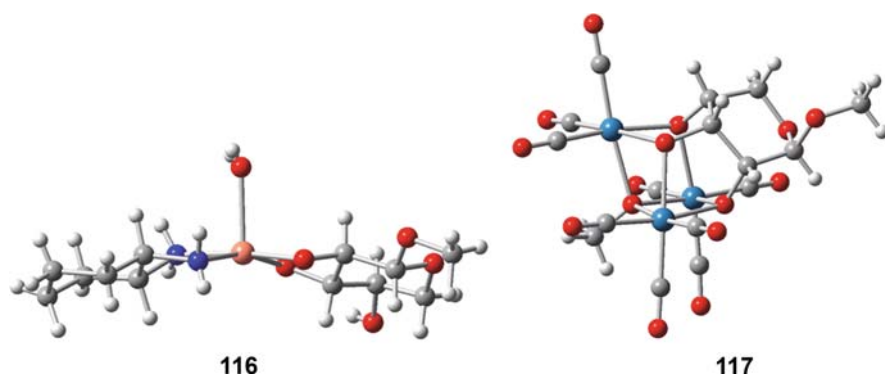
◻ **Figure 25**
The molecular structures of [(R,R-chxn)(H$_2$O)Cu(Me-β-D-Xyl*p*2,3H$_{-2}$)] 116 in crystals of 116 · H$_2$O and [Re$_3$(CO)$_9$-(μ_3-OMe)(μ_3-^{1}C$_4$-Me-β-D-Rib*p*2,3,4H$_{-3}$)]$^-$ 117 in crystals of (DBUH)117

6.2 Furanosides

Methyl-β-D-ribofuranoside (Me-β-D-Rib*f*) **118** comprises a *cis*-O2,O3 diol group and often shows a complexation behavior like its non-chiral analog anhydroerythritol, the complexes of which have been described above. A bis(diolato) borate similar to **121** (❯ *Fig. 26*), for example, is also formed with anhydroerythritol. The boron center is tetrahedrally coordinated by two chelating *cis*-O2,O3 diolato groups which form torsion angles of 12.8° and 9.2° with O2–O3 distances of 2.32 Å and 2.30 Å respectively. These rather small angles and distances are accessible by furanoidic diol groups but not by pyranoidic diol groups as a consequence of the small boron atom. Solutions with a molar ratio of B:**118** of 1:2 contain two diastereomeric forms of **121** (❯ *Fig. 26*) as well as monodiolato-dihydroxo borate [87]. In the ruthenium complex cation [(*mer*-dien)(NO)Ru(Me-β-D-Rib*f*2,3H$_{-2}$)]$^+$, the O3 and O2 ligator atoms of the diolato moiety occupy two equatorial sites trans to NO and the central nitrogen atom of dien, respectively. The *trans*-influence of the NO group results in a Ru–O distance which is
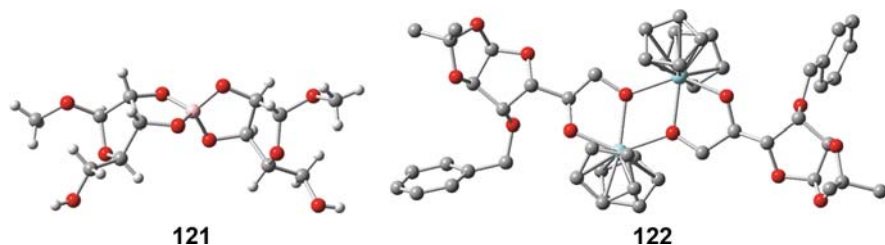
◻ Figure 26
The molecular structures of [B(Me-β-D-Rib*f*2,3H_−2)]⁻ 121 in crystals of Na121 · 2 H₂0 and [{Zr(Cp)₂(3-*O*-benzyl-1,2-*O*-isopropylidene-α-D-Glc*f*5,6H_−2)}₂] 122 in crystals of 122 · C₇H₈. The hydrogen atoms have been omitted for clarity in 122

about 0.15 Å shorter than the other Ru–O distance. Two species have been identified in the mother liquor, both showing a ^{13}C NMR downfield shift of about 15 ppm for the carbon atoms of the chelating diolato residue [81]. Three isomers already described for silicate complexes of anhydroerythritol have also been identified in solutions of [SiR(Me-β-D-Rib*f*2,3H_−2)2]⁻ (R = Ph, OMe): *anti/anti*, *syn/anti*, and *syn/syn*. A downfield shift of 1.4–2.5 ppm is observed for the carbon atoms of the chelating diolato moiety [92].
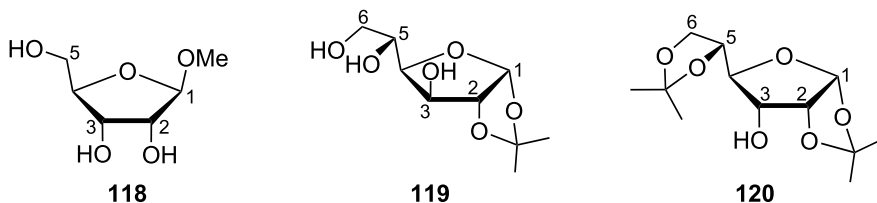

The 5-methyl-protected derivative of **118** has been found to act as a chelating ligand in vanadate esters in which only one of the two coordinating hydroxyl groups of the *cis*-diol moiety is deprotonated [119,120]. 1,2-*O*-isopropylidene-α-D-glucofuranose **119** is bonded to a Ru₃(CO)₈$^{2-}$ residue as a tetradentate ligand, namely through the hydroxyl function at C6, two μ_2-alkoxido functions at C3 and C5, respectively, and the oxygen atom of the furanose ring [131]. The three hydroxyl oxygen atoms of **119** act as facially coordinating sites in an octahedral platinum(IV) complex, which is, interestingly, also obtained when the 5,6-*O*-isopropylidene derivative of **119** is used as the starting material. The same complexation behavior is shown by 1,2:5,6-di-*O*-isopropylidene-α-D-allofuranose **120** [132,133]. These and many more furanoside and other carbohydrate complexes with platinum-group metals have been described already in a comprehensive review written by Steinborn and Junicke [7].

The two remaining hydroxyl functions at C5 and C6 of the 3-*O*-benzyl derivative of **119** are deprotonated and act as the chelation site in the dinuclear zirconium(IV) complex **122** (❯ *Fig. 26*) in which the less-stressed terminal alkoxido functions are in a bridging mode in the solid state as well as in solution [134].

6.3 Nucleosides

An *N*-glycosidic linkage between *β*-D-ribose and the nucleobases adenine, guanine, hypox-anthine, cytosine, and uracile leads to the ribonucleosides adenosine (ado) **123**, guanosine (guo) **124**, inosine (ino) **125**, cytidine (cyd) **126**, and uridine (urd) **127**, respectively. In the following, complexes and esters using the chelating sites of the ribose moiety are discussed.

123

124

125

126

127
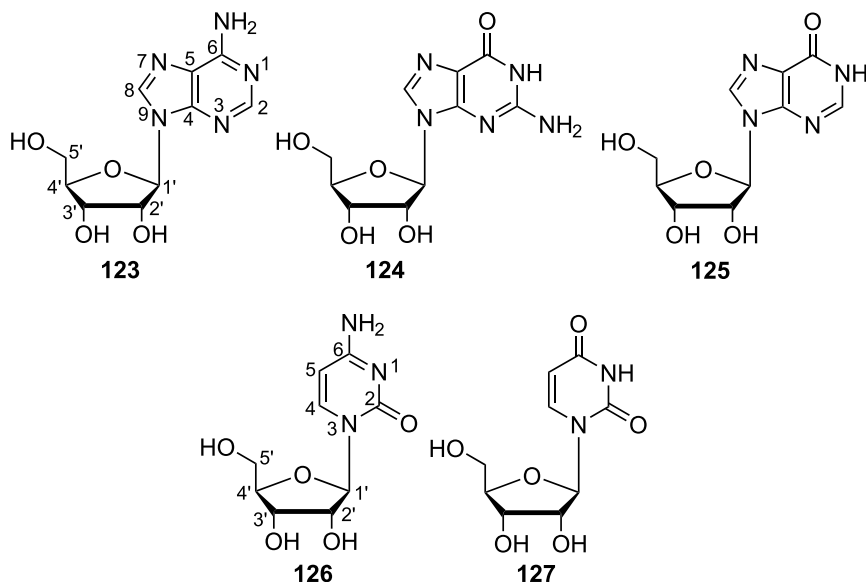
In the 1970s structural investigations of osmium(VI) and uranium(VI) complexes with adenosine **123** and its 5′-phosphate derivatives emphasized the chelation ability of the furanoidic *cis*-diol group. In the crystal structure of the mononuclear heteroleptic complex [OsO$_2$(py)$_2$(Ado2′,3′H$_{-2}$)] (py = pyridine), adenosine acts as diolato ligand with its ligator atoms O2′ and O3′ being *trans* to the nitrogen atoms of the two coordinating pyridine molecules. The reported π stacking of the adenine bases is a structural feature typical for solid-state nucleoside complexes [135]. With 2,2′-bipyridyl instead of the two pyridine molecules, osmium(VI) complexes similar to that described above are also obtained in neutral aqueous solution with 5′-phosphate derivatives of adenosine **123** and uridine **127**, respectively [136]. Di- and tetranuclear UO^{2+} complexes are formed at pH 11 with adenosine-5′-monophosphate with O3′ of the chelating diolato moiety bridging between two uranium centers (compare dinuclear VO^{2+} complex **128**, ❷ *Fig. 27*) while at pH 7.5 the uranium centers are coordinated by phosphate oxygen atoms only [137]. The same behavior is also shown by adenosine-5′-di- and -triphosphate with the exception that no dinuclear species is observed with the diphosphate [138]. The dimeric dinuclear solid-state structure of the vanadium(V)-adenosine complex anion **128** (❷ *Fig. 27*) has been found to be maintained as the main species besides several minor products in a solution of pH 6.5 [139]. The dimeric structure has been suggested by most of the groups working on the investigation of the solution structures of vanadium

128   **129**
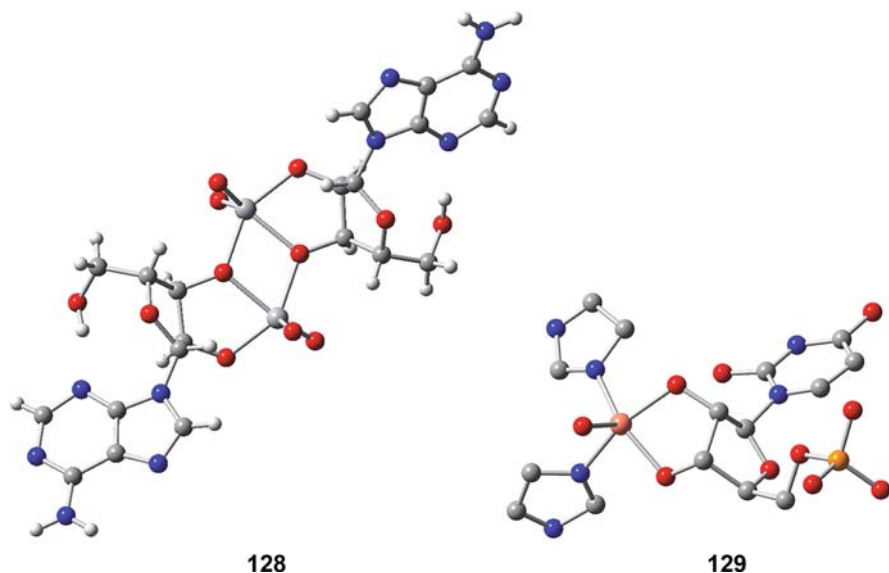
■ **Figure 27**
The molecular structures of [{VO$_2$(Ado2′,3′H$_{-2}$)}$_2$]$^{2-}$ **128** in crystals of [NEt$_4$]$_2$**128** · 4.74 H$_2$O and [Cu(5′-UMP2′,3′H$_{-2}$)(im)$_2$(H$_2$O)] **129** in crystals of **129** · 4 H$_2$O (hydrogen atoms omitted for clarity). Abbreviations: UMP = uridine monophosphate, im = imidazole

complexes with the nucleosides **123–127** as well as their 5′-derivatives in the years before the detection of **128** (❷ *Fig. 27*) [117,140,141,142,143,144,145,146].

Dinuclear subunits similar to **128** are also found in the octanuclear copper-uridine complex anion [Cu$_8$(Urd3,2′,3′H$_{-3}$)$_8$]$^{8-}$, in which two square-planar coordinated copper atoms are linked by two O2′ ligator atoms of two triply deprotonated uridine moieties. The coordination sphere of the copper centers is completed by a nitrogen atom (N1) of the nucleobase of uridine [147]. The mononuclear copper complex **129** (❷ *Fig. 27*) is formed with uridine-5′-monophosphate in neutral aqueous solution in which the diol is deprotonated as a result of the chelation at the copper center while the non-coordinating nucleobase is not deprotonated under these conditions [148]. 3-Acetamidophenylboronic acid reacts with the diol group of adenosine to a cyclic monoester with tricoordinate boron [149], whereas the reaction of boric acid and guanosine in strong alkaline aqueous solution leads to reaction products similar to those described above for the boron-anhydroerythritol system: two stereoisomers of bis(diolato)borates (compare **121**, ❷ *Fig. 26*) exist in addition to monodiolato-dihydroxo borate ester [87]. The coordination behavior of CpMo^{2+} towards the ribonucleosides **123**, **124**, **126**, and **127** and the corresponding 5′-monophosphates has been shown to be pH-dependent. At a pH of 9, the molybdocene centers are chelated exclusively by the diolato moiety, while in neutral solution a coordination of the nucleobase and phosphate oxgen atoms is also observed [150].

The reaction of cytidine **126** with [*mer*-(dien)(NO)RuCl$_2$]PF$_6$ in an aqueous solution of a pH of 12.5 leads to two isomers of diolato complexes similar to those described above with **118** while guanosine and uridine—both providing deprotonated amide functions under these conditions—are bonded to the ruthenium center by their nucleobases [81].

Homoleptic bis(diolato) bismuthates and antimonates are formed with adenosine as well as with guanosine in alkaline solutions with a pH of at least 11. The coordination pattern of all the complexes resembles the one in the bis(adenosinato)antimonate **130** (❯ *Fig. 28*): two nucleosides act as diolato ligands and occupy four of five coordination sites of the metal centers which are coordinated in a distorted trigonal-bipyramidal geometry with the stereochemically active lone pair in an equatorial orientation. Being identical in all the structures, the packing of the guanosinato complex anions is stabilized by two intermolecular hydrogen bonds of the type N2–H···N3 between two adjacent guanine base pairs. A CIS of 3–6 ppm of the carbon atoms C2′ and C3′ involved in the five-membered chelate ring formed by bismuth(III) and antimony(III) with adenosine **123**, guanosine **124**, and inosine **125** indicates that the coordination mode is maintained in alkaline solution [151,152].

The formation of several penta- or hexacoordinated silicate complexes is observed on the addition of adenosine, guanosine, and cytidine to aqueous alkaline silicate solutions. Hexacoordination is favored by an increase of the pH and high molar ratios of furanoidic cis-diol:silicon [94]. Hexacoordinate silicon is present in the homoleptic tris(diolato)silicate **131** (❯ *Fig. 28*) with cytidine **126** as chelating ligand. Pentacoordinate methoxy- or phenyl-bis(nucleosidato)silicates of the type [SiR(Nuc2′,3′H$_{-2}$)2]$^-$ (R = Ph, OMe) are obtained with the nucleosides (Nuc) adenosine and cytidine in methoxide-containing methanolic solutions. Different *syn/anti*-isomers similar to those observed with anhydroerythritol or methyl-β-D-ribofuranoside can be identified by ^{29}Si- and ^{13}C NMR data [92].

130   **131**
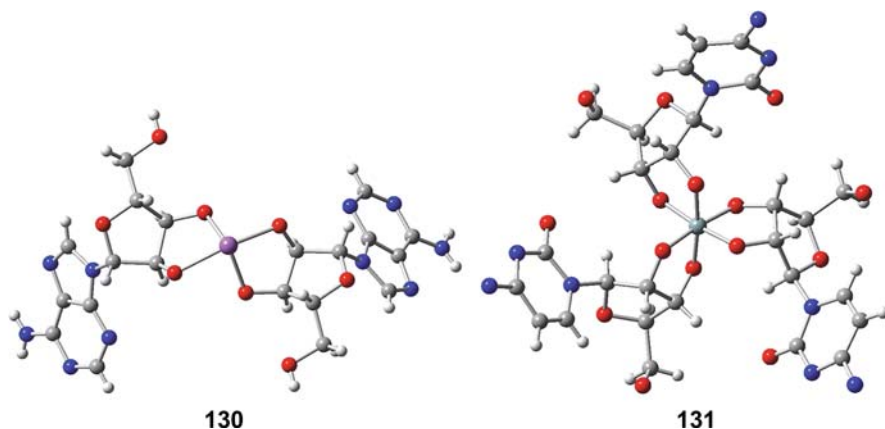
◨ **Figure 28**
The molecular structures of [Sb(Ado2′,3′H$_{-2}$)]$^-$ **130** in crystals of Na**130** · H$_2$O and [Λ-Si(Cyd2′,3′H$_{-2}$)$_3$]$^{2-}$ **131** in crystals of Cs$_2$**131** · 21.5 H$_2$O

4

6.4 Non-Reducing Disaccharides

Metal complexes of non-reducing disaccharides such as sucrose (β-D-Fru$f$-(2↔1)-α-D-Glc$p$) **132** or α,α-trehalose (α-D-Glc$p$-(1↔1)-α-D-Glc$p$) **133** not only deserve interest in their own right but also as model compounds for the corresponding complexes with oligo- and polysaccharides. Thus the action of the coordinating cellulose solvents [Pd(en)(OH)$_2$] (Pd-en), [Cu(en)(OH)$_2$] (Cu-en), [Ni(tren)(OH)$_2$] (Ni-tren), and [Cd(tren)(OH)$_2$] (Cd-tren) on the polysaccharide were derived from crystal structures with **132** and **133** (compare ❯ *Sect. 6.6*).

132   **133**
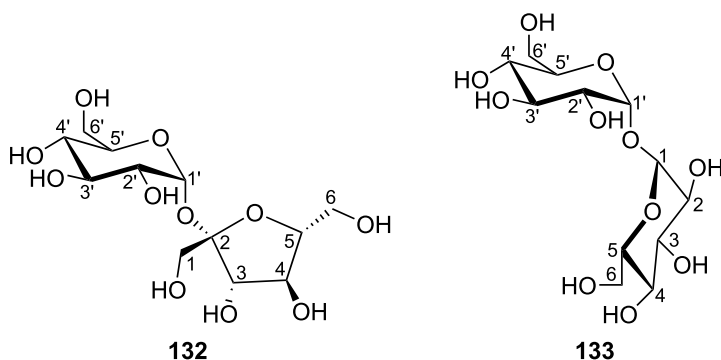
In the dinuclear complex **134** (❯ *Fig. 29*), two Pd^{II}(en) moieties are chelated by the Glc$p$-O3′,O4′- and the Fru$f$-O1,O3-diolato moieties of sucrose **132**, that is, in five- and six-membered chelates, respectively. The selection of the Glc$p$-O3′,O4′ site instead of the similar Glc$p$-O2′,O3′ site is reasonable since an intramolecular hydrogen bond of the type O2′–H···O1$^-$ stabilizes the sucrose residue in a conformation which is also found for the free carbohydrate (there with a hydrogen bond of the type O1–H···O2′ in the reversed direction) [84,153]. A similar coordination and hydrogen-bond pattern is found with Cu^{II}(en) [153]. However, only a mononuclear complex with the Ni^{II}(tren) residue bonded to the Glc$p$-O2′,O3′ diolato site is obtained in a reaction of Ni-tren and sucrose in molar ratio of 2:1. In this complex, the intramolecular hydrogen bond O1–H···O2′ which is also found in free sucrose is retained [125,153]. A dicationic Δ-configured complex is formed by sucrose and bis(phenanthroline)cobalt(III) in which the metal center is involved in an eight-membered ring with the Glc$p$-O2′- and the Fru$f$-O1 chelation sites. NMR data reveal that O2′ is deprotonated and they support the structure of the Δ-configured complex by the observation of an NOE involving the sucrose and phenanthroline residues [154].

Two crystal structures of metal complexes of α,α-trehalose **133** are reported. Two Cd^{II}(tren) residues are chelated by the Glc$p$-O2,O3 and the Glc$p$-O2′,O3′ diolato moieties, respectively, in the dinuclear complex **135** (❯ *Fig. 29*). As in free α,α-trehalose in the crystalline state, direct intramolecular hydrogen bonds are not found due to conformational restraints, but two sequences of the type O2$^-$···H–O^w···H–O6′ with a linking water molecule H$_2$O^w are observed (the reversed direction is found in free α,α-trehalose) [153]. Only one of the two Glc$p$-O2,O3-chelation sites of α,α-trehalose is chosen in a mononuclear complex with Ni-Me$_3$tren, the $N,N′,N''$-trimethyl analog of Ni-tren, in which no support by an intramolecular
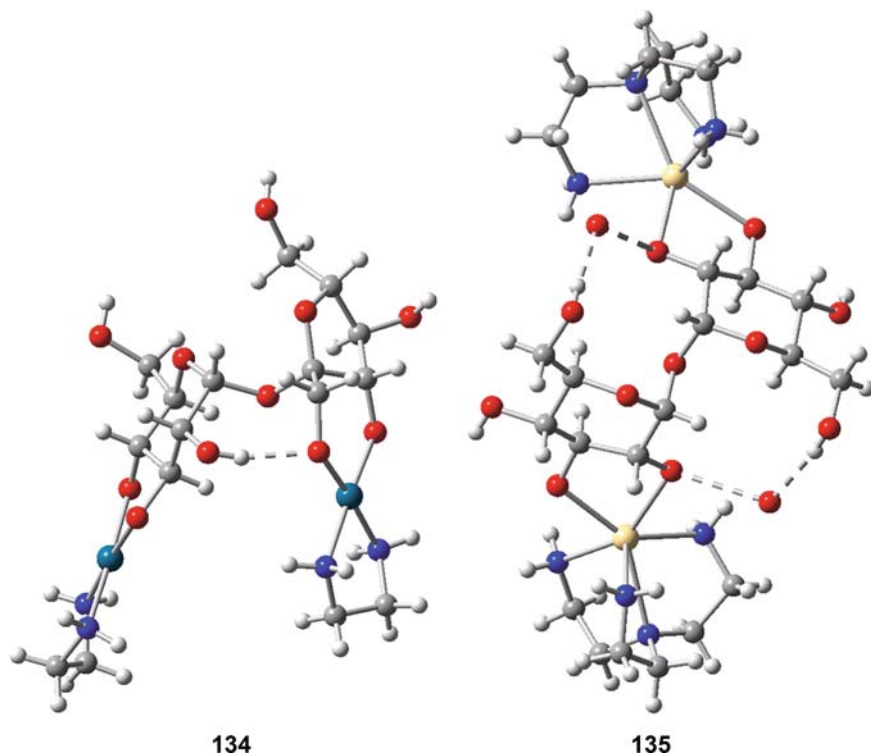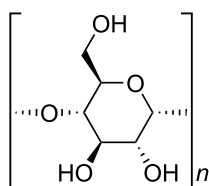
▣ Figure 29
The molecular structures of [(en)$_2$Pd$_2$(Suc1,3,3′,4′H$_{-4}$)] 134 in crystals of 134 · 11 H$_2$O and [(tren)$_2$Cd$_2$(α,α-Tre2,3,2′,3′H$_{-4}$)] · 2 H$_2$O 135 in crystals of 135 · 15 H$_2$O. *Dashed lines*: hydrogen bonds

hydrogen bond is observed. It seems that in this case the chelation is governed by the enhanced acidity of the Glc$p$-O2,O3 site compared to the Glc$p$-O3,O4 site [125].

6.5 Cyclodextrins

Cyclodextrins (CD) are cyclic torus-shaped oligosaccharides with n α-(1↔4)-glycosidic-linked glucose molecules ($n=6$: α-CD, $n=7$: β-CD, $n=8$: γ-CD) (**136**). All the Glc$p$-O2,O3 diol functions are oriented to the same side of the torus resulting in a regularly arranged coordination site pattern. This enables the formation of sandwich-type complexes in which the metal centers are enclosed between the bisdiol moieties of two CD molecules (double torus). The number of metals being chelated by the diol functions depends on factors such as the Lewis acidity of the metal or the size of the alkali counterion. Six bismuth(III) centers are bonded by six bisdiolato moieties provided by two α-cyclodextrin molecules in the electrically neutral C_2-symmetric structure **137** (❷ *Fig. 30*, a = view through the double torus, b = view onto the double torus) though a molar ratio of bismuth:α-CD of 3:2 was present during the reaction in aqueous sodium hydroxide. This indicates that the reaction is governed less by stoichiometry than by molecular recognition, and, as a consequence, **137** (❷ *Fig. 30*) may

be considered a supramolecular assembly. The Lewis acidity of the bismuth(III) atoms is sufficient to force complete deprotonation of the bisdiol moieties (compare the structures with adenosine, guanosine or methyl-α-D-mannopyranoside, for example). This leads to almost square O_4 patterns between adjacent bisdiolato moieties which are suited to coordinate sodium ions located within the double torus (**138**). The coordination sphere of the six sodium ions is completed by six water molecules, respectively, which are arranged in a homodromic hexaqua cycle (**137a**, ❷ *Fig. 30*). A similar structure is obtained with oxo-vanadium(IV) instead of bismuth(III) in which the oxo group bonded to the vanadium atom replaces the stereochemically active lone pair of the bismuth(III) centers [155]. Complete deprotonation of two γ-CD tori is also observed in the hexadecanuclear lead(II) complex [$Pb_{16}(\gamma$-CDH$_{-16})_2$] which has been crystallized from a reaction mixture containing excessive γ-CD. Eight lead atoms each are located within the double torus (compare the sodium sites in **137**, ❷ *Fig. 30*) and outside the double torus (compare the bismuth sites in **137**, ❷ *Fig. 30*), respectively. The resulting lead-alkoxido substructure is comparable to that observed in **78** (❷ *Fig. 16*) [156].
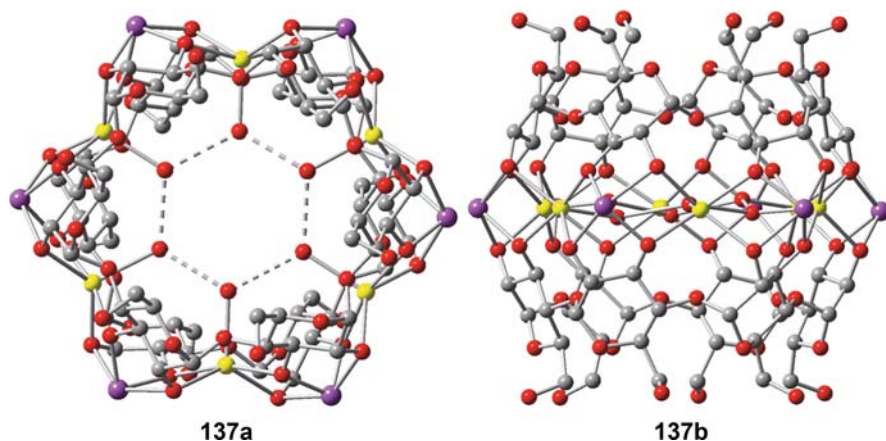

136

bold lines: hydrogen bonds
dashed lines: alkali ion-oxygen bonds

glucose-atom-numbering scheme on
the top left side

hydrogen atoms omitted for clarity

138

139

140

137a **137b**
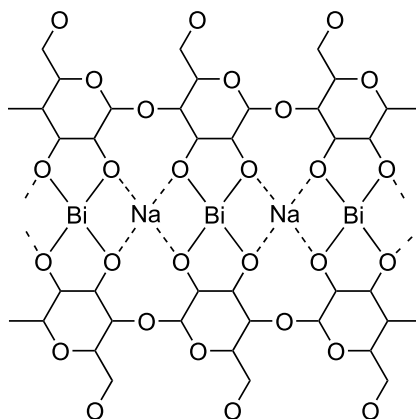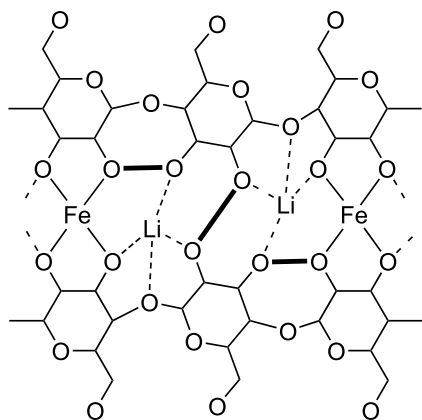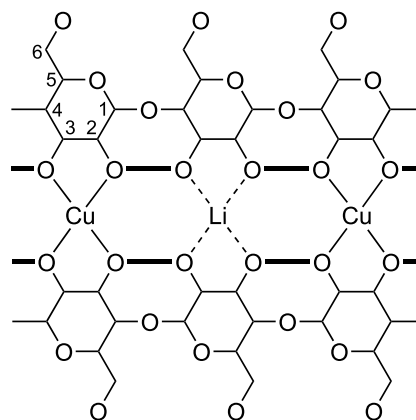
◾ **Figure 30**
The molecular structure of [Na$_6$(H$_2$O)$_6$Bi$_6$(α-CDH$_{-12}$)$_2$] **137** in crystals of **137** · 47 H$_2$O in a view through the double torus (**137a**) and in a view onto the double torus (**137b**). Bi atoms (violet), Na atoms (yellow). Hydrogen atoms omitted for clarity. *Dashed lines*: hydrogen bonds

Less Lewis acidic metals such as iron and manganese in their oxidation states +II cannot afford complete deprotonation but three of them are bonded by every second bisdiolato moiety in an α-CD double torus with the formula [Li$_6$(H$_2$O)$_6$M$_3$(H$_2$O)$_3$(α-CDH$_{-12}$)$_2$]$^{5-}$ (M = Mn, Fe). The fact that Fe^{II} or Mn^{II} are chelated by diolato functions of cyclodextrins might be surprising since no diolato complexes with simpler carbohydrates are known, but is comprehensible on a closer look at the structure **139**. The increased acceptor functions of the deprotonated diolato sites are stabilized by hydrogen bonds as well as by Li cation contacts. One of the adjacent not iron- or manganese-bonded glucose units is tilted towards a chelating glucose unit resulting in a shortening of the O2′–O3′ hydrogen bonds (O2′–O3′ distance about 2.5 Å in **139**). This way two optimal sites for the coordination of two lithium ions are generated between two bisdiolato moieties. Each of the six lithium ions occupying these sites bears an additional water molecule which, in turn, is arranged in a homodromic hexaqua cycle comparable to that in **137a** (❷ *Fig. 30*) [155]. A similar coordination and hydrogen bond pattern is established in a sandwich-type tetracuprate with β-CD, [Li$_7$(H$_2$O)$_7$Cu$_4$(β-CDH$_{-11.5}$)$_2$]$^{4-}$. However, one lithium ion is bonded to the O$_4$ site between two adjacent bisdiolato-cuprates comparable to the sodium atoms in **137** (❷ *Fig. 30*) [157].

Trinuclear sandwich-type cuprates of the type [A$_3$(H$_2$O)$_3$Cu$_3$(α-CDH$_{-6}$)$_2$]$^{6-}$ are formed with lithium and sodium as counterions A, whereas dinuclear [Cu$_2$(α-CDH$_{-4}$)$_2$]$^{4-}$ are isolated as potassium and rubidium salts. The lithium- and sodium cuprates contain the substructure **140** in which the copper atoms are coordinated by two bisdiolato moieties in a slightly distorted square planar geometry and the alkali ions mainly occupy the bisdiol sites located between two cuprates. Stabilizing hydrogen bonds of the type O–H···O$^-$ between non-deprotonated diol moieties and the adjacent diolato moieties are formed. Each of the alkali ions bears a water molecule as a fifth ligand. These bonds are directed towards the outside of the cylindic tricuprates (compare the in-torus bonded aqua ligands in **137**, ❷ *Fig. 30*). In the less-

deprotonated dicuprates, however, no incorporation of the larger, less-polarizing alkali metals potassium and rubidium is observed. These compounds are stabilized by short cooperative hydrogen bonds depicted in **141**. The anhydroglucose units not bearing a copper atom have to be tilted slightly to enable inter-cyclodextrin hydrogen bonds of the type O3–H···O3 [158].

bold lines: hydrogen bonds

hydrogen atoms omitted for clarity

141
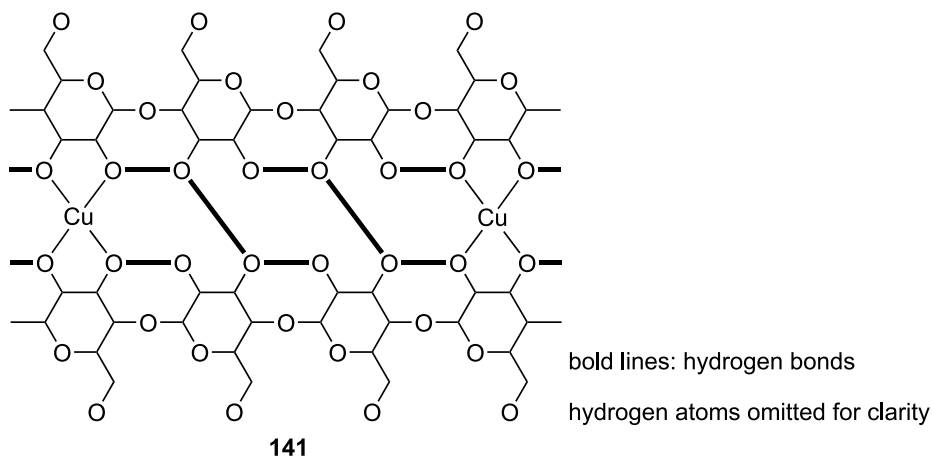
$Co^{III}(en)_2$ and $Co^{III}(cyclen)$ (cyclen = 1,4,7,10-tetraazacyclododecane) residues are coordinated by a diolato moiety of α-CD or β-CD in an aqueous alkaline solution (compare $Co^{III}(en)_2$ complexation by a pyranosidic diolato moiety in **109**, ❷ *Fig. 21*). This coordination mode could be confirmed by a large downfield shift of the the carbon atoms involved in the five-membered diolato-chelate ring [159].

6.6 Polysaccharides

The disaccharide structures described above give first evidence of how cellulose, a polymer formed by (1↔4)-glycosidic linking of β-D-glucose molecules, is present in coordinating solvents like Pd-en, Cu-en, Ni-tren, or Cd-tren. Supporting information could be gained by ^{13}C NMR data obtained from Pd-en solutions of DP 40 cellulose (cellulose with an average degree of polymerization of 40). A downfield coordination-induced shift of about 10 ppm of the carbon atoms C2 and C3, which is also observed for the 1,2-diolate complexation of sucrose (compare 6.4), and unsplit main signals of all of the glucose carbon atoms strongly indicate the formation of entirely palladated and molecularly dispersed cellulose **142**. The formation of intramolecular hydrogen bonds of the type $O6'$–H···$O2^-$ leads to a significant increase in chain stiffening [84,160]. The same coordination mode is suggested for Cu-en and cuoxam, an aqueous solution of copper(II)-hydroxide in ammonia, as well as for Ni-tren and Cd-tren [161,162].

142
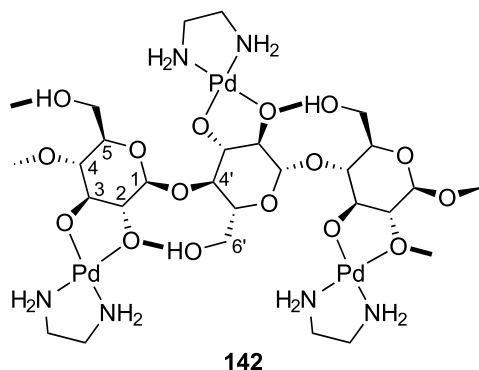
7 Reducing Carbohydrates

Although there are many data for model compounds for carbohydrates, relatively little is known about the reducing carbohydrates as ligands in metal complexes. One of the reasons for this may be the high reactivity of the reducing sugars. Furthermore their ease of oxidation and their instability in alkaline solution must be accounted for, and most importantly the monosaccharides are mixtures in solution. When a coordinating metal moiety is exposed to glucose, for example, it is hardly predictable whether the sugar will react through its α- or β-furanose, α- or β- pyranose or a less stable form. Nevertheless, the number of structurally characterized coordination compounds with reducing carbohydrates is increasing.

From the reaction between ammonium molybdate and the pentose xylose, a complex composed of a dimolybdenum core and one sugar moiety **143** [163] could be obtained.

143
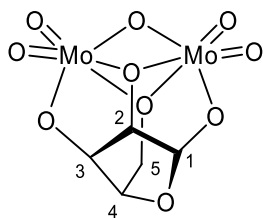
As Bilik [164,165,166] has demonstrated Mo(VI) will catalyze epimerization of pentose sugars at C2. So it is not surprising that with a reducing sugar, the first structure analysis with a transition metal complex shows lyxose as the monosaccharide in complex. The metal center is dinuclear with a triple oxygen bridge linking the two molybdenum atoms without remarkable Mo–O distances. The dinuclear metal center fixes the lyxose in an unusual furanose form, the β-D-lyxofuranose. The pseudo-rotation formulae have been applied to this form of lyxose. A phase angle of 247.7° together with a normal amplitude of pucker (reflecting the degree of non-planarity of the ring) of 35.6° is calculated. The conformation of lyxose is thus midway between the discrete descriptions ^{C4}E and $^{C4}T_{O1}$.

As the pentose sugar is able to provide an O_4 rhomb, structure analyses have shown that the O_5 pattern provided by β-mannofuranose turned out to be an ideal building block of M_2O_{10} double octahedra of binuclear metallates(III).

Thus, a series of isotypic sugar complexes of trivalent metals with the formula $Ba_2[M_2(\beta$-D-Man$f$H$_{-5})_2] \cdot$ n H$_2$O (M = Fe, V, Cr, Al, Ga, Mn; n $\approx$ 13), as shown for Mn^{III} in ❷ *Fig. 31*, has been developed [167,168].

The compounds contain a homoleptic sugar-metal complex as anion, which includes no hydroxido or oxido ligands. Instead, all the protons of the five hydroxyl groups of mannose are split off to form a pentaanionic polyolato ligand. The polyolate is derived from the β-furanose form of mannose, which is insignificant in solution [169], but is the only form with all the hydroxyl groups on one side of the ring. According to the already described epimerization of xylose towards lyxose in the presence of oxidomolybdenum(VI), D-fructose and D-glucose isomerize to the sugar ligand with the highest possible denticity, the β-mannofuranose [167].

The environments of the two metal atoms in **144** are not equivalent. M1 forms five- and six-membered chelates with the open-chain part of the ligand, whereas M2 is surrounded by two oxolanetriolato fragments in a distorted E_2 conformation. [Fe$_2$(rac-Man$f$H$_{-5})_2]^{4-}$ **145** [31] with iron as the central metal is also known. In contrast to **144**, in the C_i symmetric **145** the two Fe centers are equivalent. Besides the structure of [Mn$^{III}_2(\beta$-D-Man$f$H$_{-5})_2]^{4-}$ there is an additional structure with two different oxidation states, [Mn^{IV}Mn$^{III}(\beta$-D-Man$f$H$_{-5})_2]^{3-}$ [168]. The unexpected oxidation state +VI for one of the central atoms was unambiguously assigned and became apparent for the mean Mn–O bond length in the octahedral MnO$_6$ coordination. For Mn^{III}, the mean Mn–O distance is 2.01 ± 0.13 Å and for Mn^{VI}, it is 1.89 ± 0.03 Å.

In the structures, introduced so far, an O_4 rhomb or O_5 patterns turned out to be ideal building blocks for carbohydrate-metal complexes. The most important monosaccharide, D-glucose, in any of its hemiacetal forms does not exceed the simple O2 diol pattern (a consequence is the epimerization reaction of glucose to β-mannofuranose in the presence of trivalent metal ions).

144　　　　　　**145**
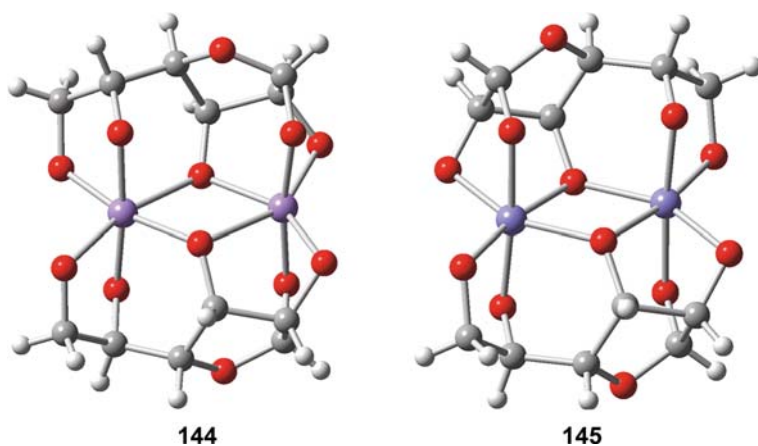
◼ **Figure 31**
Molecular structures of the tetraanions [Mn$^{III}_2(\beta$-D-Man$f$H$_{-5})_2]$^{4-}$ 144 and [Fe$_2$(rac-Man$f$H$_{-5})_2]$^{4-}$ 145 in crystals of Ba$_2$[Mn$^{III}_2(\beta$-D-Man$f$H$_{-5})_2] \cdot$ 13 H$_2$0 and Ba$_2$[Fe$_2$(rac-Man$f$H$_{-5})_2] \cdot$ 13 H$_2$0

This steric restriction is taken into account by exclusively providing the (en)Pd^{II} moiety, which is a diol chelator.

Although palladium is a good oxidant, oxidation of the aldose could be avoided to such an extent that even crystallization became possible. The first crystal structure of a metal derivative of glucose, [(en)$_2$Pd$_2$(α-D-Glc$p$1,2;3,4H$_{-4}$)] · 7 H$_2$O (**146** · 7 H$_2$O) was obtained from a solution with a 3:1 Pd:D-glucose molar ratio [170]. **146** shows the O1–O4 deprotonated α-D-glucopyranose tetraanion, which is coordinated as a bis(chelate) ligand to two palladium(II) central atoms with the Pd–O distance averages at 2.00 Å, the O–C–C–O angles are 43 and −50°. ^{13}C NMR data give evidence for the existence of an additional species [(en)$_2$Pd$_2$(β-D-Glc$p$1,2;3,4H$_{-4}$)] in solution. Reduction of the Pd:D-glucose molar ratio to 1:1 results in a mixture of monometallated glucoses. The 1,2-metallated species are of particular significance, owing to the maximum acidity of the hydroxy group at C1.
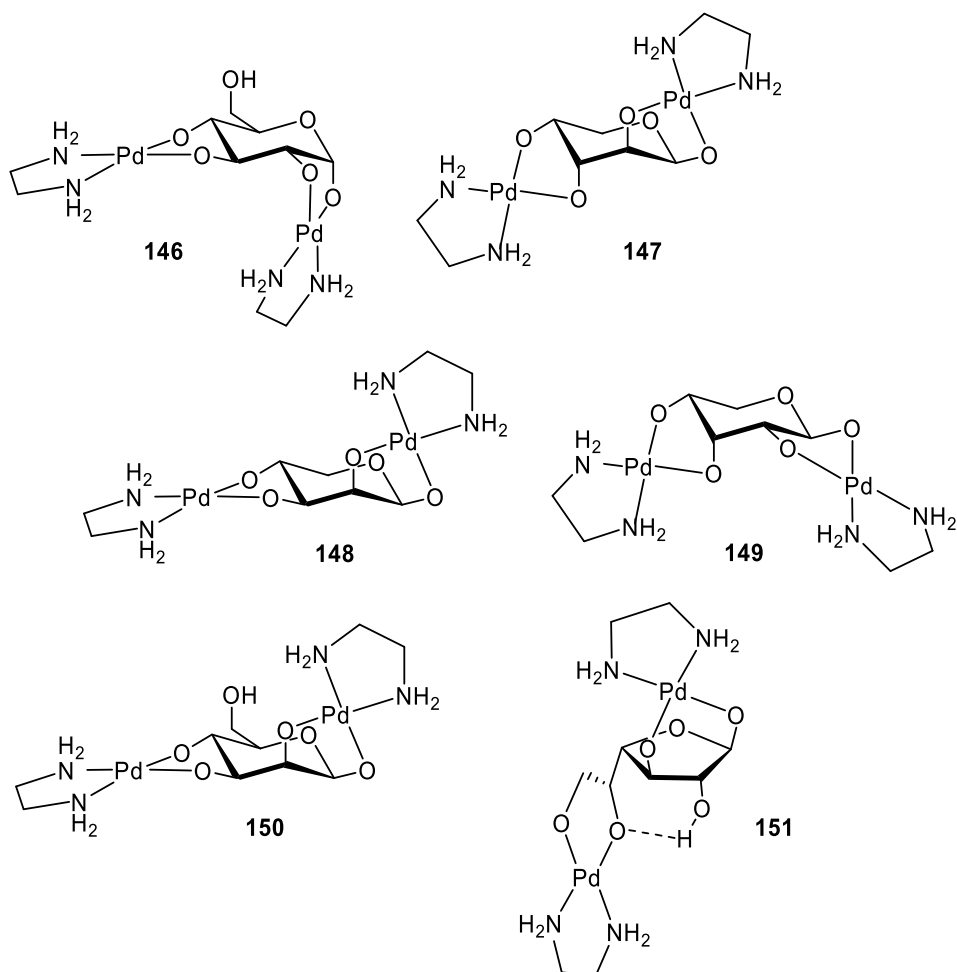
In this way several Pd_2 complexes **2**[171,172], namely [(en)$_2$Pd$_2$(β-D-Ara$p$1,2;3,4H$_{-4}$)] · 5 H$_2$O (**147** · 5 H$_2$O), [(en)$_2$Pd$_2$(β-D-Lyx$p$1,2;3,4H$_{-4}$)] · 7 H$_2$O (**148** · 7 H$_2$O), [(en)$_2$Pd$_2$(β-D-Rib$p$1,2;3,4H$_{-4}$)] · 6.5 H$_2$O (**149** · 6.5 H$_2$O), [(en)$_2$Pd$_2$(β-D-Man$p$1,2;3,4H$_{-4}$)] · 9.4 H$_2$O (**150** · 9.4 H$_2$O), which are the main species in solution, and [(en)$_2$Pd$_2$(β-D-Gal$f$1,3;5,6H$_{-4}$)] · 5 H$_2$O · C$_2$H$_5$OH (**151** · 5 H$_2$O · C$_2$H$_5$OH) could be obtained.

With the exception of **151** one of the two Pd(en) ligands binds to the O1 and O2 and the other to the O3 and O4 diol function of the β-D-pyranose form of the carbohydrate in all compounds. Further, the Pd–O distances and the O–C–C–O angles are in comparable ranges, too. **151**, however, shows a furanose form of D-galactose. Contrary to the other pyranose structures with Pd(en) moieties, a strong intramolecular hydrogen bond of the O–H···O$^-$ type is established with O2-H as the donor and O5 as the acceptor. One of the palladium atoms is coordinated by a 1,3-diolato(2-) ligand. Though this bonding mode is unusual, it is not unique, as shown for levoglucosan which binds to palladium(II) in a similar way. The second Pd(en) ligand binds to the remaining diol fragment with O5 and O6.

^{13}C NMR data show, that there exist in solution more palladium–carbohydrate species than could be obtained in crystals. Besides the above-mentioned compounds there are signals for the following species identified by the palladium induced shift of about 8 to 15 ppm: [(en)$_2$Pd$_2$(α-D-Ara$p$1,2;3,4H$_{-4}$)], [(en)Pd(β-D-Lyx$p$1,2H$_{-2}$)], [(en)Pd(β-D-Lyx$p$2,3H$_{-2}$)], [(en)$_2$Pd$_2$(α-D-Rib$p$1,2;3,4H$_{-4}$)], [(en)$_2$Pd$_2$(α-D-Xyl$p$1,2;3,4H$_{-4}$)], [(en)$_2$Pd$_2$(β-D-Xyl$p$1,2;3,4H$_{-4}$)], [(en)$_2$Pd$_2$(α-D-Gal$p$1,2;3,4H$_{-4}$)] and [(en)$_2$Pd$_2$(β-D-Gal$p$1,2;3,4H$_{-4}$)]. The dimetallation of the carbohydrates influences the distribution of the different forms of sugars in solution in contrast to the forms in equilibrium without coordination. Formation of dimetallated pyranoses requires two diol functions that are not *trans*-diaxial. Hence, for lyxopyranose and its homologue mannopyranose, only the β-anomer in its $^4C_1$ conformation can be dimetallated. The major dimetallated species in solutions of ribose and galactose can be predicted as well, since the most stable form of the free sugars in aqueous solution (β-pyranose) provides two diol functions that are well suited for palladium bonding without rearrangement. The same appears to hold true first glance for the xylose/glucose pair. However, the actual anomer distribution deviates from that of the free sugars by a shift of the concentrations towards the α-anomer. The bonding modes of dimetallated arabinopyranoses cannot be predicted. Suitable bisdiol conformations are adopted for the β-anomer both in its $^1C_4$ and $^4C_1$ conformations (two axial substituents in each case) and in its $^1C_4$-α-anomer, the latter and the $^4C_1$-β-anomer being handicapped by an anomeric effect when the findings in the xylose/glucose case are generalized. In fact, the spectra show the β-form is preferred.

While (en)Pd fragments bind to diol groups without loss of the ethylenediamine ligand (nitrogen ligation is clearly favored over alkoxide bonding), at cupric centers the prediction of a particular structure is complicated by the ability of diolato ligands to substitute nitrogen ligands. In crystals of [(NH$_3$)$_4$Cu$_3$(β-D-Lyx$p$1,2,3H$_{-3}$)$_2$(H$_2$O)$_2$] · 4 H$_2$O [172] (**152** · 4 H$_2$O), two bridging lyxose ligands adopt the β-pyranose form in C2 symmetrical, trinuclear molecules; they are each threefold deprotonated along the *cis-cis* sequence of the hydroxy groups with C1, C2, and C3.

152   **153**
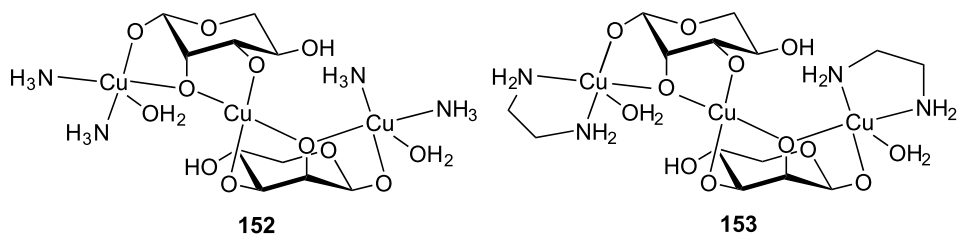
The coordination chemistry of the cupric centers is normal, that is, the bis-diolato-bonded Cu1 atom is square-planar coordinated with no further ligands, whereas Cu2, which is coordinated by a diolato ligand derived from the anomeric and the epimeric hydroxy groups, is surrounded by a square pyramid consisting of the two alkoxy oxygens, two ammine ligands and a water ligand at a longer distance. Intramolecular hydrogen bonds are established from N2–H donors and O3 acceptors. The ability of a polyolato ligand to replace ammine ligands is a prerequisite for the formation of **152**. The molecular structure of $[(en)_2Cu_3(\beta\text{-}D\text{-}Lyxp1,2,3H_{-3})_2(H_2O)_2]$ · 4 H_2O [172] (**153** · 4 H_2O) resembles that in the ammine complex, including the detail of intramolecular hydrogen bonding from amine donors to alkoxide acceptors. The structure determination demonstrates that the stronger ethylenediamine ligand is also replaced by the lyxose anions.

More examples for the higher reactivity of copper centers, in relation to the preference of diolato ligands to substitute nitrogen ligands, are given in structures **154** and **155** [173], shown in ❷ *Fig. 32*.

Complex **154** is an anionic homoleptic complex in which the five square-plane-coordinated copper(II) atoms are exclusively bound to the deprotonated $\beta\text{-}D$-mannopyranose in $^4C_1$ conformation. The increased redox stability therefore is not a consequence of the spatial separation of the oxidizing Cu(II) atoms and the half-acetal function of the monosaccharide. However, it is a consequence of the involvement of the O atoms, at the anomer C atoms, in the coordination of copper, as it is for the homoeptic lyxose complexes.
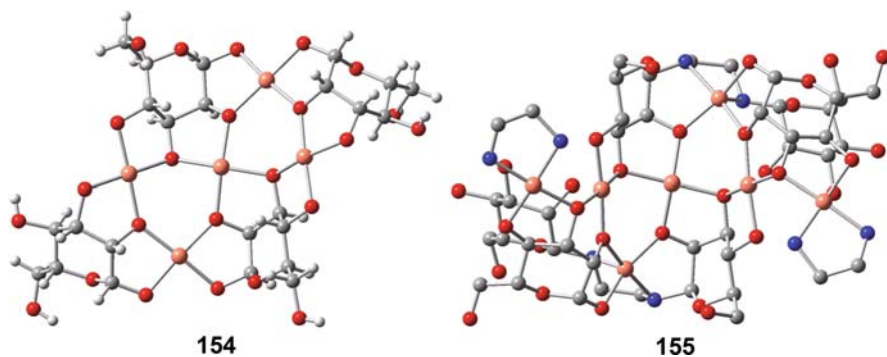

154   **155**

❏ **Figure 32**
Structure of $[Cu_5(\beta\text{-}D\text{-}Manp)_4H_{-13}]^{3-}$ (**154**) in K_3 **154** · $\alpha\text{-}D\text{-}Manp$ · 16.5 H_2O and $[(en)_2Cu_7(\beta\text{-}D\text{-}Manp1,2,3,4H_{-4})_2(L2,3,4H_{-3})_2]$ (**155**) in **155** · 26.6 H_2O with L = *N,N'*-bis($\beta\text{-}D$-mannopyranosyl)-ethylendiamine

In contrast to the other aldoses, the copper atoms find an especially favorable coordination environment for lyxose and mannose. Cu(II), indeed, has the ability to build stable complexes with the pyranoid *trans*-diol fragments, shown for the complexed 3,4-diol functions, but the more flat chelate five-membered rings, which are built with the with pyranoid *cis*-diol fragments, seemed to be more favorable for copper centers.

The *cis,cis*-orientation of the triol function with O1, O2 and O3 probably leads to an increased complex stability in the environment of the anomeric center and, as a consequence, to decreased tendency for reduction of copper.

A second compound, **155**, contains a reaction product with ethylenediamin and two moieties of mannose. Although the structure of the pentacuprate is quite complex, the composition of **155** could be derived from the simple educts. Besides oxidation, the building of *N*-glycosides is another reaction of the aldoses.
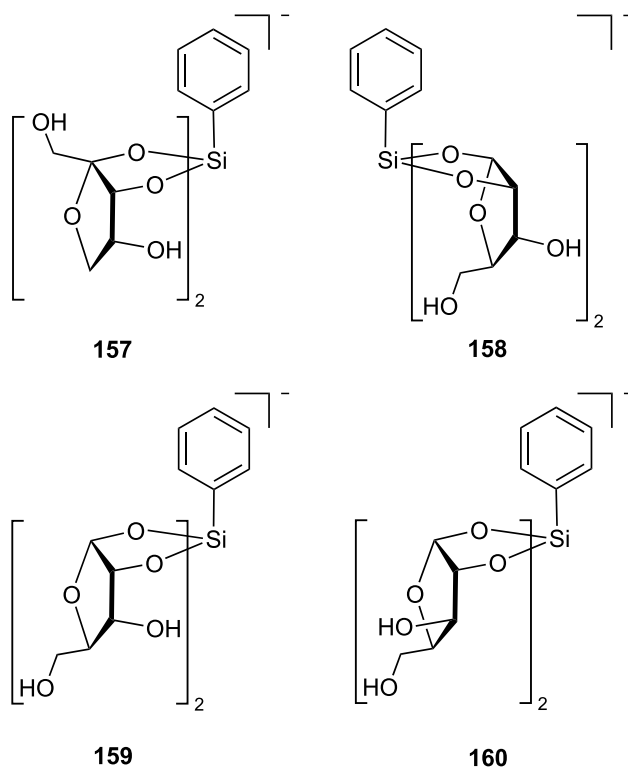
For silicon, the metal-coordinating properties, as found in AnEryt, should, in principle, be shared by each of the monosaccharides. A particular monosaccharide is expected to act as a good ligand if its *cis*-furanose form is of considerable stability, so that the stability constant of the complex is not charged with the isomerization energy of the ligand. In fact, almost all of the monosaccharides enrich alkaline aqueous silicate solutions with five- and six-coordinate silicon species, to some extent. However, the determination of the compositions and structures of the involved species is largely complicated by the mere number of the species in equilibrium. This has recently been demonstrated for D-ribose solutions by Kinrade et al., who detected a vast amount of various five- and six-coordinate species in such solutions [94]. For monosaccharides other than D-ribose, the situation is not any better.

To avoid these problems, the hydroxide ligand is substituted by an inert phenyl residue. In this way a series of phenylsilicates was crystallized. Five complexes have been isolated and characterized with two ketoses and three aldopentoses [174]. The silicon central atom in [K([18]crown-6)]**156** · MeOH is part of two chelate rings, with the ligands being O^2,O^3-β-D-fructofuranose dianions (❿ *Fig. 33*).

156
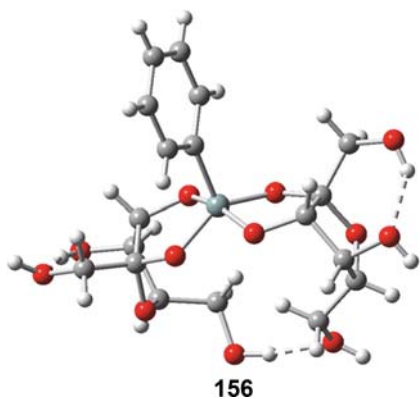
⬛ **Figure 33**
Structure of the anion [PhSi(β-D-Fru*f* 2,3H$_{-2}$)$_2$]$^-$ **156** in the crystal structure of [K([18]crown-6)][PhSi(β-D-Fru*f* 2,3H$_{-2}$)$_2$] · MeOH

The β-furanose isomer is best suited for silicon ligation because it exhibits a torsion angle close to 0° for the most acidic diol function, thus assuring a flat chelate ring. The same structural principles are also found in the anions [PhSi(a-D-Rul$f$2,3H$_{-2}$)$_2$]$^-$ **157**, [PhSi(β-D-Ara$f$1,2H$_{-2}$)$_2$]$^-$ **158**, [PhSi-(a-D-Rib$f$1,2H$_{-2}$)$_2$)]$^-$ **159** and [PhSi(a-D-Xyl$f$1,2H$_{-2}$)$_2$]$^-$ **160**.

157   **158**


159   **160**

Continuing with the furanoses, in **161** [133] 2,3-O-isopropylidene-α-L-sorbofuranose acts as a neutral tridentate ligand which is coordinated by three hydroxyl groups ($\kappa^3 O^1, O^4, O^6$ coordination).

The six-, seven-, and eight-membered 1,3,2-dioxaplatinacyclohexane rings exhibit boat, chair, and distorted chair conformations, respectively. The cyclic system is not free of bond angle strain, as indicated by the O–Pt–O angles in particular. One of these angles is distinctly smaller than 90° (O4–Pt–O6 = 82.5° vs. O1–Pt–O6 = 95.3° and O1–Pt–O4 = 91.2°. Two Pt–O bonds (O1, O4) average 2.25 Å and are equivalent to those in **162**. In contrast, the Pt–O6 bond with 2.16 Å is significantly shorter. The furanose ring assumes an envelope conformation in which C4 is displaced from the C5,O4,C2,C3 plane by 0.37 Å. A similar distortion of 0.57 Å but in the opposite direction is observed in the furanose ring of 1,2-O-isopropylidene-α-D-glucofuranose in **162** [133].

In **163** [133], 2,3;4,5-di-O-isopropylidene-β-D-fructopyranose acts as a neutral bidentate ligand which is coordinated by the hydroxyl group (O1) and the acetal oxygen atom (O6) of the pyranose ring ($\kappa^2 O^1, O^6$ coordination). The octahedral coordination of the platinum is com-

pleted by an aqua ligand. The five-membered 1,3,2-dioxaplatina cyclohexane ring exhibits a half-chair conformation. This ring is not free of bond angle strain, which is revealed by the small O1–Pt–O6 angle (75.3°) and the Pt–O bonds average 2.24 Å. The pyranose ring of the free ligand 2,3;4,5-di-O-isopropylidene-β-D-fructopyranose exhibits a $^2S_0$ conformation in the solid state [175]. In contrast, in the crystal structure of **163** [133], the twisted boat conformation of the pyranose ring is distorted due to complexation with platinum. This distortion is caused by changes in the dihedral angles in the sugar ring; in particular, the dihedral angle C3–C4–C5–C6 is reduced by 7° and C4–C5–C6–O6 is increased by 6°. Another structurally characterized β-D-fructopyranose is [$B_2(C_6H_5)_2(\beta$-D-Fru$p$2,3;4,5H$_{-4}$)] · acetone [176], shown in ❯ *Fig. 34*.

161

162

163
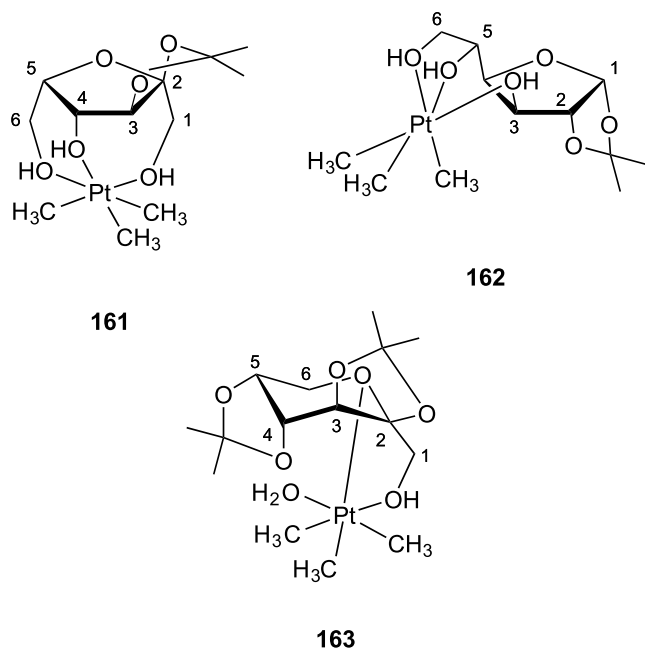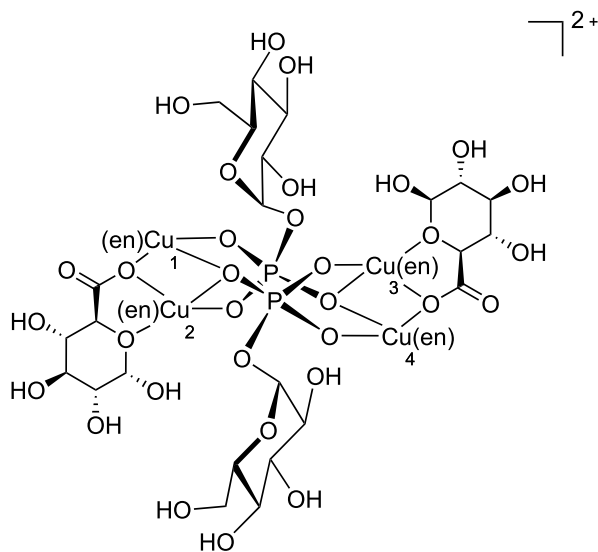
In **164**, phenylboronic acid forms five-membered cyclic boronates with the 2,3 and 4,5 diol function of the β-D-fructopyranose.

164
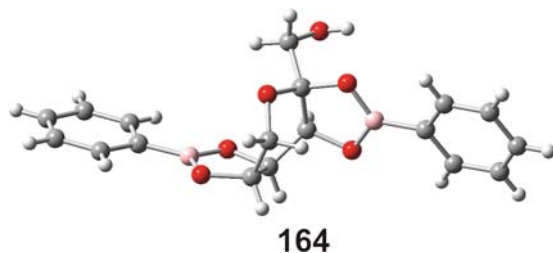
◨ **Figure 34**
Stucture of [$B_2(C_6H_5)_2(\beta$-D-Fru$p$2,3;4,5H$_{-4}$)] (164) in crystals of [$B_2(C_6H_5)_2(\beta$-D-Fru$p$2,3;4,5H$_{-4}$)] · acetone

In **165** [62], two D-glucoronate anions are introduced onto a tetracopper(II) scaffold of $[Cu_4\{\mu\text{-}(\alpha\text{-}D\text{-}Glc\text{-}1P)\}_2(bpy)_4]^{4+}$.

165

Of the two D-glucoronate ligands, one adopts the α-D-pyranose form, bridging the Cu1 and Cu2 ions, and the other adopts the β-D-pyranose form, connecting the Cu3 and Cu4 atoms. The C6 carboxylate group of each D-glucoronate connects the two Cu atoms in a η^1,η^1 monoatom bridging mode. The five-membered chelation by axial coordination is completed of the C5 cyclic O atom. The metal binding of the pyranose ring-O atom of D-glucoronate may accelerate interconversion between the α and β anomers through an intermediate open-chain form in solution.

Besides these complexes characterized by crystal-structure analysis, there is an extensive number of compounds containing reducing sugars, investigated only by various spectroscopic methods. Examples include borate esters of carbohydrates that have been investigated in depth by ^{11}B and ^{13}C NMR spectroscopy [177,178]. Furthermore, there is a great deal of literature that provides NMR spectroscopic data for molybdenum and tungsten complexes of carbohydrates as reviewed in [1]. However, it has remained as an ambitious goal for future work to support the NMR-derived conclusions by solid-state work. Hence, the above-mentioned oxido-molybdenum-lyxose complex, which demands an O_4 rhomb pattern for coordination, provides the only crystal-structure analysis in this substance class.

8 Concluding Remarks

While structural information about metal complexes of reducing carbohydrates was only sparsely available 10 years ago, a considerable increase has been observed in recent years.

In our opinion, this development was facilitated mainly by two key factors: the technical progress of all analytical methods, particularly in the fields of NMR spectroscopy and X-ray diffractometry, and the plenty of structural data meanwhile available for metal complexes of model compounds of carbohydrates. The basic research on the structural chemistry of the latter complexes followed by a transfer of the thereby gained knowledge in stability and regioselectivity of metal coordination into reducing carbohydrates has proved to be very successful. By this way, the improvement of existing and the development of new applications of metal complexes of carbohydrates, which provide a cheap and renewable feedstock, is merely a matter of time.

References

1. Verchere JF, Chapelle S, Xin F, Crans DC (1998) Prog Inorg Chem 47:837
2. Yano S (1998) Chin J Polym Sci 16:193
3. Yano S, Mikata Y (2002) Bull Chem Soc Jpn 75:2097
4. Gyurcsik B, Nagy L (2000) Coord Chem Rev 203:81
5. Nagy L, Szorcsik A (2002) J Inorg Biochem 89:1
6. Nagy L, Yamaguchi T, Yoshida K (2003) Struct Chem 14:77
7. Steinborn D, Junicke H (2000) Chem Rev 100:4283
8. Alexeev Y, Vasilchenko IS, Kharisov BI, Blanco LM, Garnovsk AD, II, Zhdanov Y (2004) J Coord Chem 57:1447
9. Zhdanov YA, Alekseev YE (2002) Russ Chem Rev 71:969
10. Petrou AL (2002) Coord Chem Rev 228:153
11. Baruah B, Das S, Chakravorty A (2003) Coord Chem Rev 237:135
12. Zamojski A, Jarosz S (2003) Curr Org Chem 7:1
13. Lomozik L, Gasowska A, Bregier-Jarzebowska R, Jastrzab R (2005) Coord Chem Rev 249:2335
14. Karakhanov EE, Maksimov AL, Runova EA, Kardasheva YS, Terenina MV, Buchneva TS, Guchkova AY (2003) Macromol Symp 204:159
15. Engeldinger E, Armspach D, Matt D (2003) Chem Rev 103:4147
16. Jeunesse C, Armspach D, Matt D (2005) Chem Commun 5603
17. Varma AJ, Deshpande SV, Kennedy JF (2004) Carbohydr Polym 55:77
18. Kästele X, Klüfers P, Kunte T (2001) Z Anorg Allg Chem 627:2042
19. Allscher T, Kästele X, Kettenbach G, Klüfers P, Kunte T (2007) Chem Asian J 2:1037
20. Habermann N, Klaassen M, Klüfers P (1993) Carbohydr Res 241:9
21. Klüfers P, Schuhmacher J (1994) Angew Chem 106:1839
22. Andrews MA, Voss EJ, Gould GL, Klooster WT, Koetzle TF (1994) J Am Chem Soc 116:5730
23. Klüfers P, Labisch O (2003) Z Anorg Allg Chem 629:1441
24. Ma L, Liu S, Zubieta J (1989) Polyhedron 8:1571
25. Chapelle S, Verchere JF, Sauvage JP (1990) Polyhedron 9:1225
26. Matulova M, Bilik V, Alfoldi J (1989) Chem Pap 43:403
27. Chapelle S, Verchere JF (1992) Inorg Chem 31:648
28. Burger J, Klüfers P (1997) Angew Chem Int Ed Engl 36:776
29. Ishi I, Nakashima K, Shinkai S, Araki K (1998) Tetrahedron 54:8679
30. Munoz A, Lamande L (1992) Carbohydr Res 225:113
31. Burger J, Klüfers P (1997) Z Anorg Allg Chem 623:1547
32. Hinrichs M, Hofbauer FR, Klüfers P (2006) Chem Eur J 12:4675
33. Benner K, Klüfers P, Vogt M (2003) Angew Chem Int Ed 42:1058
34. Burgmayer SJN, Stiefel EI (1988) Inorg Chem 27:2518
35. Chapelle S, Sauvage JP, Koell P, Verchere JF (1995) Inorg Chem 34:918
36. Burger J, Klüfers P (1998) Z Anorg Allg Chem 624:359
37. Chapelle S, Sauvage JP, Verchere JF (1994) Inorg Chem 33:1966
38. Junicke H, Steinborn D (2003) Inorg Chim Acta 346:129

39. Gupta A, Kirfel A, Will G, Wulff G (1977) Acta Crystallogr Sect B: Struct Sci B33:637

40. Van Duin M, Peters JA, Kieboom APG, Van Bekkum H (1985) Tetrahedron 41:3411

41. Hedman B (1977) Acta Crystallogr Sect B: Struct Sci B33:3077

42. Godfrey JE, Waters JM (1975) Cryst Struct Comm 4:5

43. Chapelle S, Verchere JF (1991) Carbohydr Res 211:279

44. Herdin S, Klüfers P, Kunte T, Piotrowski H (2004) Z Anorg Allg Chem 630:701

45. Klüfers P, Schuhmacher J (1995) Angew Chem Int Ed Engl 34:2119

46. Norrild JC (2001) J Chem Soc Perkin Trans 1719

47. Matulova M, Hricoviniova Z (2002) Carbohydr Res 337:1745

48. Chapelle S, Verchere JF (1995) Carbohydr Res 266:161

49. Chapelle S, Koll P, Verchere JF (1998) Carbohydr Res 306:27

50. Chapelle S, Sauvage JP, Koell P, Verchere JF (1995) Inorg Chem 34:918

51. Lis T (1979) Acta Crystallogr Sect B: Struct Crystallogr Cryst Chem B35:1699

52. Lis T (1984) Acta Crystallogr Sect C: Cryst Struct Commun C40:374

53. Tsubomura T, Yano S, Yoshikawa S (1988) Bull Chem Soc Jpn 61:3497

54. Tajmir-Riahi HA (1990) J Inorg Biochem 39:33

55. Gajda T, Gyurcsik B, Jakusch T, Burger K, Henry B, Delpuech JJ (1998) Inorg Chim Acta 275–276:130

56. Szorcsik A, Nagy L, Gyurcsik B, Vanko G, Kraemer R, Vertes A, Yamaguchi T, Yoshida K (2004) J Radioanal Nucl Chem 260:459

57. Giroux S, Rubini P, Henry B, Aury S (2000) Polyhedron 19:1567

58. Junicke H, Arendt Y, Steinborn D (2000) Inorg Chim Acta 304:224

59. Escandar GM, Salas Peregrin JM, Gonzalez Sierra M, Martino D, Santoro M, Frutos A, Garcia SI, Labadie G, Sala LF (1996) Polyhedron 15:2251

60. Escandar GM, Olivieri AC, Gonzalez-Sierra M, Frutos AA, Sala LF (1995) J Chem Soc Dalton Trans 799

61. Frutos AA, Sala LF, Escandar GM, Devillers M, Peregrin JMS, Sierra MG (1999) Polyhedron 18:989

62. Kato M, Sah AK, Tanase T, Mikuriya M (2006) Inorg Chem 45:6646

63. Llopis E, Ramirez JA, Cervilla A (1986) Transition Met Chem 11:489

64. Ramos ML, Caldeira MM, Gil VMS (2000) J Chem Soc Dalton Trans 2099

65. Ramos ML, Caldeira MM, Gil VMS (1997) Carbohydr Res 297:191

66. Ramos ML, Calderia MM, Gil VMS (1997) Carbohydr Res 299:209

67. Van Duin M, Peters JA, Kieboom APG, Van Bekkum H (1986) Rec Trav Chim Pays-Bas 105:488

68. Lakatos A, Bertani R, Kiss T, Venzo A, Casarin M, Benetollo F, Ganis P, Favretto D (2004) Chem Eur J 10:1281

69. Ferrier F, Avezou A, Terzian G, Benlian D (1998) J Mol Struct 442:281

70. Abrahams BF, Moylan M, Orchard SD, Robson R (2003) Angew Chem Int Ed 42:1848

71. Sheldrick B, Mackie W (1989) Acta Crystallogr Sect C: Cryst Struct Commun C45:1072

72. Klüfers P, Kramer G, Piotrowski H, Senker J (2002) Z Naturforsch B: Chem Sci 57:1446

73. Saladini M, Candini M, Iacopino D, Menabue L (1999) Inorg Chim Acta 292:189

74. Ramos ML, Caldeira MM, Gil VMS (1991) Inorg Chim Acta 180:219

75. Ramos ML, Caldeira M, Gil VMS, Van Bekkum H, Peters JA, Van Bekkum H, Peters JA (1994) Polyhedron 13:1825

76. Ramos ML, Caldeira MM, Gil VMS, Van Bekkum H, Peters JA (1994) J Coord Chem 33:319

77. Venema FR, Peters JA, Van Bekkum H (1993) Rec Trav Chim Pays-Bas 112:445

78. Van Duin M, Peters JA, Kieboom APG, Van Bekkum H (1987) J Chem Soc Perkin Trans 2473

79. Van Duin M, Peters JA, Kieboom APG, Van Bekkum H (1987) J Chem Soc Dalton Trans 2051

80. Burger J, Klüfers P (1995) Chem Ber 128:75

81. Barth M, Kästele X, Klüfers P (2005) Eur J Inorg Chem1353

82. Klüfers P, Krotz O, Ossberger M (2002) Eur J Inorg Chem1919

83. Achternbosch M, Klüfers P (1994) Acta Crystallogr Sect C: Cryst Struct Commun C50:175

84. Ahlrichs R, Ballauff M, Eichkorn K, Hanemann O, Kettenbach G, Klüfers P (1998) Chem Eur J 4:835

85. Habermann N, Jung G, Klaassen M, Klüfers P (1992) Chem Ber 125:809

86. Klaassen M, Klüfers P (1993) Z Anorg Allg Chem 619:661
87. Benner K, Klüfers P (2000) Carbohydr Res 327:287
88. Klüfers P, Mayer P, Schuhmacher J (1995) Z Anorg Allg Chem 621:1373
89. Klüfers P, Schuhmacher J (1995) Z Anorg Allg Chem 621:19
90. Burger J, Klüfers P (1996) Z Anorg Allg Chem 622:1740
91. Benner K, Klüfers P, Schuhmacher J (1999) Z Anorg Allg Chem 625:541
92. Kästele X, Klüfers P, Kopp F, Schuhmacher J, Vogt M (2005) Chem Eur J 11:6326
93. Tacke R, Bertermann R, Burschka C, Dragota S (2005) Angew Chem Int Ed 44:5292
94. Kinrade SD, Deguns EW, Gillson AM, Knight CTG (2003) Dalton Trans 3713
95. Kinrade SD, Balec RJ, Schach AS, Wang J, Knight CTG (2004) Dalton Trans 3241
96. Lambert JB, Lu G, Singer SR, Kolb VM (2004) J Am Chem Soc 126:9611
97. Kästele X, Klüfers P, Tacke R (2006) Angew Chem Int Ed 45:3212
98. Blank G (1973) Acta Crystallogr Sect B: Struct Crystallogr Cryst Chem 29:1677
99. Rabinowitz IN, Kraut J (1964) Acta Cryst 17:159
100. Yang L, Wang Z, Zhao Y, Tian W, Xu Y, Weng S, Wu J (2000) Carbohydr Res 329:847
101. Yang L, Tao D, Sun Y, Jin X, Zhao Y, Yang Z, Weng S, Wu J, Xu G (2001) J Mol Struct 560:105
102. Neidle S, Gaffney PRJ, Reese CB (1998) Acta Crystallogr Sect C: Cryst Struct Commun C54:1191
103. Kumara Swamy KC, Kumaraswamy S (2001) Acta Crystallogr Sect C: Cryst Struct Commun C57:1147
104. Salazar-Pereda V, Martinez-Martinez L, Flores-Parra A, Rosales-Hoz MdJ, riza-Castolo A, Contreras R (1994) Heteroat Chem 5:139
105. Grainger CT (1981) Acta Crystallogr Sect B: Struct Crystallogr Cryst Chem B37:563
106. Hausherr-Primo L, Hegetschweiler K, Ruegger H, Odier L, Hancock RD, Schmalle HW, Gramlich V (1994) J Chem Soc Dalton Trans 1689
107. Hegetschweiler K (1997) Bol Soc Chil Quim 42:257
108. Hegetschweiler K, Hausherr-Primo L, Koppenol WH, Gramlich V, Odier L, Meyer W, Winkler H, Trautwein AX (1995) Angew Chem Int Ed Engl 34:2242
109. Hegetschweiler K, Raber T, Reiss GJ, Frank W, Worle M, Currao A, Nesper R, Kradolfer T (1997) Angew Chem Int Ed Engl 36:1964
110. Morgenstern B, Sander J, Huch V, Hegetschweiler K (2001) Inorg Chem 40:5307
111. Park YJ, Kim HS, Jeffrey GA (1971) Acta Crystallogr Sect B: Struct Crystallogr Cryst Chem 27:220
112. Gack C, Klüfers P (1996) Acta Crystallogr Sect C: Cryst Struct Commun C52:2972
113. Junicke H, Bruhn C, Stroehl D, Kluge R, Steinborn D (1998) Inorg Chem 37:4603
114. Jeffrey GA, McMullan RK, Takagi S (1977) Acta Crystallogr Sect B: Struct Crystallogr Cryst Chem B33:728
115. Klüfers P, Mayer P (1998) Acta Crystallogr Sect C: Cryst Struct Commun C54:583
116. Shannon RD (1976) Acta Crystallogr Sect A: Cryst Phys Diffr Theor Gen Cryst A32:751
117. Zhang B, Zhang S, Wang K (1996) J Chem Soc Dalton Trans 3257
118. Rajak KK, Rath SP, Mondal S, Chakravorty A (1999) Indian J Chem Sect A: Inorg Bio-inorg Phys Theor Anal Chem 38A:405
119. Rajak KK, Rath SP, Mondal S, Chakravorty A (1999) J Chem Soc Dalton Trans 2537
120. Rajak KK, Rath SP, Mondal S, Chakravorty A (1999) Inorg Chem 38:3283
121. Rajak KK, Baruah B, Rath SP, Chakravorty A (2000) Inorg Chem 39:1598
122. Takagi S, Jeffrey GA (1979) Acta Crystallogr Sect B: Struct Crystallogr Cryst Chem B35:902
123. Barili PL, Catelani G, Fabrizi G, Lamba D (1993) Carbohydr Res 243:165
124. Johansson MJ, Bergh A, Larsson K (2004) Acta Crystallogr Sect C: Cryst Struct Commun C60:o312
125. Herdin S, Kettenbach G, Klüfers P (2004) Z Naturforsch B: Chem Sci 59:134
126. Kuentzer D, Jessen L, Heck J (2005) Chem Commun 5653
127. Jessen L, Haupt ETK, Heck J (2001) Chem Eur J 7:3791
128. Cameron TS, Bakshi PK, Thangarasa R, Grindley TB (1992) Can J Chem 70:1623
129. Klaassen M, Klüfers P (1994) Acta Crystallogr Sect C: Cryst Struct Commun C50:686
130. Klaassen M, Klüfers P (1994) Z Anorg Allg Chem 620:1631
131. Bhadrui S, Sapre N, Khwaja H, Jones PG (1992) J Organomet Chem 426:C12
132. Steinborn D, Junicke H, Bruhn C (1997) Angew Chem Int Ed Engl 36:2686

133. Junicke H, Bruhn C, Kluge R, Serianni AS, Steinborn D (1999) J Am Chem Soc 121:6232

134. Meyer zu Berstenhorst B, Erker G, Kehr G, Froehlich R (2006) Dalton Trans 3200

135. Conn JF, Kim JJ, Suddath FL, Blattmann P, Rich A (1974) J Am Chem Soc 96:7152

136. Daniel FB, Behrman EJ (1976) Biochemistry 15:565

137. Feldman I, Rich KE (1970) J Am Chem Soc 92:4559

138. Feldman I, Rich KE, Agarwal RT (1970) J Am Chem Soc 92:6818

139. Angus-Dunne SJ, Batchelor RJ, Tracey AS, Einstein FWB (1995) J Am Chem Soc 117:5292

140. Sakurai H, Goda T, Shimomura S, Yoshimura T (1982) Nucleic Acids Symp Ser 11:253

141. Geraldes CFGC, Castro MM (1989) J Inorg Biochem 35:79

142. Richter J, Rehder D (1991) Z Naturforsch B: Chem Sci 46:1613

143. Crans DC, Harnung SE, Larsen E, Shin PK, Theisen LA, Trabjerg I (1991) Acta Chem Scand 45:456

144. Tracey AS, Leon-Lai CH (1991) Inorg Chem 30:3200

145. Zhang X, Tracey AS (1992) Acta Chem Scand 46:1170

146. Richter J, Rehder D, Wyns L, Haikal A (1995) Inorg Chim Acta 238:155

147. Galy J, Mosset A, Grenthe I, Puigdomenech I, Sjoeberg B, Hulten F (1987) J Am Chem Soc 109:380

148. Begum NS, Manohar H (1992) Polyhedron 11:2823

149. Cai SX, Keana JFW (1991) Bioconjug Chem 2:317

150. Erxleben A, Yovkova L (2006) Inorg Chim Acta 359:2350

151. Klüfers P, Mayer P (1997) Z Anorg Allg Chem 623:1496

152. Klüfers P, Mayer P (2007) Z Anorg Allg Chem 633:903

153. Kettenbach G, Klüfers P, Mayer P (1997) Macromol Symp 120:291

154. Parada J, Bunel S, Ibarra C, Larrazabal G, Moraga E, Gillitt ND, Bunton CA (2001) Carbohydr Res 333:185

155. Geisselmann A, Klüfers P, Kropfgans C, Mayer P, Piotrowski H (2005) Angew Chem Int Ed 44:924

156. Klüfers P, Schuhmacher J (1994) Angew Chem 106:1925

157. Fuchs R, Habermann N, Klüfers P (1993) Angew Chem 105:895

158. Klüfers P, Piotrowski H, Uhlendorf J (1997) Chem Eur J 3:601

159. Yamanari K, Nakamichi M, Shimura Y (1989) Inorg Chem 28:248

160. Burger J, Kettenbach G, Klüfers P (1995) Macromol Symp 99:113

161. Saalwaechter K, Burchard W, Klüfers P, Kettenbach G, Mayer P, Klemm D, Dugarmaa S (2000) Macromolecules 33:4094

162. Burchard W, Habermann N, Klüfers P, Seger B, Wilhelm U (1994) Angew Chem 106:936

163. Taylor GE, Waters JM (1981) Tetrahedron Lett 22:1277

164. Bilik V, Petrus L, Farkas V (1975) Chem Zvesti 29:690

165. Bilik V, Voelter W, Bayer E (1972) Ann Chem 759:189

166. Bilik V (1972) Chem Zvesti 26:372

167. Burger J, Gack C, Klüfers P (1996) Angew Chem Int Ed Engl 34:2647

168. Geisselmann A, Klüfers P, Pilawa B (1998) Angew Chem Int Ed Engl 37:1119

169. Wilbur DJ, Williams C, Allerhand A (1977) J Am Chem Soc 99:5450

170. Klüfers P, Kunte T (2001) Angew Chem Int Ed 40:4210

171. Klüfers P, Kunte T (2003) Chem Eur J 9:2013

172. Klüfers P, Kunte T (2002) Eur J Inorg Chem 1285

173. Klüfers P, Kunte T (2004) Z Anorg Allg Chem 630:553

174. Klüfers P, Kopp F, Vogt M (2004) Chem Eur J 10:4538

175. Lis T, Weichsel A (1987) Acta Crystallogr Sect C: Cryst Struct Commun C43:1954

176. Draffin SP, Duggan PJ, Fallon GD (2004) Acta Crystallogr Sect E: Struct Rep Online E60:o1520

177. Chapelle S, Verchere JF (1988) Tetrahedron 44:4469

178. van den BR, Peters JA, van BH (1994) Carbohydr Res 253:1